UNIVERSITAT POLITÈCNICA DE CATALUNYA

MASTER THESIS

TITLE: Design of a DVB-T2 simulation platform and network optimization with Simulated Annealing

MASTER DEGREE: Master in Science in Telecommunication Engineering & Management

AUTHORS: Carlos Enrique Herrero
Carlos Alberto López Arranz

DIRECTORS: Silvia Ruiz Boqué
Mario García Lozano

DATE: July 15th 2009

Title: Design of a DVB-T2 simulation platform and network optimization with Simulated Annealing

Authors: Carlos Alberto López Arranz, Carlos Enrique Herrero

Directors: Silvia Ruiz Boqué, Mario García Lozano

Date: July, 15th 2009

Overview

The implementation of the Digital Terrestrial Television is becoming a reality in the Spanish territory. In this context, with the satellite and cable systems, this technology is one of the possible mediums for the television signal transmission. Its development is becoming crucial for the digital transition in those countries which mainly depend on the terrestrial networks for the reception of multimedia contents.

However, due to the maturity of the current standard, and also to the higher requirements of the customer needing (HDTV, new contents, etc.), a revision of the current standard becomes necessary. The DVB organisation in collaboration with other entities and organisms has developed a new standard version capable to satisfy those requirements.

The main objective of the project is the design and implementation of a physical layer simulation platform for the DVB-T2 standard. This simulator allows the theoretical evaluation of the new enhanced proposals, making easier a later field measurement stage and the future network deployment.

The document describes the implementation of the simulation platform as well as its subsequent validation stage, including large graphical results that allow the evaluation and quantification of the improvements introduced over the current standard version (DVB-T).

On the other hand, and as future investigation lines, a solution for the future DVB-T2 network deployment is performed, enhancing the coverage capacity of the current network by the use of iterative meta-heuristic techniques.

Finally it has to be mentioned that this work has been performed within the context of a project called FURIA, which is a strategic research project funded by the Spanish Ministry of Industry, Tourism and Commerce.

Título: Diseño de una plataforma de simulación para DVB-T2 y optimización de la red mediante Simulated Annealing

Autores: Carlos Alberto López Arranz, Carlos Enrique Herrero

Directores: Silvia Ruiz Boqué, Mario García Lozano

Fecha: 15 de julio de 2009

Resumen

La implementación de la Televisión Digital Terrestre es ya una realidad en el territorio nacional. En este contexto, junto con el cable y el satélite, esta tecnología es uno de los posibles soportes para la transmisión de la señal televisiva, cuyo desarrollo se está revelando crucial para la transición digital en aquellos países que dependen principalmente de las redes terrestres para recibir contenidos multimedia.

No obstante, debido a la madurez del estándar actual y las cada vez más exigentes necesidades de los usuarios (HDTV, nuevos contenidos, etc.), se hace necesaria una revisión del estándar actual. A partir de esta necesidad, la Organización DVB en colaboración con otros organismos y entidades ha desarrollado una nueva versión capaz de satisfacer estas demandas.

El objetivo principal del proyecto es el diseño y la implementación de un simulador de capa física de DVB-T2 sobre el cual se puede evaluar teóricamente las mejoras propuestas por este nuevo estándar, facilitando las posteriores pruebas de campo y el despliegue de la red.

El documento describe la implementación de la plataforma de simulación así como su posterior etapa de validación, incluyendo numerosos resultados gráficos que permiten evaluar y cuantificar las mejoras introducidas respecto a la versión actual del estándar (DVB-T).

Por otro lado, y como líneas futuras de investigación, se plantea una solución para la optimización del despliegue de la futura red DVB-T2 mejorando la capacidad de cobertura de la red actual mediante técnicas meta-heurísticas iterativas.

Por último, se debe mencionar que este proyecto está enmarcado dentro del contexto del FURIA, un Proyecto Singular Estratégico de Investigación propuesto por el Ministerio de Industria, Turismo y Comercio.

INDEX

TABLE INDEX

FIGURE INDEX

DEFINITIONS, SYMBOLS AND ABBREVIATIONS

Definitions

- **OFDM cell:** The modulation value for one OFDM carriers during one OFDM symbol.
- **Active cell:** An OFDM cell carrying a constellation point for L1 signalling or PLP.
- **Data cell:** An OFDM cell which is not a pilot or tone reservation.
- **Dummy Cell:** An OFDM cell carrying a pseudo-random value used to fill the remaining capacity not used for L1 signalling, PLPs or Auxiliary Streams.
- **Auxiliary Stream:** A sequence of cells carrying data of as yet undefined modulation and coding, which may be used for future extensions or as required by broadcasters.
- **OFDM symbol:** Waveform TS in duration comprising all the active carriers modulated with the corresponding modulation values and including the guard interval.
- **Data symbol:** An OFDM symbol in a T2-frame which is not a P1 or P2 symbol.
- **Normal symbol:** An OFDM symbol in a T2-frame which is not a P1, P2 or Frame Closing symbol.
- **Frame Closing Symbol:** An OFDM symbol with higher pilot density used at the end of a T2-frame in certain combinations of FFT size, guard interval and scattered pilot pattern.
- **sub-slice:** Group of cells from a single PLP, which before frequency interleaving are transmitted on active OFDM cells with consecutive addresses over a single RF channel.
- **T2 system:** The input for T2 system is one or more TS or GSE streams. The output is the RF signal in one frequency (FF mode) or in multiple frequencies (TFS mode).
    - T2 system means an entity where one or more PLPs are carried, in a particular way, within a DVB-T2 signal on one or more frequencies.
    - T2 system is unique within the T2 network and it is identified with T2_system_id. Two T2 systems with the same T2_system_id and network_id have identical physical layer structure and configuration, except for the cell_id which may differ.
    - The T2 system is transparent to the data that it carries (including transport streams and services).
- **T2_SYSTEM_ID:** This 16-bit field identifies uniquely the T2 system within the T2 network.

- **Physical Layer Pipe:** physical layer TDM channel that is carried by the specified sub-slices.
- **Type 1 PLP:** PLP having one slice per T2 frame, transmitted before any Type 2 PLPs.
- **Type 2 PLP:** PLP having two or more sub-slices per T2 frame, transmitted after any Type 1 PLPs,
- **Common PLP**: PLP having one slice per T2 frame, transmitted just after the L1 signalling, this may contain data shared by multiple PLPs.
- **Data PLP:** A PLP of Type 1 or Type 2
- **PLP_ID:** This 8-bit field identifies uniquely a PLP within the T2 system, identified with the T2_system_id. The same PLP_ID may occur in one or more frames of the superframe.
- **T2 frame:** Fixed physical layer TDM frame that is further divided into variable size sub-slices. T2 frame starts with one P1 and one or multiple P2 symbols.
- **Slice:** The set of all cells of a PLP which are mapped to a particular T2-frame. May be divided into sub-slices.
- **P1 symbol:** Fixed pilot symbol that carries S1 and S2 signalling fields and is located in the beginning of the frame within each RF-channel. It is mainly used for fast initial signal scan to detect T2 subsignal, frequency offset, and FFT size. Uses 2k mode with 1/4 guard interval.
- **P2 symbol:** Pilot symbol located right after P1 with the same FFT-size and guard interval as the data symbols. The number of P2 symbols depends on the FFT-size. Used for fine frequency and timing synchronization as well as for initial channel estimate. Carries L1 and L2 signalling information and may also carry data.
- **FEF part:** The part of the super-frame between two T2-frames which contains FEFs. A FEF part shall always start with a P1 symbol. The remaining contents of the FEF part shall be ignored by a DVB-T2 receiver.
- **Time interleaving block (TI-block):** A set of cells within which time interleaving is carried out, corresponding to one use of the time interleaver memory.
- **Interleaving frame:** The unit over which dynamic capacity allocation for a particular PLP is carried out, made up of a integer, dynamically varying number of FEC blocks and having a fixed relationship to the T2-frames. The Interleaving frame may be mapped directly to one T2-frame or may be mapped to multiple T2-frames. It may contain one or more TI-blocks.
- **T2 Super-frame:** A set of T2 frames consisting of a particular number of consecutive T2 frames. A superframe may in addition include FEF parts.
- **P1 signalling:** Signalling carried by the P1 symbol and used to identify the basic mode of the DVB-T2 symbol.
- **L1 pre-signalling**: Signalling carried in the P2 symbols having a fixed size, coding and modulation, including basic information about the T2 system as well as

information needed to decode the L1 post-signalling. L1 pre-signalling remains the same for the duration of a super-frame.

- **L1-post-signalling**: Signalling carried in the P2 symbol carrying more detailed L1 information about the T2 system and the PLPs.
- **Dynamic L1-signalling**: L1 signalling consisting of parameters which may change from one T2-frame to the next.
- **Configurable L1-signalling**: L1 signalling consisting of parameters which remain the same for the duration of one super-frame.
- **FFT size**: The nominal FFT size used for a particular mode, equal to the active symbol period *T*s expressed in cycles of the elementary period *T*.
- **Elementary Period**: Time period which depends on the system bandwidth and is used to define the other time periods in the T2 system.
- **MISO group:** The group (1 or 2) to which a particular transmitter in a MISO network belongs, determining the type of processing which is performed to the data cells and the pilots. Signals from transmitters in different groups will combine in an optimal manner at the receiver.
- **BBFRAME:** The set of K_{bch} bits which form the input to one FEC encoding process (BCH and LDPC encoding).
- **FECFRAME**: The set of N_{ldpc} (16200 or 64800) bits from one LDPC encoding operation.
- **FEC Block**: A set of N_{cells} OFDM cells carrying all the bits of one LDPC FECFRAME.

Symbols

Δ	Guard interval duration
λ_i	LDPC codeword bits
$\eta_{MOD}(i)$	Number of transmitted bits per constellation symbol (for PLP *i*)
1_{TR}	Vector containing ones at positions corresponding to reserved carriers and zeros elsewhere
$a_{m,l,p}$	Frequency-Interleaved cell value, cell index *p* of symbol *l* of T2-frame *m*
A_{CP}	Amplitude of the continual pilot cells
A_{P2}	Amplitude of the P2 pilot cells
A_{SP}	Amplitude of the scattered pilot cells
$b_{BS,j}$	Bit j of the BB scrambling sequence
$b_{e,do}$	Output bit of index *do* from substream *e* from the bit-to-sub-stream demultiplexer
$c(x)$	BCH codeword polynomial
C/N	Carrier-to-noise power ratio
C/N+I	Carrier-to-(Noise+Interference) ratio
C_{data}	Number of active cells in one normal symbol
C_{FC}	Number of active cells in one frame closing symbol
$c_{m,l,k}$	Cell value for carrier *k* of symbol *l* of T2-frame *m*
C_{P2}	Number of active cells in one P2 symbol

$C_{SSS1,i}$	Bit *i* of the S1 modulation sequence
$C_{SSS2,i}$	Bit *i* of the S2 modulation sequence
C_{tot}	Number of active cells in one T2 frame
D_{FL}	Data Field Length
D_i	Number of cells mapped to each T2 frame of the Interleaving frame for PLP *i*
$D_{i,aux}$	Number of cells carrying auxiliary stream i in the T2 frame
$D_{i,common}$	Number of cells mapped to each T2 frame for common PLP *i*
$D_{i,j}$	Number of cells mapped to each T2 frame for PLP *i* of type *j*
D_{L1}	Number of OFDM cells in each T2 frame carrying L1 signalling
D_{L1post}	Number of OFDM cells in each T2 frame carrying L1 post-signalling
D_{L1pre}	Number of OFDM cells in each T2 frame carrying L1 pre-signalling
$d_{n,s,r,q}$	Time Interleaver input / Cell interleaver output for cell *q* of FEC block *r* of TIblocks of Interleaving Frame *n*
D_{PLP}	Number of OFDM cells in each T2 frame available to carry PLPs
$d_{r,q}$	Cell interleaver output for cell *q* of FEC block *r*
D_x	Difference in carrier index between adjacent scattered-pilot-bearing carriers
D_y	Difference in symbol number between successive scattered pilots on a given carrier
$e_{m,l,p}$	Cell value for cell index *p* of symbol *l* of T2-frame *m* following MISO processing
f_c	Centre frequency of the RF signal
$f\_post_{m,i}$	Cell *i* of coded and modulated L1 post-signalling for T2-frame *m*
$f\_pre_{m,i}$	Cell *i* of coded and modulated L1 pre-signalling for T2-frame *m*
f_q	Constellation point normalised to mean energy of 1
f_{SH}	Frequency shift for parts 'B' and 'C' of the P1 signal
$g(x)$	BCH generator polynomial
$g_1(x)... g_{12}(x)$	Polynomials to obtain BCH code generator polynomial
g_q	OFDM cell value after constellation rotation and cyclic Q delay
$H(p)$	Frequency interleaver permutation function, element *p*
$H_0(p)$	Frequency interleaver permutation function, element *p*, for even symbols
$H_1(p)$	Frequency interleaver permutation function, element *p,* for odd symbols
$I_{JUMP}(i)$	Frame interval: difference in frame index between successive T2-frames to which a particular PLP is mapped (for PLP *i*)
i_j	BCH codeword bits which form the LDPC information bits
j	$\sqrt{-1}$
k'	Carrier index relative to the centre frequency
k	OFDM carrier index
K_{bch}	number of bits of BCH uncoded Block
K_{ext}	Number of carriers added on each side of the spectrum in extended carrier mode.
$K_{L1\_PADDING}$	Length of L1_PADDING field
K_{ldpc}	Number of bits of LDPC uncoded Block
K_{max}	Carrier index of last (highest frequency) active carrier
K_{min}	Carrier index of first (lowest frequency) active carrier
K_{mod}	Modulo value used to calculate continual pilot locations
$k_{p1}(i)$	Carrier index *k* for active carrier *i* of the P1 symbol.
K_{post}	Length of L1 post-signalling field including the padding field
$K_{post\_ex\_pad}$	Number of information bits in L1 post-signalling excluding the padding field.
K_{pre}	Information length of the L1 pre-signalling
K_{sig}	Number of signalling bits per FEC block for L1 pre- or post-signalling
K_{total}	Number of OFDM carriers
l	Index of OFDM symbol within the T2-frame

L_{data}	Number of data symbols per T2 frame including any frame closing symbol but excluding P1 and P2
L_F	Number of OFDM symbols per T2 frame excluding P1
L_{normal}	Number of data symbols, not including P1, P2 or any frame closing symbol, in a T2-frame
$L_r(q)$	Cell interleaver permutation function for FEC block r of the TI-block
m	T2-frame number
M_{aux}	Number of auxiliary streams in the T2 system
M_{common}	Number of common PLPs in the T2 system
m_i	BCH message bits
M_j	Number of PLPs of type j in the T2 system
M_{max}	Sequence length for the frequency interleaver
MSS_DIFF_i	Bit i of the differentially modulated P1 sequence
MSS_SCR_i	Bit i of the scrambled P1 modulation sequence
MSS_SEQ_i	Bit i of the overall P1 modulation sequence
M_{TI}	Maximum number of cells required in the TI memory
n	Interleaving frame index within the superframe
N_{bch}	Number of bits of BCH coded Block
N_{bch_parity}	Number of BCH parity bits
$N_{BLOCKS\_IF}(i,n)$	Number of FEC blocks in Interleaving Frame n (for PLP i)
$N_{BLOCKS\_IF\_MAX}$	Maximum value of $NBLOCKS\_IF(n)$
$N_{cells}(i)$	Number of OFDM cells per FEC Block (for PLP i)
N_{data}	Number of data cells in an OFDM symbol (including any unmodulated data cells in the frame closing symbol)
N_{dummy}	Number of dummy cells in the T2-frame
$N_{FEC\_TI}(n,s)$	Number of FEC blocks in TI-block s of interleaving frame n
N_{FEF}	Number of FEF parts in one super frame
N_{FFT}	FFT size
N_{group}	Number of bit-groups for BCH shortening
N_{ldpc}	Number of bits of LDPC coded Block
$N_{MOD\_per\_Block}$	Number of modulated cells per FEC block for the L1 post-signalling
N_{MOD_Total}	Total number of modulated cells for the L1 post-signalling
N_{P2}	Number of P2 symbols per T2 frame
N_{pad}	Number of BCH bit-groups in which all bits will be padded for L1 signalling
N_{PN}	Length of the frame-level PN sequence
N_{post}	Length of punctured and shortened LDPC codeword for L1 post-signalling
$N_{post\_FEC\_Block}$	Number of FEC blocks for the L1 post-signalling
N_{post_temp}	Intermediate value used in L1 puncturing calculation
N_{punc}	Number of LDPC parity bits to be punctured
N_{punc_groups}	Number of parity groups in which all parity bits are punctured for L1 signalling
N_{punc_temp}	Intermediate value used in L1 puncturing calculation
N_r	Number of bits in Frequency Interleaver sequence
N_{RF}	Number of RF channels used in a TFS system
$N_{subslices}$	Number of sub-slices per T2 frame on each RF channel
$N_{subslices\_total}$	Number of sub-slices per T2 frame across all RF channels
$N_{substreams}$	Number of substreams produced by the bit-to-sub-stream demultiplexer
N_{T2}	Number of T2 frames in a super frame
N_{TI}	Number of TI blocks in an Interleaving Frame
p	Data cell index within the OFDM symbol prior to frequency interleaving and pilot insertion
$P(r)$	Cyclic shift value for cell interleaver in FEC block r of the TI-block.
$p_1(t)$	Time-domain complex baseband waveform for the P1 signal

$p_{1A}(t)$	Time-domain complex baseband waveform for part 'A' of the P1 signal
P_I , $P_I(i)$	Number of T2 frames to which each Interleaving Frame is mapped (for PLP (i)
p_i	LDPC parity bits
p_{nl}	Frame level PN sequence value for symbol l
q	Index of cell within coded and modulated LDPC codeword
Q_{ldpc}	Code-rate dependent LDPC constant
r	FEC block index within the TI-block
$R_{eff\_16K\_LDPC\_1\_2}$	Effective code rate of 16K LDPC with nominal rate 1/2
R_{eff_post}	Effective code rate of L1 post-signalling
r_i	BCH remainder bits
R_i	Value of element i of the frequency interleaver sequence following bit permutations
R'_i	Value of element i of the frequency interleaver sequence prior to bit permutations
$r_{l,k}$	Pilot reference sequence value for carrier k in symbol l
R_{RQD}	Complex phasor representing constellation rotation angle
s	Index of TI-block within the Interleaving Frame
S_i	Element i of cell interleaver PRBS sequence
T	Elementary time period for the bandwidth in use
t_c	Column-twist value for column c
T_F	Duration of one T2-frame
T_F	Frame duration
T_{FEF}	Duration of one FEF part
T_P	Time interleaving period
T_{P1}	Duration of the P1 symbol
T_{P1A}	Duration of part 'A' of the P1 signal
T_{P1B}	Duration of part 'B' of the P1 signal
T_{P1C}	Duration of part 'C' of the P1 signal
T_S	Total OFDM symbol duration
T_{SF}	Duration of one super frame
T_U	Active OFDM symbol duration
u_i	Parity-interleaver output bits
UPL	User Packet Length
v_i	Column-twist-interleaver output bits
w_i	Bit i of the symbol-level reference PRBS
X_i	The set of bits in group j of BCH information bits for L1 shortening
$x_{m,l,p}$	Complex cell modulation value for cell index p of OFDM symbol l of T2-frame m
$y_{i,q}$	Bit i of cell word q from the bit-to-cell-word demultiplexer
z_q	Constellation point prior to normalisation
π_p	Permutation operator defining parity bit groups to be punctured for L1 signalling
π_s	Permutation operator defining bit-groups to be padded for L1 signalling

The symbols s, t, i, j, k are also used as dummy variables and indices within the context of some clauses or equations.

In general, parameters which have a fixed value for a particular PLP for one processing block (e.g. T2-frame, Interleaving Frame, TI-block as appropriate) are denoted by an upper case letter. Simple lower-case letters are used for indices and dummy variables.

Abbreviations

16QAM	16-ary Quadrature Amplitude Modulation
64QAM	64-ary Quadrature Amplitude Modulation
256QAM	256-ary Quadrature Amplitude Modulation
ACM	Adaptive Coding and Modulation
AWGN	Additive White Gaussian Noise
BB	BaseBand
BCH	Bose-Chaudhuri-Hocquenghem multiple error correction binary block code
BER	Bit Error Ratio
BICM	Bit Interleaved Coding and Modulation
CBR	Constant Bit Rate
CCM	Constant Coding and Modulation
CI	Cell Interleaver
CRC	Cyclic Redundancy Check
D	Decimal notation
DBPSK	Differential Binary Phase Shift Keying
DEMUX	DEMUltipleXer
DNP	Deleted Null Packets
DFL	Data Field Length
DVB	Digital Video Broadcasting project
DVB-T	DVB System for terrestrial broadcasting specified in EN 300 421
DVB-T2	DVB-T2 System as specified in the present document.
EBU	European Broadcasting Union
FEC	Forward Error Correction
FEF	Future Extension Frame
FFT	Fast Fourier Transform
FIFO	First In First Out
GCS	Generic Continuous Stream
GF	Galois Field
GFPS	Generic Fixed-length Packetized Stream
GS	Generic Stream
GSE	Generic Encapsulated Stream
HEM	High Efficiency Mode
HEX	Hexadecimal notation
IF	Intermediate Frequency
IFFT	Inverse Fast Fourier Transform
IS	Interactive Services
ISCR	Input Stream Time Reference
ISI	Input Stream Identifier
ISSY	Input Stream SYnchronizer
ISSYI	Input Stream SYnchronizer Indicator
Kbit	1024 bits
LDPC	Low Density Parity Check (codes)
LSB	Least Significant Bit
M_{bit}	2^{20} bits
MIS	Multiple Input Stream
MISO	Multiple Input, Single Output (meaning multiple transmitting antennas but one receiving antenna)
MPEG	Moving Pictures Experts Group
MSB	Most Significant Bit
MSS	Modulation Signalling Sequences
MUX	MUltipleX

NA	Not Applicable
NM	Normal Mode
NPD	Null-Packet Deletion
PAPR	Peak to Average Power Ratio
PER	(MPEG TS) Packet Error Rate
PID	Packet IDentifier
PLP	Physical Layer Pipe
PLL	Phase-Locked Loop
PLS	Physical Layer Signalling
PRBS	Pseudo Random Binary Sequence
QEF	Quasi-Error-Free
QPSK	Quaternary Phase Shift Keying
RF	Radio Frequency
SIS	Single Input Stream
SISO	Single Input Single Output (meaning one transmitting and one receiving antenna)
SoAC	Sum of AutoCorrelation
TDM	Time Division Multiplex
TF	Time/Frequency
TFS	Time-Frequency Slicing
TS	Transport Stream
TSPS	Transport Stream Partial Stream
TSPSC	Transport Stream Partial Stream Common
TV	TeleVision
UP	User Packet

INTRODUCTION

0.1 Main goals of the project

During the last years, the mobile telephone has revolutionized society habits and there are also coming up new concepts: terminal associated to people instead of terminals associated to places, multimedia entertainment while people is waiting, streaming on demand; in other words personalised solutions.

Nowadays mobile phone operators offer different multimedia services, for example: music video-clips, web mail access, TV programs, etc. by means of third generation networks (3G) and HSDPA. However the inefficiency of these networks in transmitting the same content to different users, puts a limit in the maximum number of active users supported by the system, and also determines the high cost of these services.

All these factors make necessary a convergence/cooperation between telecommunications and broadcasting networks, but also imply broadcast community to reconsider its technical approach in terms of deciding how to manage new services and opportunities.

In this scenario, and knowing that these requirements were not satisfied by the provided services in the last years, it has become necessary the deployment of new standards including specifications for the new mobile broadcast scenarios, and with the capability to support the future market demand. The Digital Video Broadcasting (DVB) organization, works to develop, set and promote technical guidelines, standards and specifications to benefit and advance digital media markets world-wide. With this objective in mind the DVB organization started to renew the Digital Video Broadcasting - Satellite standard (DVB-S) which was ratified by the ETSI organization in the year 2005. Up to the date: DVB-C, DVB-T, DVB-H and other broadcasting standards have been reviewed and/or are in review process. This document is focused on the DVB-T2 standard, which is on ETSI standardization stage, and it is a continuation of the previous work performed in our Final Bachelor Degree Project from the Telecommunications Engineering specializing in Telecommunications Systems [1].

In this context it must be noted that the DVB-T standard was developed at the beginning of the 1990's. Along these years new radio communications systems have been appearing using different OFDM modulation techniques, so it's easy to think that this systems are employing coders, interleavers, modulation techniques, pilots, transmission diversity, etc. offering better features than DVB-T standard does.

One of the main goals of this project is to develop a simulation platform of the defined DVB-T2 standard and test the new results obtained in E_b/N_0 requirements in front of the DVB-T standard. On the other hand, since one of the main problems for the network operators is to maximize the coverage area, a study for the optimisation of the current DVB network is performed taking into account the new parameters of the DVB-T2 standard.

This project has been developed under a more ambitious national project named FURIA [2]. FURIA is a SSP project (Strategically Singular Project) in the field of Network Audiovisual Technologies, which main objective is **to develop and validate the integration of emergent technologies for the spreading of audiovisual contents in fixed and mobile devices**. Joining forces from the different national organisations (companies, technological centres and universities) with the final purpose of hold on the national high technological level.

FURIA consortium has the capability to finish the investigation and development stages in the new contents of broadcasting audiovisual technologies, and will realise valuable contributions to the main standardization bodies in an industrial forum context, collaborating with technical proposals in the definition of the new Terrestrial Digital Video Broadcasting standard in the recent years.

It is expected that the generated research results of the consortium will be immediately applied, in means of generating pre-industrial results.

Other objectives of the FURIA project are:

- The establishment of relationships with other national and European projects, which will allow the enrichment of Spanish technological level, and the generation of:
- Contributions to forums and European standards, to grow up Spanish technological consortium acknowledgment and to have influence in the standardisation section.

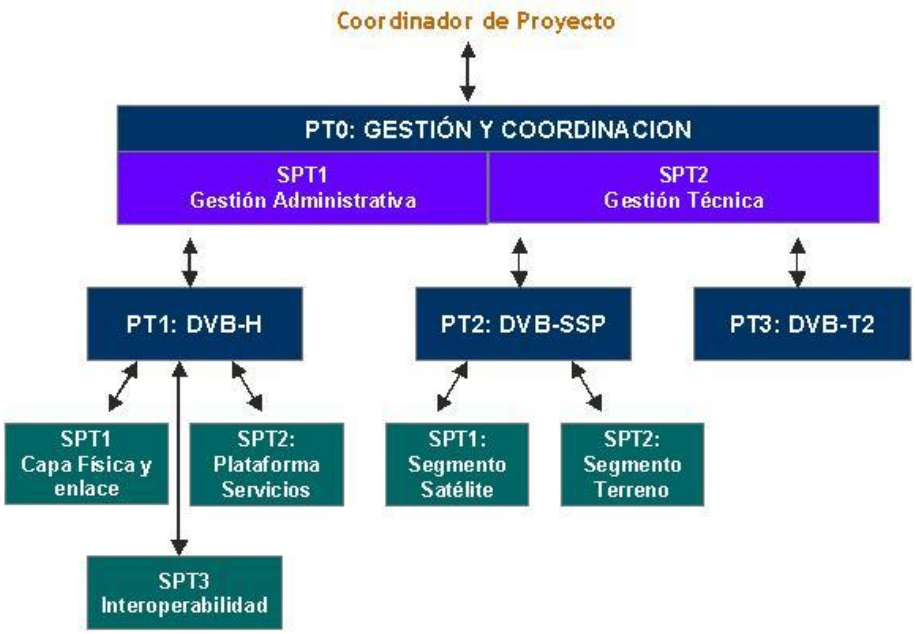

Fig. 0.1: General Scheme of FURIA council

It is worth highlighting that FURIA project is developed in the framework of the technological Spanish platform e-NEM, national mirror of its European homonymic NEM (Networked and Electronic Media).

The technological Spanish platform eNEM is an open forum promoted by the industry of Audiovisual Technologies Network, with the main objective of obtaining a mass critical investigation in fundamental issues for the Spanish development in this area. It's constituted by groups or excellence poles and a coordination of technical-scientist, composed by relevant actors in the Network Audiovisual Technologies area. The list of participating entities in the FURIA project is depicted below:

Project Manager

Fig. 0.2: Participating entities

0.2 Structure of the written report

Within this project framework, Radio Communications Research Group (together with the Fundació i2CAT) participates in the PT3, realising studies, simulations and the solution campaigns that are pretty needed to manage the deployment in an optimal way.

The guidelines for the new DVB-T2 have been published by the DVB organisation within the DVB bluebook denomination [3]. During the initial process of this project the version A122-TM3980 Rev.5 has been followed for the standard implementation. However a new version of this bluebook was published during the realisation of the project and its modifications have been also included in the simulation platform. The second part of our project has been the study of the Simulated Annealing algorithm to optimize the coverage area of the current network.

In this memory all the work realised during these six working months is summarized, in a theoretical and practical framework in the simulator development. The integration task has been difficult and time consuming, as well as the number of test running to validate that every stage of the simulation platform were working properly. These are tasks usually are not reflected at the written report, but are one of the critical tasks in big engineering projects.

The task programmed for this project contains two main stages. The first stage has been the deployment of transmission, modulation and receiver blocks for the system and the validation of the results with other FURIA platform members. The second stage consisted in the development and implementation of network optimization algorithms in the real Catalonia DVB-T network. Along this memory a detailed explanation of both systems will be given.

The project is composed by three significant blocks. First, the *chapters' one* and *two* introduce the reader in the DVB-T context, with a short description of the DVB-T in Spain and specifying the initial scenarios for the simulator platform. In the second block (*Chapters 3, 4* and *5*), the implemented simulator is described at both, theoretical and programming level. Finally, in *Chapter 6,* a description of the optimization proposed for the DVB-T network for the T2 mode, just as the conclusions, are performed.

CHAPTER 1: INTRODUCTION TO DVB-T2

Along that chapter, a brief introduction to the second generation of the Digital Terrestrial Television Broadcasting System (DVB-T2) is realized. Also in this section, the technical bases of this system will be analyzed in order to provide to the reader the reasons and benefits to implement this new standard, as well as the main advantages and drawbacks of the digital television.

Nowadays, there are four main DTTB (Digital Terrestrial Television Broadcasting) standards coexisting in the international scenario:

- USA-based ATSC (Advanced Television System Committee) standard.
- Europe-based DVB-T (Digital Video Broadcasting-Terrestrial) standard.
- Japan-based ISDB-T (Integrated Services Digital Broadcasting-Terrestrial) standard.
- Chinese-based DTMB (Digital Terrestrial/Television Multimedia Broadcasting) standard.

In this context, in March 2006 DVB decided to study options for an upgraded DVB-T standard. In June 2006, a formal study group named TM-T2 (Technical Module on Next Generation DVB-T) was established by the DVB Group to develop an advanced modulation scheme that could be adopted by a second generation digital terrestrial television standard, to be named **DVB-T2**.

According to the commercial requirements and call for technologies issued in April 2007, the first phase of DVB-T2 will be devoted to provide optimum reception for stationary (fixed) and portable receivers (i.e., units which can be nomadic, but not fully mobile) using existing aerials, whereas a second and third phase will study methods to deliver higher payloads (with new aerials) and the mobile reception issue. The novel system should provide a minimum 30% increase in payload, under similar channel conditions already used for DVB-T.

1.1 Digital Terrestrial Television: Isofrequential networks

DVB-T2 is based in the Orthogonal Frequency Division Modulation (OFDM), a well know transmission technique that has been used on the last radio broadcast applications (DAB), ADSL modems or in other standards like *IEEE 802.11* [4].

In one hand the main advantage of OFDM modulation is to transform a frequency selective channel in to a group of different non selective sub-channels (narrower channels). This feature makes OFDM be the most spectral efficient system, providing a deeply multipath immunity. In an OFDM system, data is transmitted in parallel in a group of subcarriers providing natural diversity and frequency interleaving. These subcarriers were orthogonal in time domain (consecutive pilots spaced by the inverse of symbol time) and tolerating spectrum overlap in frequency domain warranting an efficient spectrum use.

OFDM signals can be easy generated and demodulated using Fourier Fast Transform (FFT and IFFT). It's immunity to multipath allows the implementation of easy equalizers and channel estimators, and makes them more tolerant to synchronization errors in broadcast applications. Another advantage of the OFDM techniques is the easily adoption of adaptative coding and modulation techniques, and OFDM symbol windowing allows the implementation of spectrum conformation filters.

In the other hand, the main disadvantages of OFDM modulation are basically two: high peak power and average power relationship. Those characteristics force the use of lineal filters and amplifiers and make the system sensitive to frequency offsets (sampling frequency errors), generated by synchronization errors and Doppler effects, which introduces orthogonal loses between subcarriers.

OFDM also allows isofrequency networks (SFN, Single Frequency Networks), where different transmitters send the same signal simultaneously. At receiver, the signals from different transmitters can be constructive combined to generate a diversity gain. The fact that bandwidth is subdivided in different sub channels, and all of them are modulated at low transmission velocity, makes symbol delay large enough to erase delay spread effects. The cyclic prefix (also denominated guard period) between consecutive OFDM symbols reduces intersymbolic interference (ISI) effects.

However it is possible, that the signal generated by different delays between different transmitters, could not be eliminated generating interferences between symbols. At *Chapter 6* the Catalonian area planning for an optimal deployment of the DVB-T2 system is analyzed in order to reduce these effects.

Another way to solve this problem is to consider that the different signals arriving from different transmitters are transmitted in independent paths that can be isolated knowing the arrival angle to de receptor (DOA. Direction Of Arrival). Using multiple antennas at the receiver, a MIMO (Multiple-Input Multiple-Output) would be performed.

1.2 DVB-T2 system

The DVB-T2 [3] system is part of the new generation of standards developed by the DVB organization [5]. This new generation includes the improvement of the different television broadcasting services. The first standard that has been improved is the satellite standard (DVB-S [6]) becoming the DVB-S2 [7] standard. Following this line the digital terrestrial television standard which was developed more than 15 years ago also requires a revision, in order to adapt it to the new technologies and improving its features.

The DVB-T2 draft standard ratified by the DVB Steering Board on June 26, 2008, and published on the DVB homepage as *DVB-T2 standard BlueBook* [3], has been handed over to the European Telecommunications Standards Institute (ETSI) by DVB Project on June 20, 2008.

The Digital Video Broadcasting Project (DVB) is an industry-led consortium of over 260 broadcasters, manufacturers, network operators, software developers, regulatory bodies and others in over 35 countries committed to designing global standards for the global delivery of digital television and data services. This supposes to know real necessities of electronic markets, economical situations and also broadcast television industry. Considering some of these factors, different coding and modulation schemes are defined for the following terrestrial services: LDTV (Limited Definition Television), SDTV (Standard Definition Television), EDTV (Enhanced Definition Television) and HDTV (High Definition Television).

The ETSI process is expected to take until July 2009, when the final standard will be published. The ETSI process has several phases, but the only changes expected (if any) will be text clarifications.

DVB-T2 modulators are on the market and receiver chips are under development. Prototype receivers were shown in September 2008 at the IBC08 in Amsterdam [8].

The DVB-T2 standard implements deep changes at different parts of the structure which are very similar to the DVB-S2 standard. These improvements include the possibility of higher data transmission capacity, higher immunity in hostile channels, the possibility of mobile reception and other added services.

The implementation of these new services is possible with the modification of the encoding and interleaving schemes. The following characteristics have been devised for the T2 standard:

- OFDM modulation with QPSK, 16-QAM, 64-QAM, or 256-QAM constellations.
- OFDM modes are 1k, 2k, 4k, 8k, 16k, and 32k.
- Guard intervals are 1/128, 1/32, 1/16, 19/256, 1/8, 19/128, and 1/4.
- FEC is LDPC and BCH (as in DVB-S2), with rates 1/2, 3/5, 2/3, 3/4, 4/5, and 5/6.
- There are fewer pilots, in 8 different pilot-patterns.
- In the 8k, 16k and 32k mode, a larger part of the standard 8 MHz channel can be used, adding extra capacity with an extended OFDM carrier mode.
- DVB-T2 is specified for 1.7, 5, 6, 7, 8, and 10 MHz channel bandwidth.
- MISO (Multiple-Input Single-Output) may be used (Siavash Alamouti scheme), but MIMO will not be contemplated. Diversity receivers can be used (as they are with DVB-T).

For instance, a UK MFN DVB-T profile (64-QAM, 2k mode, coding rate 2/3, guard interval 1/32) and a DVB-T2 equivalent (256-QAM, 32k, coding rate 3/5, and guard interval 1/128) allows a bit rate increase from 24.13 Mbit/s to 35.4 Mbit/s (+46.5%). Another example, for an Italian SFN DVB-T profile (64-QAM, 8k, coding rate 2/3, guard interval 1/4) and a DVB-T2 equivalent (256-QAM, 32k, coding rate 3/5, guard interval 1/16), achieves an increase in bit rate from 19.91 Mbit/s to 33.3 Mbit/s (+67%).

A comparison between the DVB-T [9] and the DVB-T2 standards in Spain can be found in **Table 1.1**

Table 1.1: DVB-T2 and DVB-T standard comparative

	DVB-T in Spain	DVB-T2
Modulation	64-QAM	256-QAM
FFT size	8 K	32 K
Guard interval	1/4	1/16
FEC	2/3 CC + RS (8%)	3/5 LDPC + BCH (0.3%)
Scattered pilots	8%	1%
Continual pilots	2.6%	0.35%
Bandwidth	Standard	Extended
Capacity	19.9 Mbits/s	33.6 Mbits/s

As it can be seen in the comparative the capacity of the DVB-T2 standard is 33.6 Mbits/s, which means an enhancement of a 69% compared to the DVB-T standard.

CHAPTER 2: SIMULATION ENVIRONMENT DESCRIPTION

Along this chapter the scenario required to develop the DVB-T2 simulation platform as well as the implied channel models and the election of the simulator platform will be described.

2.1 Initial scenario

In first place and based on the directives marked by the FURIA council defined in the introduction chapter, the proposed simulator will be orientated to the physical layer to bit level of DVB-T2. To make possible those requirements, it has been implemented a generic transmitter defined at *DVB-T2 BlueBook* [3]. The receiver block needs to be able to reconstruct the transmission signal, following the guidelines proposed by the transmitter. In the same way, the different channels models considered by the DVB organisation are described in the DVB *BlueBook* A133 [10].

Table 2.1: Interfaces for the Baseline System

Location	Interface	Interface type	Connection
Transmit Station	Input	MPEG-2 or generic transport stream(s) multiplex	From MPEG-2 multiplexer
	Output	RF signal	To aerial
Receive Installation	Input	RF	From aerial
	Output	MPEG-2 or generic transport stream(s) multiplex	To MPEG-2 demultiplexer

2.2 Baseline system and general considerations

The system is defined as the functional block of equipment performing the adaptation of the base band TV signals from the output of the transport multiplexer to the terrestrial channel characteristics. The following processes shall be applied to the data stream:

- Transport multiplex adaptation and randomization for energy dispersal;
- FEC encoding (i.e. LDPC/BCH codes);
- Bit interleaving;
- Gray mapping and constellation rotation (when it is allowed);
- Cell, Time and Frequency Interleaving;
- Mapping and modulation;
- Orthogonal Frequency Division Multiplexing (OFDM) transmission.

The system is directly compatible with MPEG-2 and MPEG-4 coded TV signals ISO/IEC 13818 [11].

Since the system is being designed for digital terrestrial television services to operate within the existing VHF and UHF (8MHz, 7MHz and 6MHz channel spacing and also 1.7MHz, 10 MHz on extended mode) spectrum allocation for analogue transmissions it is required that the system provides enough protection against high levels of Co-Channel Interference (CCI) and Adjacent Channel Interference (ACI) emanating from existing PAL/SECAM/NTSC services. Another requirement is that the System shall allow the maximum spectrum efficiency when used within the VHF and UHF bands; this requirement can be achieved by utilizing Single Frequency Network (SFN) operation.

To achieve these requirements an OFDM system with LDPC error correcting coding is being specified. To maximize commonality with the Satellite baseline specification (see *EN 302 307* [7]) and Cable baseline specifications (see DVB-C2 *BlueBook* [12]) the outer coding and outer interleaving are common, and the inner coding is common with the Satellite baseline specification. To allow optimal trade off between network topology and frequency efficiency, a flexible guard interval is specified. This will enable the system to support different network configurations, such as large area SFN and single transmitter, while keeping maximum frequency efficiency.

The system also allows different levels of QAM modulation and different encoding rates used to trade bit rate versus ruggedness. In this case the functional block diagram of the system shall be expanded to include the modules shown dashed in figure **(Fig. 2.1)**.

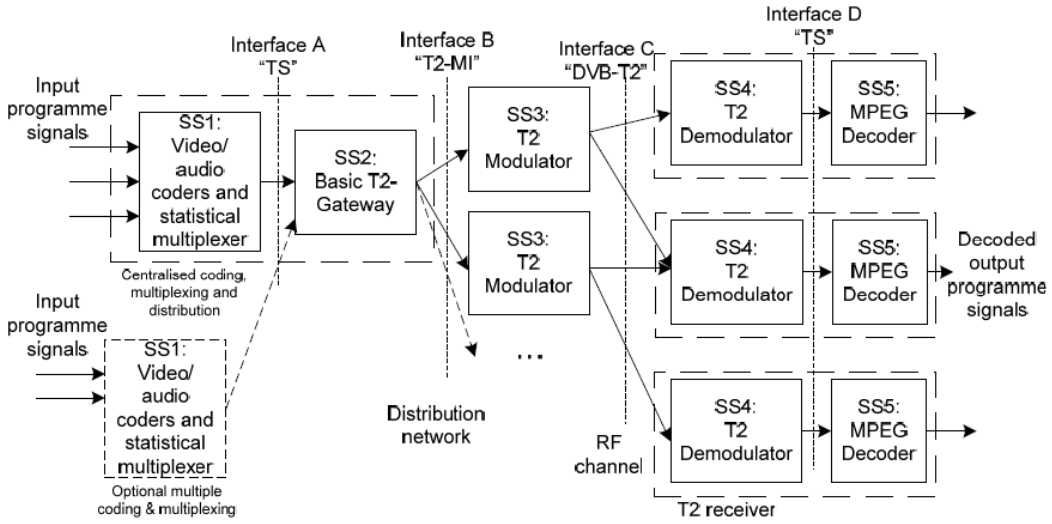

Fig. 2.1: Functional block diagram of the system

The full DVB-T2 system can be divided into three basic sub-systems on the network side (SS1, SS2 and SS3) and two subsystems on the receiver side (SS4 and SS5). Regarding interfaces, there are two corresponding interfaces on the network side (A and B), and one receiver-internal interface (D). The RF interface (C) is common to network and receiver.

On the network side the three sub-systems are:

- **SS1: Coding and multiplexing** sub-system. This includes generation of MPEG-2 Transport Streams and/or Generic Streams, e.g. GSE. For video services this includes video/audio encoding plus associated PSI/SI, or other Layer 2 signalling. Typically the video coding (and possibly audio coding) is performed with variable bitrates with a common control ensuring a total constant bit rate (excluding NULL packets) for all streams taken together. This subsystem is largely the same as for other DVB standards, but there are some T2-specific aspects of the coding and multiplexing, which are also discussed in *Chapter 3*. The coding and multiplexing sub-system interfaces to the T2-Gateway via the A interface (typically one or more MPEG-2 TSs over ASI). When DVB-T2 uses the common PLP this sub-system is responsible for the arrangement of the output TSs in line with the requirements. When a conventional statmux system, originally generating single TS, is used in connection with multiple PLPs carrying one TS each, this sub-system will also include some remultiplexing functionality such as PSI/SI handling and PCR restamping.

- **SS2: Basic T2-Gateway** sub-system. The input interface to this sub-system is exactly the same as that specified, applicable both to the basic DVB-T2 physical layer and to the extension. This includes functionality for Mode

adaptation and Stream adaptation for DVB-T2, together with scheduling and capacity allocation. The Basic T2-Gateway delivers at its output interface (B) a “T2-MI” stream: a sequence of T2-MI packets, each containing either a Baseband frame, IQ vector data for any auxiliary streams, or signalling information (L1 or SFN). The T2-MI stream contains all the information required to describe both the content and emission timing of T2-frames, and a single T2-MI stream is fed to one or more modulators in a network.

The operations performed by the Basic T2-Gateway include all those parts of the physical-layer specification that are not completely prescriptive, such as scheduling and allocation. These need to be done centrally in an SFN, to ensure that the same signal is generated by all modulators.

- **SS3: DVB-T2 Modulator** sub-system. The DVB-T2 modulators use the Baseband frames and T2-frame assembly instructions carried in the incoming T2-MI stream to create DVB-T2 frames and emit them at the appropriate time for correct SFN synchronisation. The modulators interface to the receivers via the C interfaces (the transmitted DVB-T2 signal).

In the receiver the two sub-systems are:

- **SS4: DVB-T2 demodulator** sub-system. This sub-system receives an RF signal from one or (in an SFN) more transmitters in the network and (in the transport-stream case) outputs one transport stream. SS4 interfaces to SS5 via the D interface, a syntactically correct transport stream carrying one or more of the services as well as any common signalling data derived from the common PLP. The streams passing the B interface are identical to those passing the D interface.

- **SS5: Stream decoder** sub-system. This sub-system receives the transport stream and outputs decoded video and audio. Since interface D is a syntactically correct transport stream, this sub-system is essentially the same as for other DVB standards, except that some new L2-signalling elements have been defined for DVB-T2.

2.3 Channel models

The standard *ETSI 300 744* [9] estimates three different scenarios at the reception of the DVB-T TV signals, the reception from a Gaussian channel (AWGN), the reception from a Ricean (F1) channel, and the reception through a Rayleigh (P1) channel. In addition to these well-known channels from DVB-T, some other channels have been added, some specific to DVB-T2. The channels have been chosen to verify the performance in a wide range of reception conditions including fixed, portable, mobile and even SFN and MISO. These

new channels are: TU-6 channel, Simple Two Path profile and Memoryless Rayleigh Channel with erasures.

These models have been used in our system using the channel models described at FURIA-PSE documentation, DVB Bluebook and ETSI 300 744. A deeply description of their characteristics is performed in the following paragraphs.

2.3.1 Gaussian channel

The first implemented channel to test the simulation platform was the Gaussian channel. In this channel model only white Gaussian noise (AWGN) is added to the signal, and there is only one path.

2.3.2 F1 and P1 channels

The two channel models for fixed reception F1 and portable reception P1 have been generated from the following equations where x(t) and y(t) are input and output signals respectively:

- Fixed reception F1:

$$y(t) = \frac{\rho_0 x(t) + \sum_{i=1}^{N} \rho_i e^{-j\theta_i} x(t-\tau_i)}{\sqrt{\sum_{i=0}^{N} \rho_i^{\,2}}} \qquad \textbf{(2.1)}$$

Where:

- the first term before the sum represents the line of sight ray;
- N is the number of echoes equals to 20;
- θ_i is the phase shift from scattering of the i'th path - listed in table **(Table 2.2)**;
- ρ_i is the attenuation of the i'th path - listed in table **(Table 2.2)**;
- τ_i is the relative delay of the i'th path - listed in table **(Table 2.2)**;

The Ricean factor K (the ratio of the power of the direct path (the line of sight ray) to the reflected paths) is given as:

$$K = \frac{\rho_0^2}{\sum_{i=1}^{N} \rho_i^2} \qquad \textbf{(2.2)}$$

In the simulations a Ricean factor K = 10 dB has been used. In this case:

$$\rho_o = \sqrt{10 \sum_{i=1}^{N} \rho_i^2} \qquad \textbf{(2.3)}$$

- Portable reception, Rayleigh fading (P1):

$$y(t) = k \sum_{i=1}^{N} \rho_i e^{-j\theta_i} x(t-\tau_i) \quad \text{where} \quad k = \frac{1}{\sqrt{\sum_{i=1}^{N} \rho_i^2}} \qquad \textbf{(2.4)}$$

θ_i, ρ_i and τ_i are given in table **(Table 2.2)**.

Table 2.2: Amplitudes, delays and phases to the multipath components of the radio channel to DVB-T

Table Attenuation, Phase and Delay Values for F1 and P1			
i	**ρ_i**	**ζ_i[us]**	**σ_i[rad]**
1	0.057662	1.003019	4.855121
2	0.176809	5.422091	3.419109
3	0.407163	0.518650	5.864470
4	0.303585	2.751772	2.215894
5	0.258782	0.602895	3.758058
6	0.061831	1.016585	5.430202
7	0.150340	0.143556	3.952093
8	0.051534	0.153832	1.093586
9	0.185074	3.324866	5.775198
10	0.400967	1.935570	0.154459
11	0.295723	0.429948	5.928383
12	0.350825	3.228872	3.053023
13	0.262909	0.848831	0.628578
14	0.225894	0.073883	2.128544
15	0.170996	0.203952	1.099463
16	0.149723	0.194207	3.462951

17	0.240140	0.924450	3.664773
18	0.116587	1.381320	2.833799
19	0.221155	0.640512	3.334290
20	0.259730	1.368671	0.393889

2.3.3 TU6 model

In 1989, the EU-COST207 project (1984–1988) deeply studied channel propagation models to be used for mobile communications. The Typical Urban 6-paths model (TU6) depicted in **Table 2.3** [10] proven to be representative for the typical mobile reception with Doppler frequency above 10 Hz. Assessment of mobile reception performance requires setting up a reproducible environment. The TU6 has been heavily used both for simulation and for laboratory test (using a channel simulator), and results from numerous field trials highly correlate with the obtained results. Nevertheless, concerns remain in regard to the TU6 suitability for reception with Doppler frequency below 10 Hz (i.e., the pedestrian and indoor reception) suggesting further modelling work.

Table 2.3: Proposed TU6 channel model for mobile communications

Tap Number	Delay (μs)	Power (lin)	Power (dB)	Doppler Spectrum
1	0,0	0,5	-3,0	Rayleigh
2	0,2	1,0	0,0	Rayleigh
3	0,5	0,63	-2,0	Rayleigh
4	1,6	0,25	-6,0	Rayleigh
5	2,3	0,16	-8,0	Rayleigh
6	5,0	0,1	-10,0	Rayleigh

2.3.4 Simple Two Path profile

This profile only includes two paths. Each path, '*i*', is defined by α_i, τ_i, Δ_{fi} which denote the amplitude, delay and frequency shift of the particular path '*i*', respectively. The profile parameters are given in **Table 2.4**:

Table 2.4: 0dB Echo profile

i	α_i (dB)	τ_i (μs)	Δ_{fi} (Hz)
1	0	0	0
2	0	0.9 Δ	1

The parameter 'Δ' denotes the guard interval duration in μs.

2.3.5 Memoryless Rayleigh Channel with erasures

This channel model is used to simulate the behaviour of the BICM module of DVB-T2 system over terrestrial multipath channels. The principle of this channel consists in modelling the concatenation of the frame builder, OFDM generator, wireless channel, OFDM demodulator and frame extraction as an equivalent flat fading channel. Furthermore, this channel models an OFDM-based system with perfect frequency interleaving over a multipath channel providing arbitrary probability of carrier erasures. The equivalent flat-fading coefficient *h* is modelled as a Rayleigh process concatenated with random erasures of probability *R*. **Fig. 2.2** depicts how to simulate this equivalent channel.

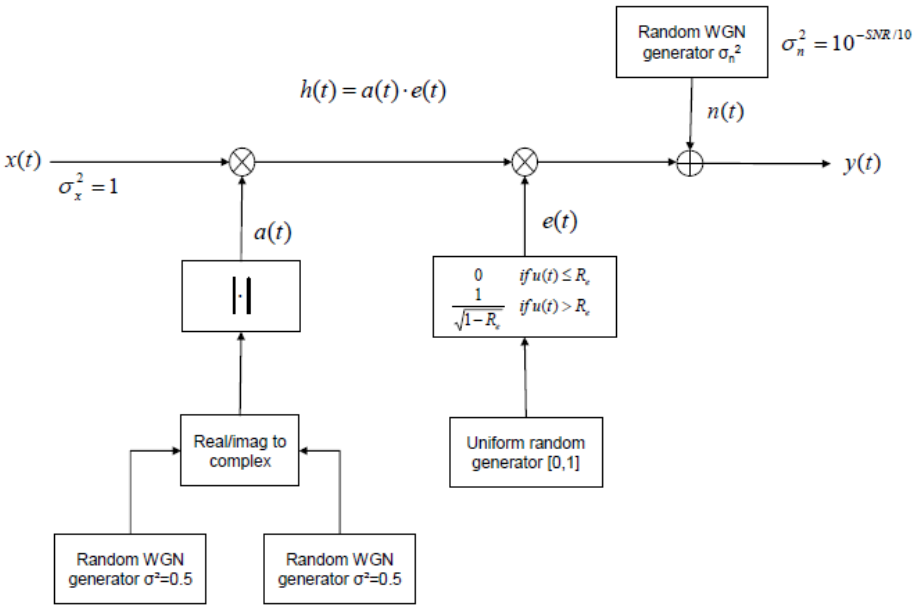

Fig. 2.2: Memoryless Rayleigh Channel with erasures

2.4 C/N calculation for DVB-T2 Simulator

In this section the type of algorithm used for the Carrier to Noise ratio calculation used in the simulator platform is explained.

For this process it has been supposed that there aren't pilots inside of each OFDM symbol, that is, all the sub carriers are data transporters (use of OFDM training symbols). So first of all the C/N relationship from the $\frac{Eb}{N_0}_{data\ carrier}$ function **(4.5)** is calculated as:

$$\frac{Eb}{N_0}_{data\ carrier} = \frac{\overline{s^2(t)} \cdot T_b \cdot \frac{1}{N_c}}{N_0} = \frac{\frac{N_c}{2} \cdot T_b \cdot \frac{1}{N_c}}{\sigma^2 T_m} = \frac{\frac{N_c}{2} \cdot \frac{T_c}{\log_2 M} \cdot \frac{1}{N_c}}{\sigma^2 \frac{T_c}{N_t}} = \frac{N_T}{2\sigma^2 \log_2 M} \qquad \textbf{(4.5)}$$

Where N_0 is noise power, E bit energy, Nc is the sub carrier number, N_T total number of carriers, T_b and T_c are bit and sub carrier duration and σ^2 is the noise spectral density. Now the $\frac{C}{N}_{Total}$ **(4.6)** ratio can be calculated as:

$$\frac{C}{N}_{Total} = \frac{\overline{s^2(t)}}{N_0 \frac{N}{T}} = \frac{\frac{N_u}{2} T}{N_0 N_T} = \frac{N_u T}{2\sigma^2 T_m N_T} = \frac{N_u T}{2\sigma^2 \frac{T}{N_T} N_T} = \frac{N_u}{2\sigma^2} \quad \textbf{(4.6)}$$

Where $N_u = N_c + (1.3)^2 N_{pilot}$ for all the modes.

To make the calculation **(4.7)**, the average signals power should be unitary in the time domain. Knowing that the average received power in the time domain is $C_{rx} = \frac{N_u}{N_T}$, it is needed to normalize it with $f_{norm} = \frac{N_T}{N_u}$, so finally:

$$N_0 = \frac{c_{rx} f_{norm}}{\frac{Nu}{N_T} \frac{Eb}{N_0} \log_2 M} = \frac{c_{rx} \frac{N_T}{N_u}}{\frac{Nu}{N_T} \frac{Eb}{N_0} \log_2 M} = \frac{1}{\frac{Nu}{N_T} \frac{Eb}{N_0} \log_2 M} \quad \textbf{(4.7)}$$

2.5 Election of the simulation platform

It exists an extensive fan of proposals for the improvement of the different subsystems from the transmitter/receiver chain inside the FURIA council. However, the objective of is this work during that project was not to make a unique simulator product to integrate the efforts of participants members. The final objective was to offer a technical debate forum where the different strategies brought to the project could be analyzed and compared. Whatever is well known that one of the principal problems found by the expert forums and the standardization institutions is that frequently is very difficult to compare lending, when details of the simulation parameters and the platforms are different. Trying to reduce this dispersion, the decision of improve simulations with Matlab was taken, tool that makes close module tests easier (without the code) in the different simulators brought by the participants.

Despite of Matlab (Simullink, Communications ToolBox etc.) counts with complete simulators of DVB-T with accessibility to the different blocks, most of them have been programmed. That decision is done looking for a better control to the system, improving the simulator execution velocity.

The designed DVB-T2 block scheme is shown in the figure below **(Fig. 2.3)**.

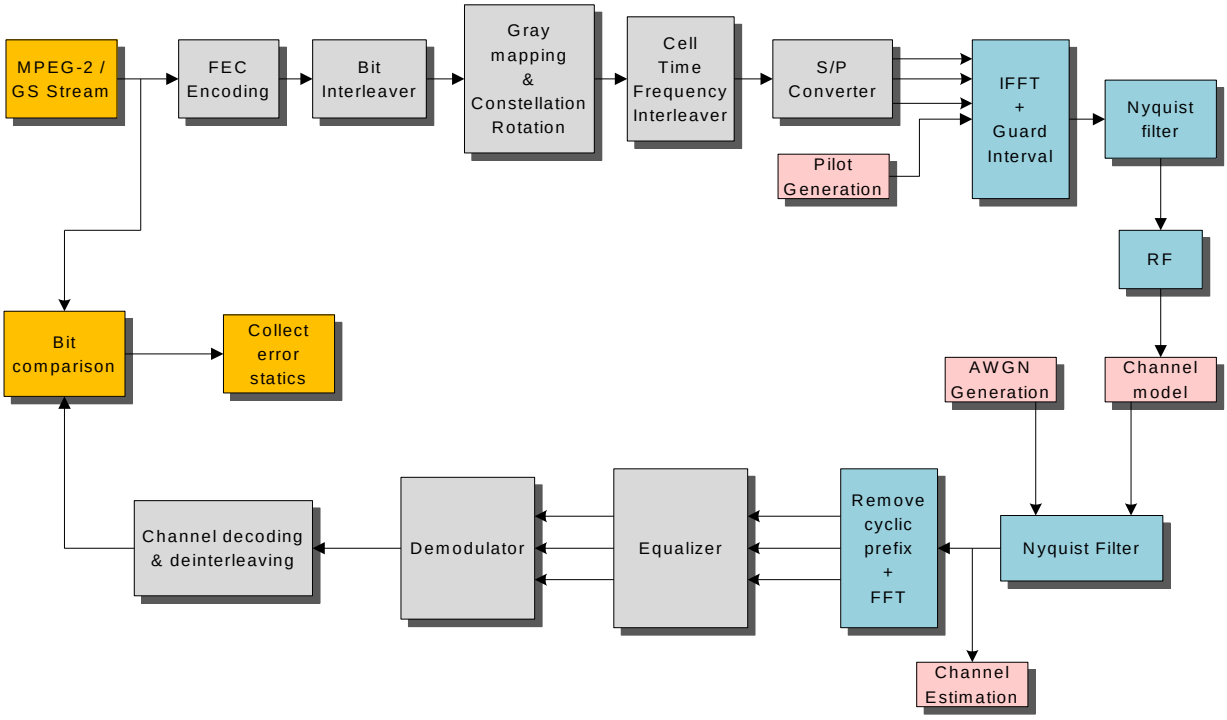

Fig. 2.3: TX/RX chain DVB-T2 system scheme

The simulator is designed to make possible changes in anyone of its blocks. These changes will be made with the minimum effort of programmation possible, due to their scalability and modularity.

In that way, at least all the codifiers and decodifiers, the type and depth of the interleavers, the modulators, the bit assignations mechanisms to the carriers, the carriers potency assignation, the pilot structure and the equalizing channel mechanisms will be reconfigurable, as well as all the variable parameters defined in the DVB-T2 bluebook.

CHAPTER 3: DVB-T2 TRANSMITTER ARCHITECTURE

The architecture of the DVB-T2 transmitter system is composed by five main blocks described during the next Sections. Figure below **(Fig 3.1)** shows the block diagram of the whole transmitter system. Along the chapter the details of the different blocks of the transmission chain will be depicted.

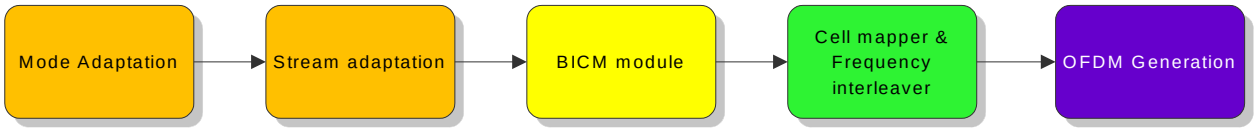

Fig. 3.1: High level block diagram of the DVB-T2 transmitter system

The input(s) of the system is one or more MPEG-2 Transport Stream(s) and/or one or more Generic Stream(s). The Input Pre-Processor, which is not part of the T2 system, is the element used for separating the services into the T2 system inputs, which are one or more logical data streams. In that case the Physical Layer Pipes (PLPs) are where the logical data streams are carried.

The input data streams shall be constant and shall not exceed the T2 available capacity of a physical layer frame for the current frame parameters. This will be achieved by putting into groups the PLPs that use the same modulation, coding, interleaving depth, constant bit-rate, statistically-multiplexed source. That group PLP may contain a common PLP, however if the T2 signal carries a single PLP no common PLP is transmitted. Generally a group of statically multiplexed services can use variable coding and modulation for different services generating a constant total output capacity.

In that chapter, a deeply explanation of the three first modules is realized. Especially analysing the BICM module, the stage with more sub-blocks in the transmitter system, and which is divided in six main parts; the FEC Encoding and the bit interleaving block, the Mapping and Constellation stage, the constellation rotation block and the cell and time interleavers.

On the other hand, a complete description of the functions and stages developed in the simulation platform are included in the depiction of each block.

3.1 Input processing

The input to the T2 system shall consist of one or more logical data streams. One logical data stream is carried by one Physical Layer Pipe (PLP). The mode adaptation modules, which operate separately on the contents of each PLP, slice the input data stream into data fields which, after stream adaptation, will form baseband frames (BB frames).

Each input PLP may take one of the following formats:

- Transport Stream (TS);
- Generic Encapsulated Stream (GSE);
- Generic Continuous Stream (GCS) (a variable length packet stream where the modulator is not aware of the packet boundaries);
- Generic Fixed-length Packetized Stream (GFPS); this form is retained for compatibility with DVB-S2 [7], but it is expected that GSE would now be used instead.

A Transport Stream shall be characterized by User Packets (UP) of fixed length O-UPL = 188 $\times$ 8 bits (one MPEG packet), the first byte being a Sync-byte (47_{HEX}). It shall be signalled in the base-band header TS/GS field.

A GSE stream shall be characterized by variable length packets or constant length packets, as signalled within GSE packet headers, and shall be signalled in the Base-band Header by TS/GS field.

A GCS shall be characterized by a continuous bit-stream and shall be signalled in the base-band header by TS/GS field and UPL = 0_D. A variable length packet stream where the modulator is not aware of the packet boundaries, or a constant length packet stream exceeding 64 Kbit, shall be treated as a GCS, and shall be signalled in the base-band header by TS/GS field as a GCS and UPL = 0_D.

A GFPS shall be a stream of constant-length User Packets (UP), with length O-UPL bits (maximum O-UPL value 64 K). O-UPL is the Original User Packet Length; UPL is the transmitted User Packet Length, as signalled in the baseband header. It shall be signalled in the base-band header TS/GS field.

3.1.2 Input interface

The input interface subsystem shall map the input into internal logical-bit format. The first received bit will be indicated as the Most Significant Bit (MSB). The Input Interface shall read a data field, composed of DFL bits (Data Field Length), where:

$$0 < DFL < (K_{BCH} - 80) \quad \textbf{(3.1)}$$

Where K_{bch} is the number of bits protected by the BCH and LDPC codes **(3.1** equation**)**.

The maximum value of DFL depends on the chosen LDPC code, carrying a protected payload of K_{bch} bits. The 10-byte (80 bits) base-band header is appended to the front of the data field, and is also protected by the BCH and LDPC codes.

The Input Interface shall either allocate a number of input bits equal to the available data field capacity, thus breaking Ups in subsequent data fields (this

operation being called “fragmentation”), or shall allocate an integer number of Ups within the data field (no fragmentation). A padding field, if applicable, shall also be allocated in the first BB-Frame of a T2-Frame, to transmit in-band signalling whether fragmentation is used or not.

3.2 Stream adaptation

The stream adaptation block is the next stage of the input processing block inside the transmission chain (see **Fig. 3.1**). This block provides:

- Scheduling.
- Padding to complete a constant length (*K*bch bits) BBFRAME and/or to carry in-band signalling.
- Scrambling for energy dispersal.

The input stream to the stream adaptation module shall be a BBHEADER followed by a DATA FIELD. The output stream shall be a BBFRAME, as shown in figure **(Fig. 3.2)**.

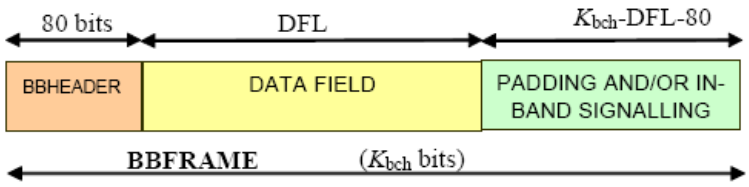

Fig. 3.2: BBFRAME format at the output of the STREAM ADAPTER

3.2.1 Scheduling

In order to generate the required L1 dynamic signalling information, the scheduler must decide exactly which cells of the final T2 signal will carry data belonging to which PLPs. Although this operation has no effect on the data stream itself at this stage, the scheduler shall define the exact composition of the frame structure.

3.2.2 Padding

Padding may be applied in circumstances when the user data available for transmission is not sufficient to completely fill a BBFRAME, or when an integer number of Ups has to be allocated in a BBFRAME. (K_{bch}-DFL-80) zero bits shall be appended after the DATA FIELD. The resulting BBFRAME shall have a constant length of *K*bch bits.

3.2.3 BB scrambler

The complete BBFRAME shall be randomized. The randomization sequence shall be synchronous with the BBFRAME, starting from the MSB and ending after *K*bch bits. The scrambling sequence shall be generated by the feed-back shift register of **Figure 3.3**. The polynomial for the Pseudo Random Binary Sequence (PRBS) generator shall be **(3.2)**:

$$1 + X^{14} + X^{15} \qquad \textbf{(3.2)}$$

Loading of the sequence (100101010000000) into the PRBS register, as indicated in Figure **(Fig. 3.3)**, shall be initiated at the start of every BBFRAME.

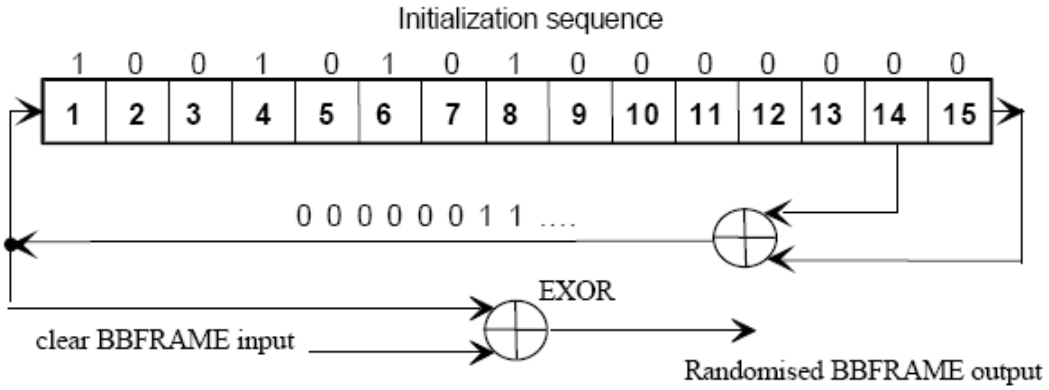

Fig. 3.3: PRBS implementation

For reasons of simulation efficiency, the input data of the simulation system is generated as random information bits grouped in TS blocks, without taking into account other input encapsulations or streams forms, and modelling the L1 signalling information as randomized bits in order to avoid possible complications in the simulator. Despite of that fact, the simulation platform is created in order to accomplish all the details of the standard specifications, opened to future revisions and extensions.

3.2.4 Designed functions for Stream Adaptation

- **gen_entrada:**

This function generates the random sequence input from *Matlab* library functions *randint*. *Randint* function generates a uniform distribution of pseudo randomly binary information. This function calculates the length of the data field needed depending on the selected codification mode, taking into account the 80 bits of signalling parameters and including the synchronism word each Transport Stream Packet (188 bytes).

- Input parameters:
  - Kbch: length of the elected BCH codification block.
- Output parameters:
  - fich: vector of Kbch length with pseudo-randomly data, including the synchronism words each TS.

❖ **gen_TSBCH:**

The main goal of this function is to apply the energy dispersal function described in *Section 3.2.*3 in order to provide the correct energy distribution of the data fields.

That objective is arranged in one iteration cycle employing the *xor (x,y)* function defined in *Matlab* library and taking profit of the matrix operation allowed in the *Matlab* environments.

- Input Parameters:
  - in: Kbch data vector.

- Output Parameters:
  - fich: Kbch randomized data vector, with the energy dispersion performed.

3.3 BICM Module

In this section a description of the different blocks composing the BICM module is performed. Figure below **(Fig. 3.4)** shows the different blocks that must be implemented in the transmission chain

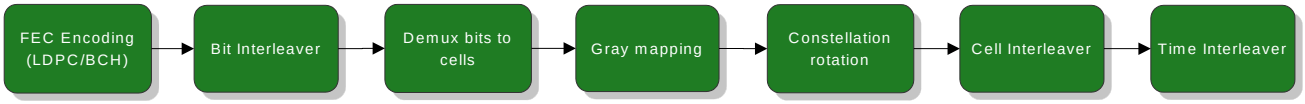

Fig. 3.4: BICM module block diagram

3.3.1 FEC Encoding

The FEC coding block consists in an outer coding (BCH), inner coding (LDPC) and a bit interleaving. The input of the block consists in BBFRAMEs (K_{bch} bits) and the output in FECFRAMEs (K_{ldpc} bits). In the figure below **(Fig. 3.5)** the depiction of a FECFRAME before bit interleaving is shown.

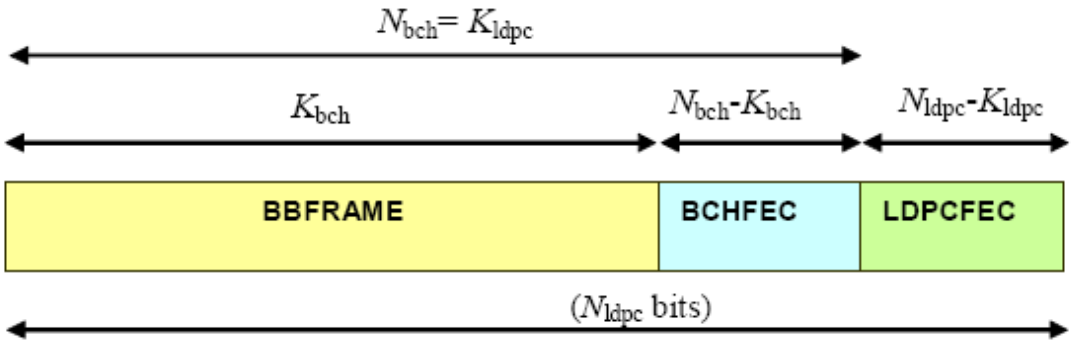

Fig. 3.5: Data format before bit interleaving

The FEC coding parameters for the normal FECFRAME (N_{ldpc} = 64800 bits) and for the short FECFRAME (N_{ldpc} = 16200 bits) are shown in **Table 3.1** and **Table 3.2**.

Table 3.1: Coding parameters for the normal FECFRAME (N_{ldpc} = 64800 bits).

LDPC Code	BCH Uncoded Block K_{bch}	BCH Coded Block N_{bch} LDPC Uncoded Block K_{ldpc}	BCH t-error correction	N_{bch} - K_{bch}	LDPC Coded Block N_{ldpc}
1/2	32 208	32 400	12	192	64 800
3/5	38 688	38 880	12	192	64 800
2/3	43 040	43 200	10	160	64 800
3/4	48 408	48 600	12	192	64 800
4/5	51 648	51 840	12	192	64 800
5/6	53 840	54 000	10	160	64 800

Table 3.2: Coding parameters for the short FECFRAME (N_{ldpc} = 16200 bits).

LDPC Code Identifier	BCH Uncoded Block K_{bch}	BCH Coded Block N_{bch} LDPC Uncoded Block K_{ldpc}	BCH t-error correction	N_{bch} - K_{bch}	LDPC Coded Block N_{ldpc}
1/4*	3 072	3 240	12	168	16 200
1/2	7 032	7 200	12	168	16 200
3/5	9 552	9 720	12	168	16 200
2/3	10 632	10 800	12	168	16 200
3/4	11 712	11 880	12	168	16 200
4/5	12 432	12 600	12	168	16 200
5/6	13 152	13 320	12	168	16 200
*NOTE: This code rate is only used for protection of L1 pre-signalling and not for data					

3.3.1.1 Designed functions for FEC Encoding

❖ codif_BCH:

That functions provides the BCH codification stage. First of all, it is mandatory to define the zero padding applied to the input data vector depending to the correction capacity of the BCH employed (t=10 or t=12), and on the code rate selected in the system (see **Table 3.1** and **Table 3.2**).

Once the padded data vector is performed, the function converts the data vector into *Galois Fields* for the codification in the BCH stage. To implement the BCH coder, the *Matlab* defined function *bchenc(msg,n,k)* is used, specifying the selected code rate. The last stage of the function is to re-convert the coded data vector from *Galois Fields* to binary information in order to affront the LDPC stage. The whole process is depicted in the following flux diagram **(Fig. 3.6)**.

Flux diagram key to icons

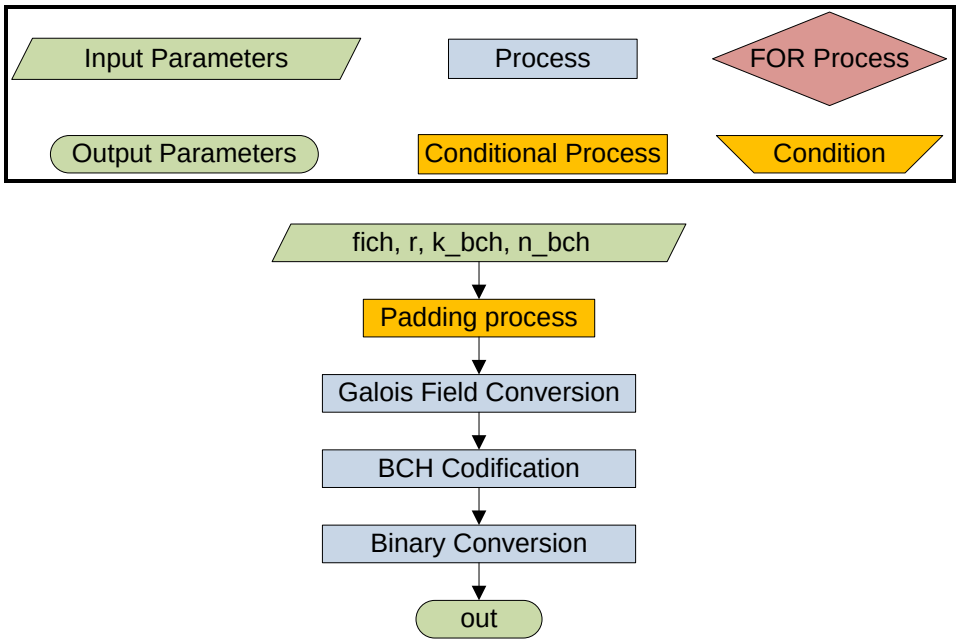

Fig. 3.6: Flux Diagram *codif_BCH*

- Input Parameters:
  - fich: Kbch data vector.
  - r: Code Rate.
  - k_bch: BCH input length.
  - n_bch: BCH output length.
- Output Parameters:
  - out: n_bch coded data vector.

❖ **LDPC_coder:**

The main goal of this function is to apply the LDPC codification to the BCH coded data stream. For that purpose, the designed functions are the LPDC codification stage used in DVB-S2 [7], and defined in *Matlab*. The LDPC stage is common in both standards, using a 16200 or a 64800 bit length output code.

The first step is to create the low density parity check matrix of the LDPC code with the code rate *r* (*H = dvbs2ldpc(r)*). Once the parity check matrix is created following the code length, the LDPC coder object is created with the corresponding *Matlab* module (*I = fec.ldpcenc(H)*). At last, the information bits are coded and the result is a data vector of the selected length (16200 or 64800 bits) **(**see **Fig. 3.7)**.

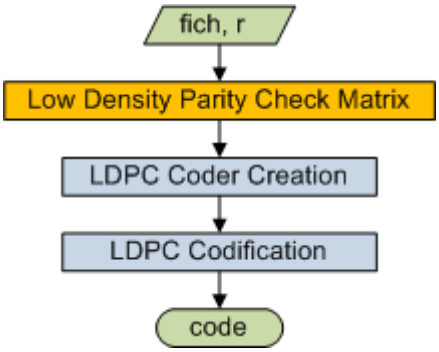

Fig. 3.7: Flux Diagram *LDPC_coder*

- Input Parameters:
  - fich: Nbch data vector.
  - r: Code Rate.
- Output Parameters:
  - code: n_ldpc coded data vector.

3.3.2 Bit Interleaver (for 16-QAM, 64-QAM and 256-QAM)

The output of the LDPC bit interleaving consists in a parity interleaving followed by a twist column interleaving, and it's only applied for 16-QAM, 64-QAM and 256 QAM modulations, in the case of the QPSK modulation, the bit interleaving stage is not performed.

The parity bits are interleaved in the first part by **(3.3)**:

$$u_i = \lambda_i \; for \; 0 \le i < K_{ldpc} \; (information \; bits \; are \; not \; interleaved)$$
$$u_{K_{ldpc}+360t+s} = \lambda_{K_{ldpc}+Q_{ldpc} \cdot s+t} \quad for \; 0 \le s < 360, 0 \le t < Q_{ldpc} \qquad \textbf{(3.3)}$$

Where:
Q_{ldpc} is defined in **Table 3.3a**
λ is the output of LDPC encoder
U is the output of the parity interleaver

Table 3.3a and **Table 3.3b** show the bit interleaving structure for each modulation format.

Table 3.3a: Q_{ldpc} values for short frames

Code Rate	Q_{ldpc} Normal Frames	Q_{ldpc} Short Frames
1/4	-	36
1/2	90	25
3/5	72	18
2/3	60	15
3/4	45	12
4/5	36	10
5/6	30	8

Table 3.3b: Bit Interleaver parameters

Modulation	Rows N_r		Columns N_c
	N_{ldpc} = 64 800	N_{ldpc} = 16 200	
16-QAM	8 100	2 025	8
64-QAM	5 400	1 350	12
256-QAM	4 050	-	16
	-	2 025	8

The output data bits from the parity interleaver are serially written into the column-twist interleaver corresponding column and serially read out row-wise as can be seen in **Fig. 3.8**.

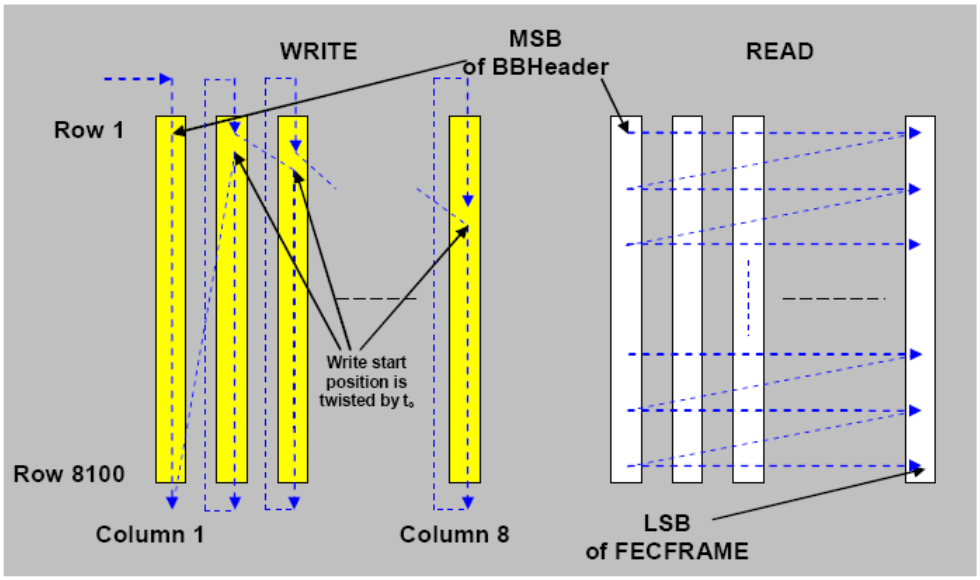

Fig. 3.8: Bit interleaving scheme for normal FECFRAME and 16-QAM

In that case, the write start position of each column is twisted by t_c according the table below **(Table 3.4)**.

Table 3.4: Column twisting parameter t_c

Modulation	Columns N_c	N_{ldpc}	Twisting parameter t_c														
			0	1	2	3	4	5	6	7	8	9	10	11	12	13	14	15
16-QAM	8	64 800	0	0	2	4	4	5	7	7	-	-	-	-	-	-	-	-
		16 200	0	0	0	1	7	20	20	21	-	-	-	-	-	-	-	-
64-QAM	12	64 800	0	0	2	2	3	4	4	5	5	7	8	9	-	-	-	-
		16 200	0	0	0	2	2	2	3	3	3	6	7	7	-	-	-	-
256-QAM	16	64 800	0	2	2	2	2	3	7	15	16	20	22	22	27	27	28	32
	8	16 200	0	0	0	1	7	20	20	21	-	-	-	-	-	-	-	-

3.3.2.1 Designed functions for Bit Interleaving

❖ out_interleaver:

The bit interleaver is the first interleaving stage in the transmitter block (without taking into account the energy dispersal block). That function is divided in three main blocks **(Fig. 3.9)**.

In the first one, the variables of the interleaver are defined, including the number of columns and rows of each combination, as well as the Q_{ldpc} factor defined above and the twisting parameter. Secondly, the parity interleaving is performed, followed by the twist column interleaver.

For the last stage, the twist column interleaver is efficiently programmed using the *reshape* function defined by *Matlab*. That function allows restructuring the size of the columns and rows of a matrix, and can be perfectly adapted to the matrix based interleavers.

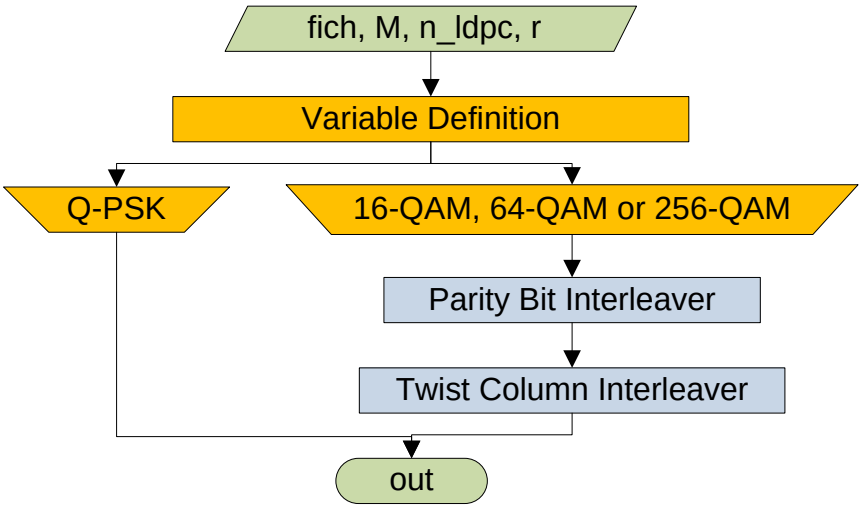

Fig. 3.9: Flux Diagram *out_interleaver*

- Input Parameters:
  - fich: Nldpc data vector.
  - M: modulation order.
  - n_bch: BCH block length.
  - r: Code Rate.
- Output Parameters:
  - out: Nldpc interleaved data vector.

3.3.3 Mapping and Constellation

The interleaved FECFRAMES (64.800 bits for normal FECFRAME or 16.200 bits for short FECFRAME) are mapped to a coded FEC block. The first step is to de-multiplex the input bits into parallel cell words and then mapping these cell words into constellation values. **Table 3.5** defines the number of output data cells and the effective number of bits per cell (η_{MOD}).

Table 3.5: Mapping parameters

LDPC block length (N_{ldpc})	Modulation Mode	η_{MOD}	Number of output data cells
64 800	256-QAM	8	8 100
	64-QAM	6	10 800
	16-QAM	4	16 200
	QPSK	2	32 400
16 200	256-QAM	8	2 025
	64-QAM	6	2 700
	16-QAM	4	4 050
	QPSK	2	8 100

3.3.3.1 Bit to cell word de-multiplexer

The output bit-stream from the bit interleaver is de-multiplexed into $N_{substreams}$ sub-streams **(**see **Fig. 3.10)**. Value of $N_{substreams}$ changes depending on the modulation as can be seen in **Table 3.6**.

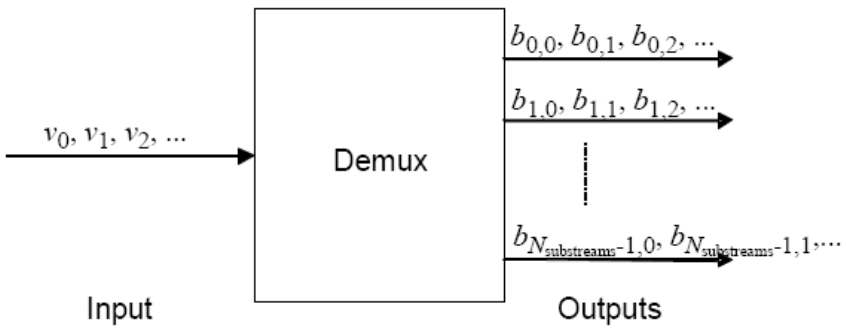

Fig. 3.10: De-multiplexing bits into sub-streams

Table 3.6: Number of sub-streams in de-multiplexer

Modulation	N_{ldpc}	Number of sub-streams, $N_{substreams}$
QPSK	Any	2
16-QAM	Any	8
64-QAM	Any	12
256-QAM	64 800	16
	16 200	8

Once formed the sub-streams, the cell words are formed interleaving the bits for each sub-streams. **Table 3.7** shows the parameters for de-multiplexing of bits to sub-streams for all code rates excluding rate 3/5. On the same way **Table 3.8** shows the parameters for rate 3/5 only.

Table 3.7: Parameters for de-multiplexing of bits to sub-streams for all code rates excluding rate 3/5

Modulation Format	QPSK															
Input bit-number, d_i mod $N_{substreams}$	0	1														
Output bit-number, e	0	1														
Modulation Format	16-QAM															
Input bit-number, d_i mod $N_{substreams}$	0		1		2		3		4		5		6		7	
Output bit-number, e	7		1		4		2		5		3		6		0	
Modulation Format	64-QAM															
Input bit-number, d_i mod $N_{substreams}$	0	1	2	3	4	5	6	7	8	9	10	11				
Output bit-number, e	11	7	3	10	6	2	9	5	1	8	4	0				
Modulation Format	256-QAM (Nldpc = 64800)															
Input bit-number, d_i mod $N_{substreams}$	0	1	2	3	4	5	6	7	8	9	10	11	12	13	14	15
Output bit-number, e	15	1	13	3	8	11	9	5	10	6	4	7	12	2	14	0
Modulation Format	256-QAM (Nldpc = 64800)															
Input bit-number, d_i mod $N_{substreams}$	0		1		2		3		4		5		6		7	
Output bit-number, e	7		3		1		5		2		6		4		0	

Table 3.8: Parameters for de-multiplexing of bits to sub-streams for rate 3/5 only

Modulation Format	QPSK															
Input bit-number, d_i mod $N_{substreams}$	0	1														
Output bit-number, e	0	1														
Modulation Format	16-QAM															
Input bit-number, d_i mod $N_{substreams}$	0	1	2	3	4	5	6	7								
Output bit-number, e	0	5	1	2	4	7	3	6								
Modulation Format	64-QAM															
Input bit-number, d_i mod $N_{substreams}$	0	1	2	3	4	5	6	7	8	9	10	11				
Output bit-number, e	2	7	6	9	0	3	1	8	4	11	5	10				
Modulation Format	256-QAM (Nldpc = 64800)															
Input bit-number, d_i mod $N_{substreams}$	0	1	2	3	4	5	6	7	8	9	10	11	12	13	14	15
Output bit-number, e	2	11	3	4	0	9	1	8	10	13	7	14	6	15	5	12
Modulation Format	256-QAM (Nldpc = 64800)															
Input bit-number, d_i mod $N_{substreams}$	0	1	2	3	4	5	6	7								
Output bit-number, e	7	3	1	5	2	6	4	0								

3.3.3.2 I/Q Constellations

Each cell word from the demultiplexer is modulated using QPSK, 16-QAM, 64-QAM or 256-QAM constellations to give a constellation point. Normalization is due after the constellation creation.

The L1 signalling is mapped with a BPSK constellation. The following table **(Table 3.9)** shows the normalization factor applied to each constellation point for each input cell word depending of the used modulation to obtain the correct complex cell value to be used.

Table 3.9: Normalization factors for each modulation

Modulation	Normalization	Modulation	Normalization
BPSK	$f_q = z_q$	64-QAM	$f_q = \frac{z_q}{\sqrt{42}}$
QPSK	$f_q = \frac{z_q}{\sqrt{2}}$	256-QAM	$f_q = \frac{z_q}{\sqrt{170}}$
16-QAM	$f_q = \frac{z_q}{\sqrt{10}}$		

3.3.3.3 Designed functions for Mapping and Constellation

❖ bit2cell:

The bit2cell function is one of the most complete functions developed for the simulator platform. It is divided in four main parts **(Fig. 3.11)**.

First of all, as in the previous functions, variable definitions depending on the selected simulator conditions are defined in order to optimize the platform efficiency.

Secondly, the demultiplexer architecture is realized taking into account the code rate selected due to their different behaviours specified in *Section 3.3.3.1*. The *Matlab* matrix capabilities have been very useful to achieve a clean programmed function avoiding boucles in that stage.

The third stage is to convert the output of the demultiplexer into a decimal vector for their immediately constellation symbol conversion. Due to that fact, a simple function is designed to convert the binary data stream into a base-M (modulation order) vector.

Finally, the data is converted into their corresponding constellation symbol (phase-quadrature) and the normalization factor is applied to guarantee that the mean envelope power of the modulated signal is equal to one.

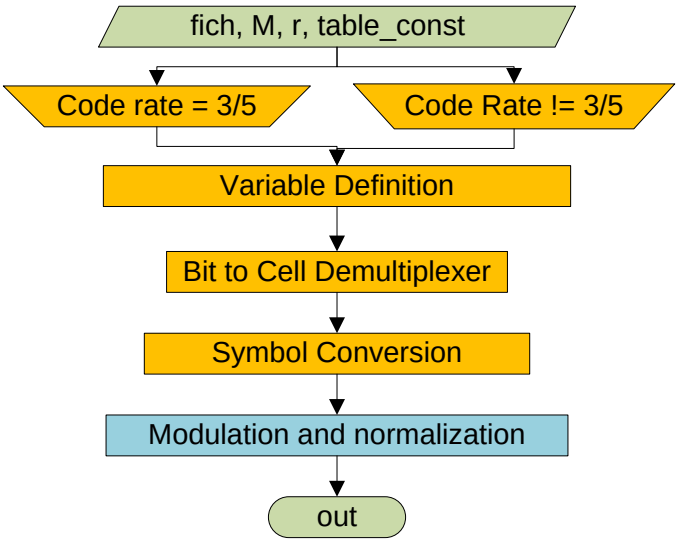

Fig. 3.11: Flux Diagram *bit2cell*

- Input Parameters:
  - fich: Nldpc data vector.
  - M: modulation order.
  - r: Code Rate.
  - table_const: vector containing the constellation values depending on the modulation.

- Output Parameters:
  - out: symbol (phase-quadrature) data stream with variable length depending on the constellation.

3.3.4 Constellation Rotation

The constellation rotation consists in the rotation in the complex plane and the cyclically delay of the imaginary part of the normalized FEC values of each FEC block. The output cells are given by **(3.4)**:

$$g_0 = \mathrm{Re}(R_{RQD} f_0) + j\ \mathrm{Im}(R_{RQD} f_{Ncells-1}),$$
$$g_q = \mathrm{Re}(R_{RQD} f_q) + j\ \mathrm{Im}(R_{RQD} f_{q-1}),\ q=1,2,\ \ldots\ N_{cells}-1, \qquad \textbf{(3.4)}$$

Where the rotation phasor $R_{RQD} = e^{j\frac{2\pi\theta}{360}}$. The rotation angle Φ depends on the modulation and is given in **Table 3.10**.

Table 3.10: Rotation angle for each modulation (in degrees)

Modulation	QPSK	16-QAM	64-QAM	256-QAM
Φ (degrees)	29,0	16,8	8,6	atan(1/16)

After rotating, the projections of the constellation points on I and Q channels carry the information regarding the m-mapped bits. For a 16-QAM, instead of $2^{m/2}$=4 projections on each axis, the constellation now has 2^m=16 projections as it can be seen in **Fig. 3.12 a)**. The insertion of the interleaving between I and Q leads to the same information being sent twice over the channel in different cells, as if an inner repetition code was used. The resulting "virtual" constellation after rotation and cyclic delay in the case of a 16-QAM is shown in **Fig. 3.12 b)**. It is equivalent to sending a higher-order irregular QAM while having the spectral efficiency of the original 16-QAM. This leads to additional diversity that improves the error-correcting performance when severely faded channels are encountered.

The constellation rotation is only used for the common and the data PLPs, never for the cells or the L1 signalling. If the constellation rotation is not used, the cells are passed onto the cell interleaver unmodified.

The rotation applies the angles defined in **Table 3.10**. The optimum choice of the angle depends on the modulation order, the channel and the mapping types. For each modulation order (constellation size), a single corresponding rotation has been chosen. This can only be strictly optimum for a particular channel type, but nevertheless the values chosen still deliver a performance improvement (compared with non-rotated constellations) for all encountered

channel models ranging from the classical faded channel (Rayleigh) to the severely faded channel (Rayleigh with erasures).

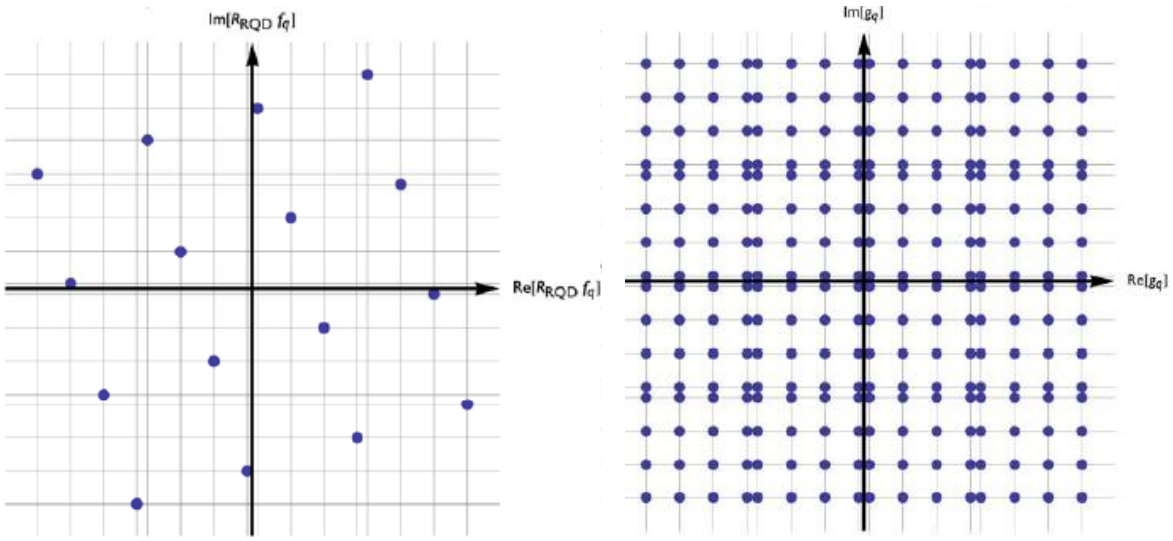

Fig. 3.12 a) and b): 16-QAM after rotation and resulting “virtual” 16-QAM constellation after rotation and cyclic delay

In order to have a deeper understanding of the rotated constellation technique, **Fig. 3.13 a)** and **Fig. 3.13 b)** show the projections as a function of the Gray mapping for the 16-QAM constellation.

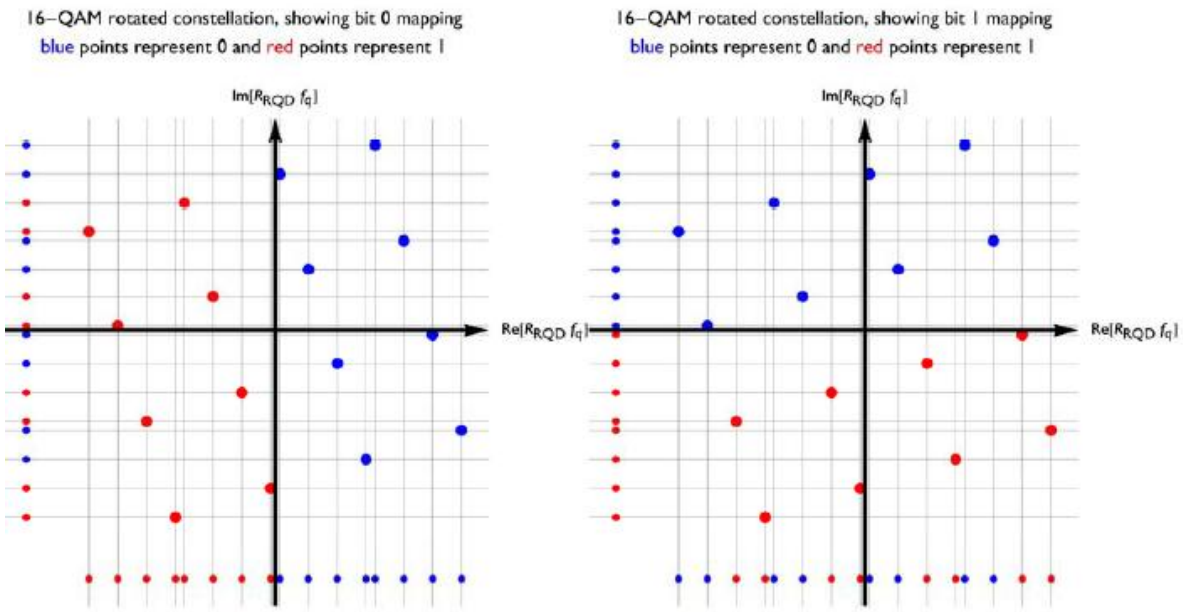

Fig. 3.13 a) and b): rotated 16-QAM constellation and its projection over components I and Q showing bit 0 and bit 1 mappings

A clear advantage with respect to non-rotated 16-QAM is observed in the extreme case where a projection over one axis is completely erased. In fact, the detection of the transmitted constellation point is still possible since the projection over the remaining axis will generally have been transmitted on a different OFDM carrier and in a different OFDM symbol.

The previous analysis corresponding to the 16-QAM case is also valid for the 4, 64 and 256-QAM schemes adopted in DVB-T2. Note however that in 256-QAM, the angle chosen is such that the projections on each axis are uniformly spaced.

This technique does not show any known disadvantages, while greatly improving the robustness of the receiver to severe channel conditions. However, the ACE PAPR reduction cannot be used in conjunction with the constellation rotation.

3.3.4.1 Designed functions for Constellation Rotation

- **constellation_rotation:**

The constellation rotation function is divided into two main blocks. In the first one, the rotation phasor is applied to all the transmitted symbols with the corresponding angle according to **Table 3.10**. At the second part of the function, the carrier interleaving is performed in order to separate I/Q components **(Fig. 3.14)**. For that second stage, the *Matlab* matrix vector processing capacity is very useful to implement it in an efficient manner.

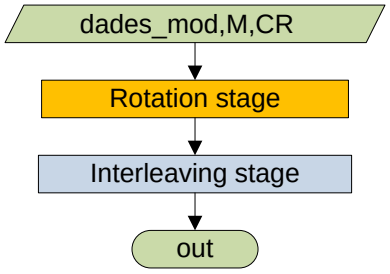

Fig. 3.14: Flux Diagram *constellation_rotation*

- Input Parameters:
  - dades_mod: input modulated data vector.
  - M: modulation order.
  - CR: binary selection of constellation rotation (1== Constellation Rotation, 0==No Constellation Rotation).
- Output Parameters:
  - out: symbol (phase-quadrature) data stream with constellation rotation.

3.3.5 Cell interleaver

The pseudorandom bit interleaver uniformly spread the cells in the FEC codeword. It ensures an uncorrelated distribution of channel distortions and interferences along the FEC codeword's at the receiver. It also differently "rotates" the interleaving sequence in each of the FEC blocks of one Time Interleaver Block (see next section).

The input of the cell interleaver is the data cells of the FEC blocks generated by the constellation rotation and cyclic Q delay. The output of the CI is a vector defined by **(3.5)**:

$$d_{r,L_r(q)} = g_{r,q} \text{ for each } q = 0,1,\ldots,N_{cells}\text{-}1, \qquad \textbf{(3.5)}$$

Where N_{cells} is the number of output data cells per FEC block and $L_r(q)$ is a permutation function applied to FEC block of the TI block.

The permutation function $L_r(q)$ is given by **(3.6)**:

$$L_r(q) = [L_0(q) + P(r)] \bmod N_{cells}, \qquad \textbf{(3.6)}$$

Where $L_0(q)$ is the basic permutation function and P(r) is the shift value to be used in FEC block r of the TI block.

For the complete creation description for the sequences $L_0(q)$ and P(r) permutation functions, see *Section 6.4* of the DVB-T2 bluebook [3].

With those specifications for the cell interleaver, a scheme for the cell interleaver is shown on **Fig. 3.15**.

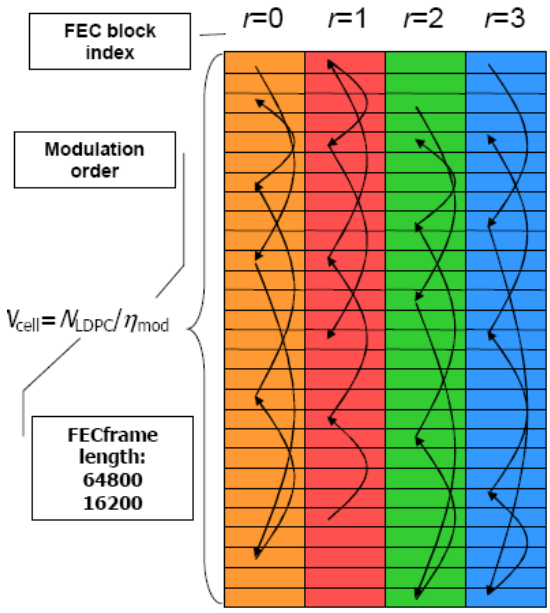

Fig. 3.15: Cell Interleaver Scheme

3.3.5.1 Designed functions for Cell Interleaver

❖ cell_interleaver:

Despite of the efforts in the simulator efficiency, the cell interleaver stage is one of the less efficient modules of the transmitter block. That fact is due to the generation of the permutation sequences. Those sequences allow the symbol dispersion through the FEC blocks, but their generation must be created using boucle sequences, one of the worst instructions to implement in *Matlab* environments due to their low calculation speed efficiency.

The function is composed by five main steps, as it can be seen in the figure below **(Fig. 3.16)**. First of all, the definition of the number of cells depending of the modulation is implemented. On the main block, the permutation sequences S_i, L_0 and P(r) are generated in order to achieve the correct L(r) sequence. At last, the data fields are interleaved following the corresponding sequence.

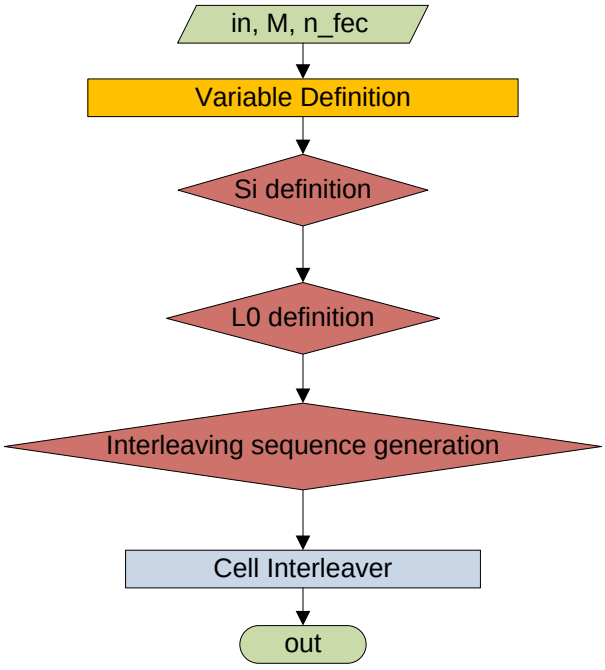

Fig. 3.16: Flux Diagram *cell_interleaver*

- Input Parameters:
  - fich: Nldpc data vector.
  - M: modulation order.
  - n_fec: total number of FEC blocks in one Time Interleaver frame (*see Section 3.3.6*).
- Output Parameters:
  - out: interleaved output data vector.

3.3.6 Time interleaver

The time interleaver operates at PLP level. The time interleaving parameters for different PLPs will be different within a T2 system.

Each of the PLP FEC blocks from the cell interleaver is grouped into Interleaving Frames. An Interleaving Frame contains a dynamically variable whole number of FEC blocks. That number is indexed as n denoted by $N_{BLOCKS\_IF\_MAX}(n)$ and is signalled as PLP_NUM_BLOCKS in the L1 signalling.

The number of blocks varies between 0 to a maximum value of $N_{BLOCKS\_IF\_MAX}$. The largest value is 1023 blocks.

There are three options for time interleaving for each PLP:

1. Each Interleaving frame contains one TI-block mapped directly to one T2-frame. This option is signalled in the L1-signalling by TIME_IL_TYPE='0' and TIME_IL_LENGTH='1'. In **Fig. 3.17** the first TI scheme is shown.

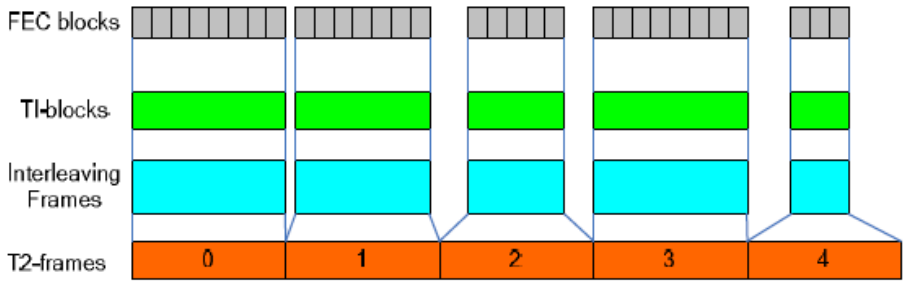

Fig. 3.17: TI for P_i=1, I_{jump}=1,N_{TI}=1

2. Each Interleaving Frame contains one TI-block mapped to more than one T2-frame. This scheme gives a greater time diversity for low-data services and is signalled by TIME_IL_TYPE='1' in L1-sgnalling. **Fig. 3.18** shows an example where one interleaving frame is mapped to two T2-frames, and FRAME_INTERVAL (I_{jump})=2.

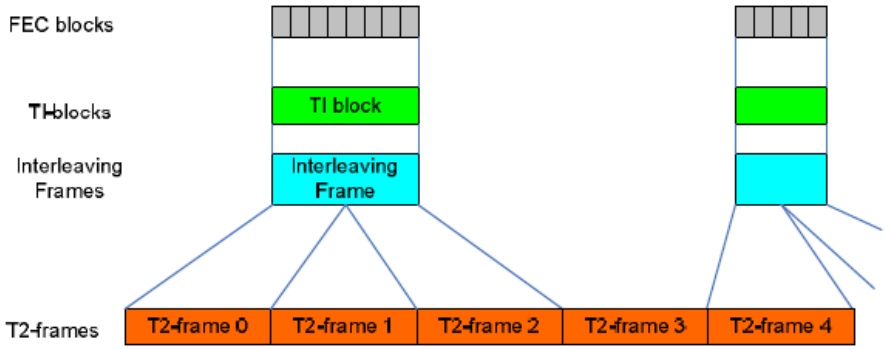

Fig. 3.18: TI for P_i=2, I_{jump}=2,N_{TI}=1

3. Each Interleaving Frame is mapped to one T2-frame and the Interleaving Frame is divided into several TI-blocks **(see Fig. 3.19)**. Each of the TI-blocks use up to the full TI memory, increasing the maximmum bit-rate for a PLP. This option is signalled by TIME_IL_TYPE='0' in the L1-signalling.

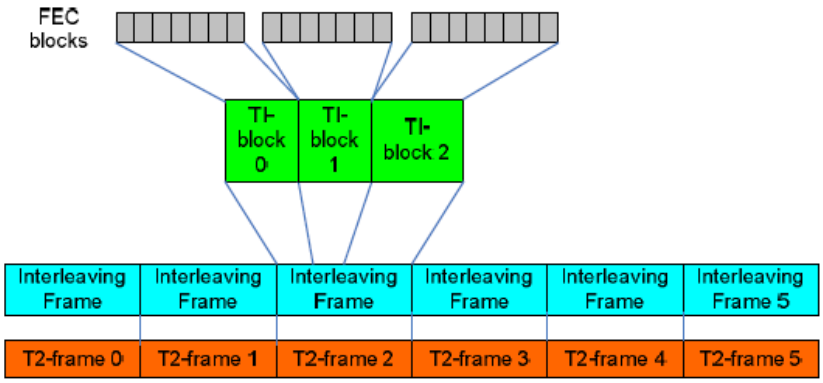

Fig. 3.19: TI for P_i=1, I_{jump}=1, N_{TI}=3

3.3.6.1 Interleaving of each TI block

The cells of the $N_{FEC}(n,s)$ FEC blocks from the output of the cell interleaver are stored in TI memories (one per PLP) due to the TI.

Otherwise, the Time Interleaver acts as a buffer for the PLP data prior to the process of frame building. That method is achieved using two memory banks for each PLP. The first bank contains the first TI block. The second TI block is written to the second memory bank while the first bank is being read. **Fig. 3.20** illustrates an example for two memory banks.

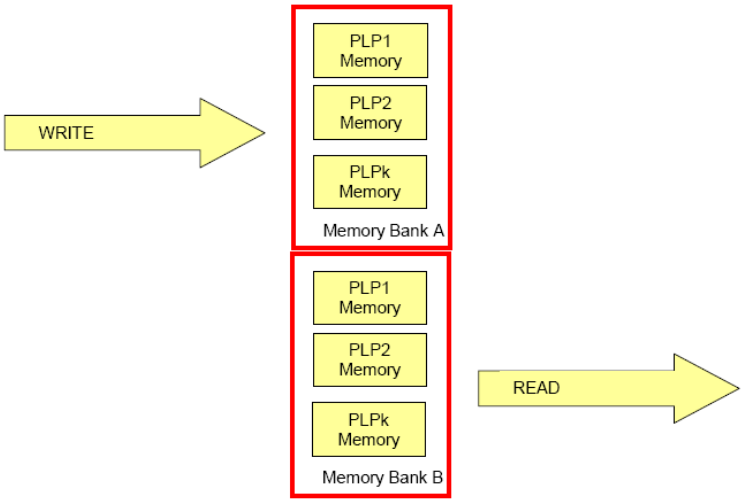

Fig. 3.20: Example of the memory bank functioning

Following the same way as the bit interleaving, the TI is a row-column block interleaver where the number of rows (N_r) is equal to the number of cells in the

FEC block (N_{cells}) divided by 5, and the number of columns (N_c) is five times the $N_{FEC}(n,s)$. The cell rates affects in the number of columns of the interleaver, varying in each TI-block. **Table 3.11** defines the parameters of the time interleaver.

Table 3.11: Time Interleaver parameters

LDPC block length (N_{ldpc})	Modulation	Number of cells per LDPC block (N_{CELLS})	Number of rows N_r
64 800	256-QAM	8 100	1 620
	64-QAM	10 800	2 160
	16-QAM	16 200	3 240
	QPSK	32 400	6 480
16 200	256-QAM	2 025	405
	64-QAM	2 700	540
	16-QAM	4 050	810
	QPSK	8 100	1 620

Fig. 3.21 shows a graphical representation of the time interleaver. The first FEC block is written column-wise into the first 5 columns of the time interleaver, the second FEC block is written into the next 5 columns and so on. The cells are read row-wise.

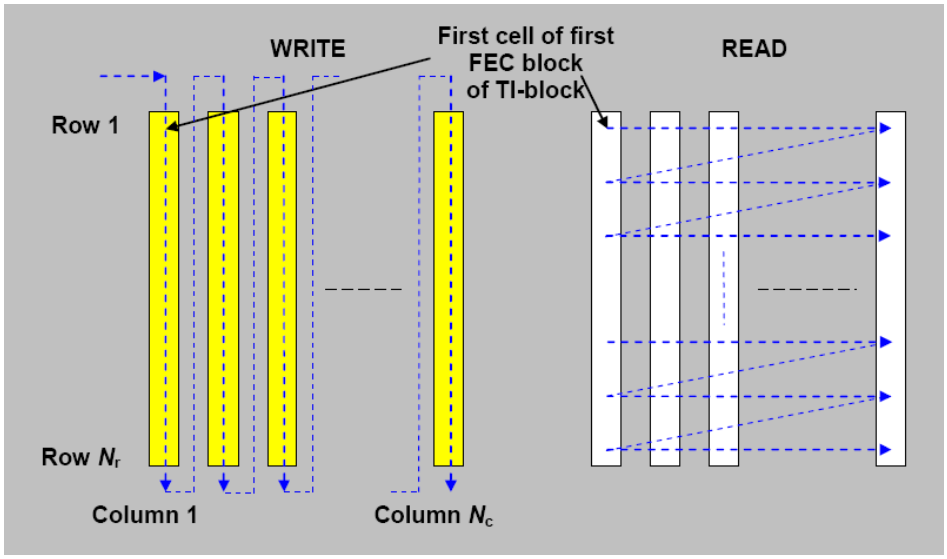

Fig. 3.21: Time Interleaver

3.3.3.2 Designed functions for Time Interleaver

❖ **Time_interleaver:**

The time interleaver is a two side efficient implemented function. On one hand, the block is easily and faster to implement in *Matlab* programming using the

reshape function defined to change the matrix appearance. In that case, this function in perfect to design a matrix interleaver, it only requires a code sentence to pass from a one row data vector into matrix of N_c by N_r. On the same way, to read the interleaver the same instruction can be applied modifying the output parameters **(Fig. 3.22)**.

On the other hand, the time interleaver requires a huge amount of memory resources, due to their Time Interleaving Frame length. In the simulator platform, the selected number of FEC blocks by Time Interleaving frame is 4 FEC blocks (259200 bits) with the first architecture defined at *Section 3.3.6*. That selection is realized in order to minimize the speed reduction effects of the simulation results. Despite of that fact, it is recommended to implement the Time Interleaver with a length of more than 30 FEC blocks by TI block to maximize the behaviour of the Constellation Rotation detector.

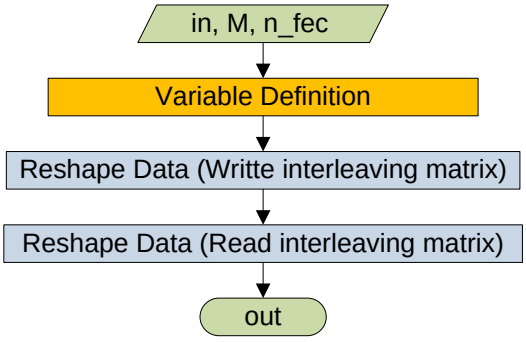

Fig. 3.22: Flux Diagram *time_interleaver*

- Input Parameters:
  - fich: Nldpc data vector.
  - M: modulation order.
  - n_fec: total number of FEC blocks in one Time Interleaver frame (*see Section 3.3.6*).
- Output Parameters:
  - out: interleaved output data vector.

CHAPTER 4: MODULATION AND CHANNEL

Along that chapter the frame builder functions applied for a T2 system with a single RF channel will be discussed. The main function of the frame builder is to assemble the cells produced by the time interleaver for each PLP and the cells of the modulated L1 signalling data into arrays of active OFDM cells corresponding to each of the OFDM symbols. In that way, the frame builder works according to the information generated by the scheduler and the configuration of the frame structure.

The function of the OFDM generation module is to take the cells produced by the frame builder, as frequency domain coefficients, to insert the relevant reference information, known as pilots, which allow the receiver to compensate for the distortions introduced by the transmission channel, and to produce from this the basis for the time domain signal for transmission. It then inserts guard intervals and, if relevant, applies PAPR reduction processing to produce the completed T2 signal. A block diagram of this module is found in figure **(Fig. 4.1).**

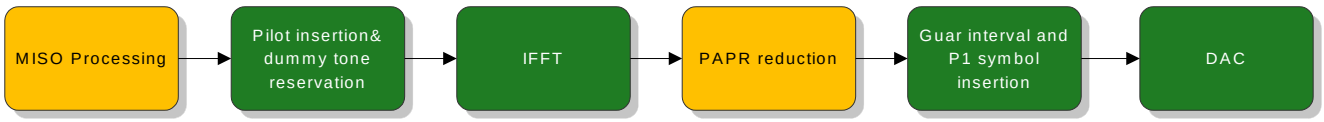

Fig. 4.1: OFDM generation block diagram

The yellow colour blocks represent the optional blocks being the green colour blocks those that must be included. A detailed description of the mandatory blocks is performed along next sections leaving the description and implementation of the optional blocks for a future implementation.

4.1 Frame Structure

The figure below **(Fig. 4.2)** shows a generic T2 frame structure. At the top level, super frames define the frame structure, which are divided into T2-frames further divided into OFDM symbols. In the following sections, each individual structure is defined.

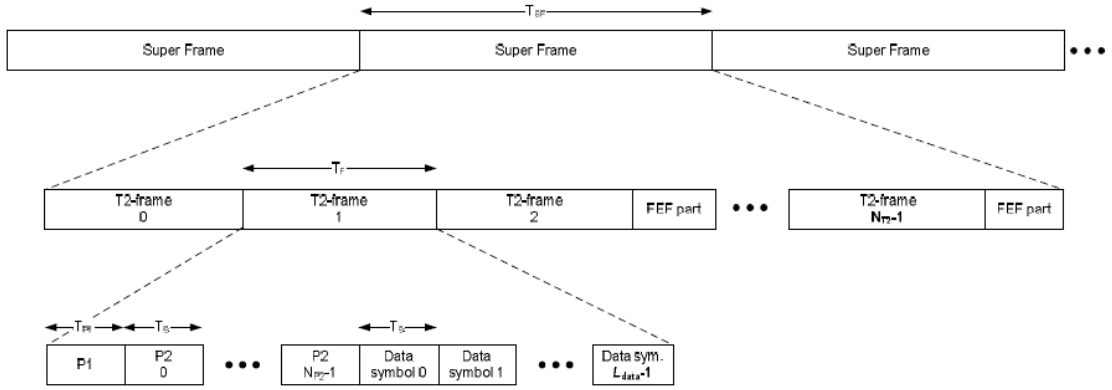

Fig. 4.2: T2-Frame structure

4.2 Super Frame

A super frame contains T2-frames and also can be contain FEF (Future Extension Frames, *see more information at DVB-Bluebook [3]*) parts. In the next figure **(Fig. 4.3)** a generic super frame with FEF parts scheme is shown.

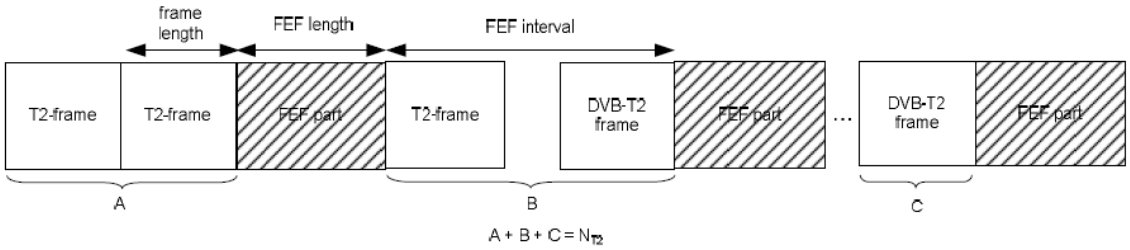

Fig. 4.3: Super Frame scheme with FEF parts

The number of T2-frames contained in a super frame is a variable parameter configured in the L1 pre-signalling data, N_{T2} (NUM_T2_FRAMES). Due to that fact, the T2-frames are marked from 0 to N_{T2}-1. The actual frame is signalled in the dynamic L1 post-signalling. Can be many FEF parts in a super frame inserted between T2-frames and shall not be adjacent to another FEF part. Thus the super frame duration T_{SF} is determined by **(4.1)**:

$$T_{SF} = N_{T2} \cdot T_F + N_{FEF} \cdot T_{FEF} \qquad \textbf{(4.1)}$$

Where:
N_{FEF} is the number of FEF parts in a super frame
T_{FEF} is the duration of the FEF parts signalled by FEF_LENGTH.

N_{FEF} can be defined by **(4.2)**:

$$N_{FEF} = \frac{N_{T2}}{FEF\ interval} \qquad \textbf{(4.2)}$$

In the case where FEF are used, the super frame may be finished with a FEF part. The maximum value for the super frame length (T_{SF}) is 64s if FEF are not used (equivalent to 256 frames of 250 ms) and 128s if FEF are used. The indexing of T2 frames and N_{T2} are independent of FEFs.

4.3 T2-Frame

The T2-frames are formed by one P1 preamble symbol, followed by one or more P2 preamble symbols, followed by a configurable number of data symbols. In some combinations of FFT size, guard interval and pilot patterns, the last data symbols shall be a frame closing symbol.

4.3.1 T2-Frame Duration

The beginning of the first preamble symbol (P1) marks the beginning of the T2-frame. The number of P symbols in a T2-Frame is determined by the FFT size whereas the number of data symbols in the T2-frame is a configurable parameter signalled in the L1 pre-signalling. The maximum value for the frame duration T_F shall be 250ms. Thus, the maximum number for L_F is as defined in **Table 4.1** (for 8MHz bandwidth).

Table 4.1: Maximum length in OFDM symbols for different FFT sizes and guard intervals

FFT Size	T_U [ms]	Guard Interval						
		1/128	1/32	1/16	19/256	1/8	19/128	1/4
32K	3.584	68	66	64	64	60	60	NA
16K	1.792	138	135	131	129	123	121	111
8K	0.896	276	270	262	259	247	242	223
4K	0.448	NA	540	524	NA	495	NA	446
2K	0.224	NA	1081	1049	NA	991	NA	892
1K	0.112	NA	NA	2098	NA	1982	NA	1784

4.3.2 Overview of the T2-frame mapping

The slices and sub-slices of the PLPs, the auxiliary streams and dummy cells are mapped into the symbols of the T2 frame as illustrated in **Fig. 4.4**. The T2 frame starts with a P1 symbol followed by *N*P2 P2 symbols. The L1-pre and -post signalling are first mapped into P2 symbol(s). After that, the common PLP's are mapped right after the L1 signalling. The data PLPs follow the common PLPs starting with type 1 PLP1. The type 2 PLPs follows the type 1 PLPs. The auxiliary stream or streams, if any, follow the type 2 PLPs, and this can be followed by dummy cells. Together, the PLPs, auxiliary streams and dummy data cells shall exactly fill the remaining cells in the frame.

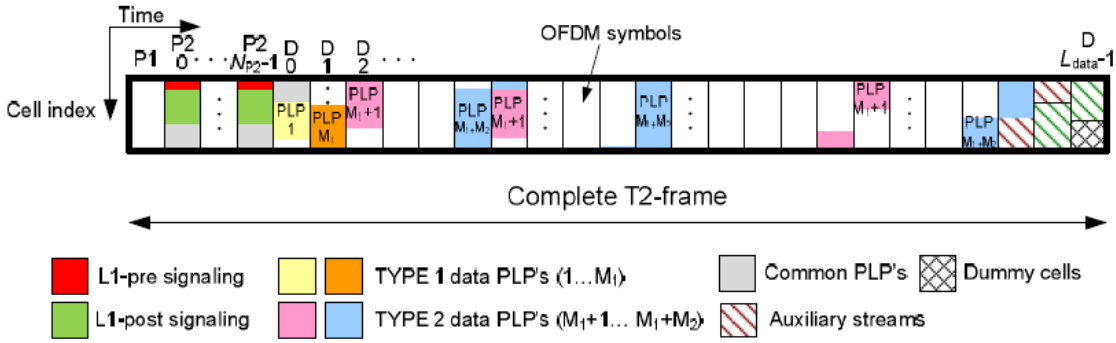

Fig. 4.4: Mapping of data PLPs into the data symbols

4.4 Frequency interleaver

The frequency interleaver operates on the data cells of one OFDM symbols to map it from the frame builder onto the available data carriers in each symbol. The number of available data carriers for the frequency interleaver depending on the FFT size is shown in **Table 4.2**.

Table 4.2: Available data carriers depending on the FFT size

FFT Size	M_{max}
1K	1024
2K	2048
4K	4096
8K	8192
16K	16384
32K	32768

The interleaved vector for the 32K mode, $A_{m,l} = (a_{m,l,0}, a_{m,l,1}, a_{m,l,2}...a_{m,l,N_{data}-1})$ is defined by:

$a_{m,l,H(p)} = x_{m,l,p}$ for even symbols of the frame (l mod 2 = 0) in mode 32K for p= 0,...,Ndata-1
$a_{m,l,p} = x_{m,l,H(p)}$ for odd symbols of the frame (l mod 2 = 1) in mode 32K for p = 0,...,Ndata-1

For other modes: 1K, 2K, 4K, 8K and 16K:

$a_{m,l,p} = x_{m,l,H0(p)}$ for even symbols of the frame (l mod 2 = 0) for p = 0,...,Ndata-1
$a_{m,l,p} = x_{m,l,H1(p)}$ for odd symbols of the frame (l mod 2 = 1) for p = 0,...,Ndata-1

$H(p)$, $H_0(p)$ and $H_1(p)$ are permutation functions based on sequences R'_i defined by the following. An (N_r - 1) bit binary word R'_i is defined, with $N_r = \log_2 M_{max}$, where R'_i takes the following values:

i = 0,1: $R'i$ [Nr-2, Nr-3,...,1,0]= 0,0,...,0,0
i = 2: $R'i$ [Nr-2, Nr-3,...,1,0] = 0,0,...,0,1
2 < i < Mmax:

{ $R'i$ [Nr-3, Nr-4,...,1,0] = $R'i$-1 [Nr-2, Nr-3,...,2,1];
in the 1k mode: $R'i$ [8] = $R'i$-1 [0] ⊕ $R'i$-1 [4]
in the 2k mode: $R'i$ [9] = $R'i$-1 [0] ⊕ $R'i$-1 [3]
in the 4k mode: $R'i$ [10] = $R'i$-1 [0] ⊕ $R'i$-1[2]
in the 8k mode: $R'i$ [11] = $R'i$-1 [0] ⊕ $R'i$-1 [1] ⊕ $R'i$-1[4] ⊕ $R'i$-1 [6]
in the 16k mode: $R'i$ [12] = $R'i$-1 [0] ⊕ $R'i$-1 [1] ⊕ $R'i$-1[4] ⊕ $R'i$-1 [5] ⊕ $R'i$-1 [9] ⊕ $R'i$-1 [11]
in the 32k mode: $R'i$ [13] = $R'i$-1 [0] ⊕ $R'i$-1 [1] ⊕ $R'i$-1[2] ⊕ $R'i$-1 [12] }

A vector R_i is derived from the vector R'_i by the bit permutations given in **Table 4.3** (from **Table 4.3a** to **Table 4.3f**).

Table 4.3a: Bit permutations for the 1k mode

R'_i bit positions	8	7	6	5	4	3	2	1	0
R_i bit positions (H_o)	4	3	2	1	0	5	6	7	8
R_i bit positions (H_1)	3	2	5	0	1	4	7	8	6

Table 4.3b: Bit permutations for the 2k mode

R'_i bit positions	9	8	7	6	5	4	3	2	1	0
R_i bit positions (H_o)	0	7	5	1	8	2	6	9	3	4
R_i bit positions (H_1)	3	2	7	0	1	5	8	4	9	6

Table 4.3c: Bit permutations for the 4k mode

R'_i bit positions	10	9	8	7	6	5	4	3	2	1	0
R_i bit positions (H_o)	7	10	5	8	1	2	4	9	0	3	6
R_i bit positions (H_1)	6	2	7	10	8	0	3	4	1	9	5

Table 4.3d: Bit permutations for the 8k mode

R'_i bit positions	11	10	9	8	7	6	5	4	3	2	1	0
R_i bit positions (H_o)	5	11	3	0	10	8	6	9	2	4	1	7
R_i bit positions (H_1)	8	10	7	6	0	5	2	1	3	9	4	11

Table 4.3e: Bit permutations for the 16k mode

R'_i bit positions	12	11	10	9	8	7	6	5	4	3	2	1	0
R_i bit positions (H_o)	8	4	3	2	0	11	1	5	12	10	6	7	9
R_i bit positions (H_1)	7	9	5	3	11	1	4	0	2	12	10	8	6

Table 4.3f: Bit permutations for the 32k mode

R'_i bit positions	13	12	11	10	9	8	7	6	5	4	3	2	1	0
R_i bit positions	6	5	0	10	8	1	11	12	2	9	4	3	13	7

The permutation function *H*(*p*) is defined by the following algorithm**(4.3)**:

$$
\begin{aligned}
&p = 0;\\
&\text{for } (i = 0;\ i < M_{\max};\ i = i + 1)\\
&\{ H(p) = (i \bmod 2).2^{N_r - 1} + \sum_{j=0}^{N_r - 2} R_i(j).2^j;\\
&\text{if } (H(p) < N_{data})\ \ p = p + 1;\ \ \}
\end{aligned}
\qquad \textbf{(4.3)}
$$

In figure below **(Fig 4.5)** a schematic representation of the algorithm used to obtain the permutation function for the 1k mode is show.

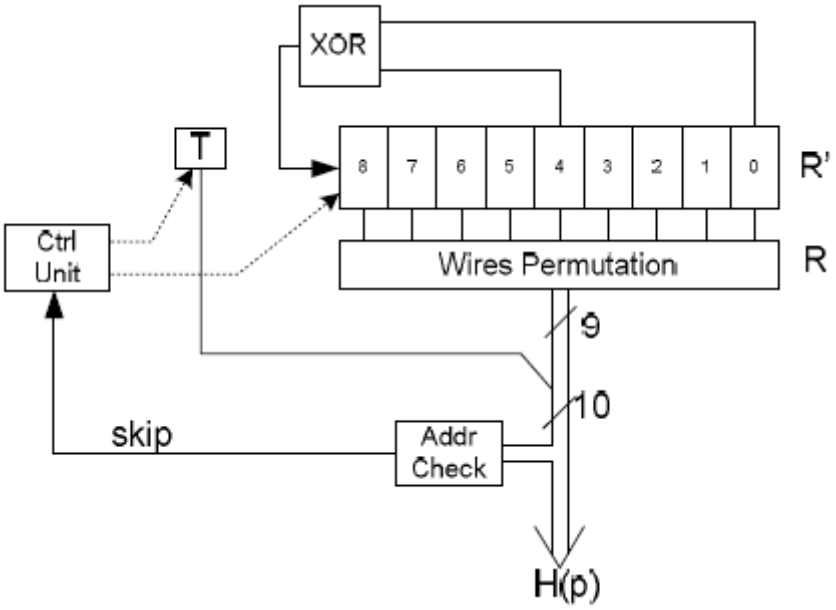

Fig. 4.5: Schematic representation for the permutation function of the frequency interleaver for the 1k mode

4.4.1 Designed functions for Frequency Interleaver

- **frequency_interleaver:**

In the Frequency Interleaver implementation the first point is to create the correct H(p) permutation function following the steps defined in *Section 4.4*. That permutation vector is designed using the *Matlab* function *xor(A,B)* which allows to perform a logical exclusive-OR gate.

Once the permutation function H(p) is calculated **(Fig. 4.6)**, the Frequency interleaver is applied into the cell data symbols in order to adapt it to their future carrier mapping process.

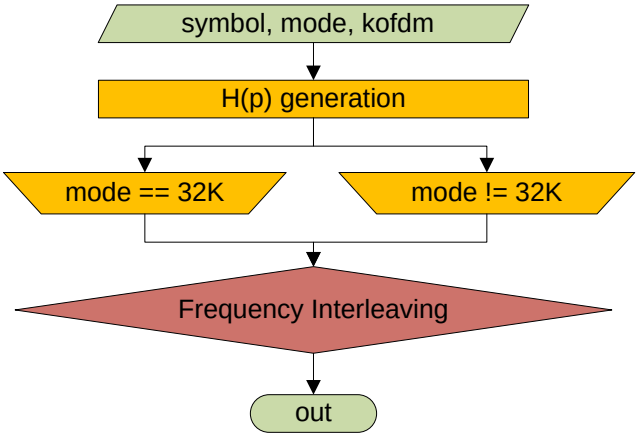

Fig. 4.6: Flux Diagram frequency_*interleaver*

- Input Parameters:
  - symbol: input cell data vector.
  - mode: OFDM selected mode.
  - kofdm: total length of the OFDM data symbol.
- Output Parameters:
  - out: interleaved output data vector.

4.5 Pilot insertion

Various cells within the OFDM frame are modulated with reference information whose transmitted value is known to the receiver. Cells containing reference information are transmitted at "boosted" power level. The information transmitted in these cells is scattered, continual, edge, P2 or frame-closing pilot cells. The locations and amplitudes of these pilots are defined in next sections for SISO transmissions, and are modified in MISO transmissions. The value of the pilot information is derived from a reference sequence, which is a series of values, one for each transmitted carrier on any given symbol.

The pilots can be used for frame synchronization, frequency synchronization, time synchronization, channel estimation, transmission mode identification and can also be used to follow the phase noise.

The pilots are modulated according to a reference sequence, $r_{l,k}$, where *l* and *k* are the symbol and carrier indices. The reference sequence is derived from a symbol level PRBS, w_k and a frame level PN-sequence, p_n. This reference sequence is applied to all the pilots (i.e. Scattered, Continual Edge, P2 and Frame Closing pilots) of each symbol of a T2-frame, including both P2 and Frame Closing symbols. The output of the symbol level sequence, w_k, is inverted or not inverted according to the frame level sequence, $p_{n'}$, as shown in Figure **(Fig. 4.7)**.

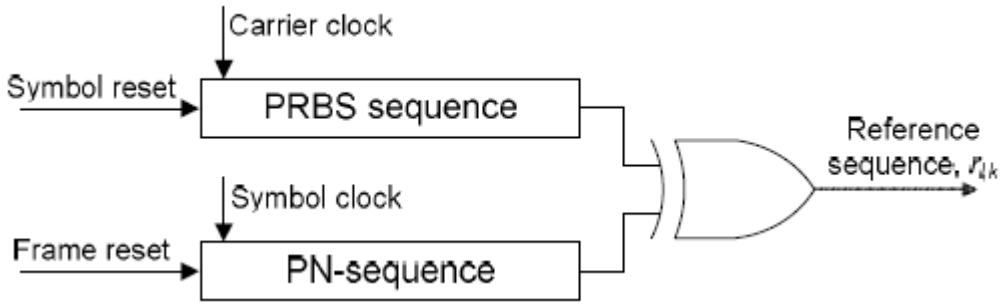

Fig. 4.7: Formation of the reference sequence from the PN and PRBS sequences

The symbol-level PRBS is mapped to the carriers such that the first output bit (w_0) from the PRBS coincides with the first active carrier ($k = K_{min}$) in 1K, 2K and 4K. In 8K, 16K and 32K bit w_0 coincides with the first active carrier ($k=K_{min}$) in the extended carrier mode. In the normal carrier mode, carrier $k=K_{min}$ is modulated by the output bit of the sequence whose index is K_{ext}. This ensures that the same modulation is applied to the same physical carrier in both normal and extended carrier modes. A new value is generated by the PRBS on every used carrier (whether or not it is a pilot) **(Fig. 4.8)**.

The polynomial for the PRBS generator shall be **(4.4)**:

$$X^{11} + X^2 + 1 \qquad \textbf{(4.4)}$$

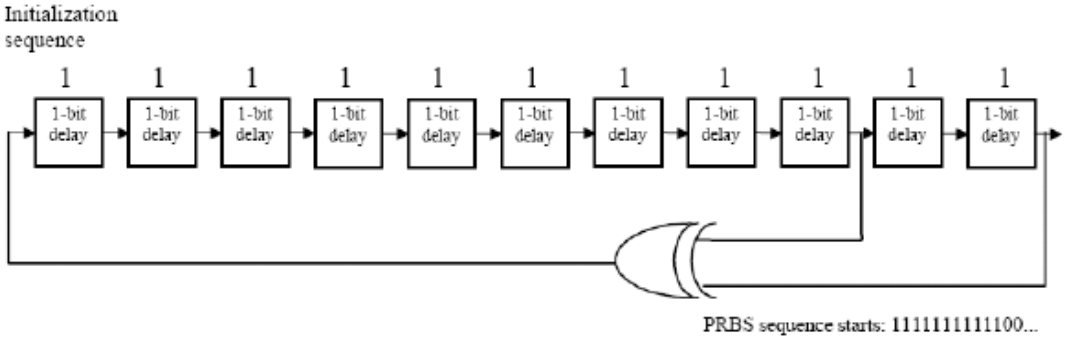

Fig. 4.8: Generation of PRBS sequence

4.5.1 Scattered pilot insertion

Reference information, taken from the reference sequence, is transmitted in scattered pilot cells in every symbol except P1, P2 and the frame-closing symbol (if applicable) of the T2-frame. The locations of the scattered pilots are defined in **Table 4.4** their amplitudes are defined in **Table 4.6**.

Table 4.4: Parameters defining the scattered pilot patterns

Pilot pattern	Separation of pilot bearing carriers (Dx)	Number of symbols forming one scattered pilot sequence (Dy)
PP1	3	4
PP2	6	2
PP3	6	4
PP4	12	2
PP5	12	4
PP6	24	2
PP7	24	4
PP8	6	16

The combinations of scattered pilot patterns, FFT size and guard interval which are allowed to be used are defined in **Table 4.5**.

Table 4.5: Scattered pilot pattern to be used for each allowed combination of FFT size and guard interval in SISO mode

FFT size	Guard interval						
	1/128	1/32	1/16	19/256	1/8	19/128	¼
32K	PP8 PP4 PP6	PP8 PP4	PP2 PP8	PP2 PP8	NA	NA	NA
16K	PP8 PP4 PP5	PP8 PP4 PP5	PP3 PP8	PP3 PP8	PP1 PP8	PP1 PP8	NA
8K	PP8 PP4 PP5	PP8 PP4 PP5	PP3 PP8	PP3 PP8	PP1 PP8	PP1 PP8	NA
4K,2K	NA	PP4 PP5	PP3	NA	PP1	NA	NA
1K	NA	NA	PP3	NA	PP1	NA	NA

The amplitudes of the scattered pilots, A_{SP}, depend on the scattered pilot pattern as shown in **Table 4.6**.

Table 4.6: Amplitudes of scattered pilots

Scattered pilot pattern	Amplitude (A_{SP})	Equivalent Boost (dB)
PP1,PP2	4/3	2.5
PP3,PP4	7/4	4.9
PP5,PP6,PP7,PP8	7/3	7.4

The modulation of the scattered pilots is given by **(4.5)**:

$$Re\{C_{m,l,k}\} = 2A_{SP}\left(\frac{1}{2} - r_{l,k}\right)$$
$$Im\{C_{m,l,k}\} = 0 \qquad \textbf{(4.5)}$$

4.5.2 Continual pilot insertion

In addition to the scattered pilots described above, a number of continual pilots are inserted in every symbol of the frame except for P1 and P2 and the frame closing symbol (if any). The number and location of continual pilots depends on both the FFT size and scattered pilot pattern PP1-PP8 in use.

The continual pilot locations are taken from one or more "CP groups" depending on the FFT mode. **Table 4.7** indicates which CP groups are used in each FFT mode. The pilot locations belonging to each CP group depend on the scattered pilot pattern in use; the concrete indices of each pilot pattern are defined in *Annex G of the DVB-T2 BlueBook* [3].

Table 4.7: Continual Pilot groups used with each FFT size

FFT size	CP Groups used	K_{mod}
1K	CP_1	1632
2K	CP_1,CP_2	1632
4K	CP_1,CP_2, CP_3	3264
8K	CP_1,CP_2, CP_3, CP_4	6528
16K	CP_1,CP_2, CP_3, CP_4, CP_5	13056
32K	CP_1,CP_2, CP_3, CP_4, CP_5, CP_6	NA

The continual pilots are transmitted at boosted power levels, where the boosting depends on the FFT size. **Table 4.8** gives the modulation amplitude A_{CP} for each FFT size. When a carrier's location is such that it would be both a continual and scattered pilot, the boosting value for the scattered pilot pattern shall be used (A_{SP}).

Table 4.8: Boosting for the continual pilots

FFT size	1K	2K	4K	8K	16K	32K
A_{CP}	4/3	4/3	$(4\sqrt{2})/3$	8/3	8/3	8/3

The modulation value for the continual pilots is given by **(4.6)**:

$$Re\{C_{m,l,k}\} = 2A_{CP}\left(\frac{1}{2} - r_{l,k}\right)$$
$$Im\{C_{m,l,k}\} = 0 \qquad \textbf{(4.6)}$$

4.5.3 Edge pilot insertion

The edge carriers, carriers $k=K_{min}$ and $k=K_{max}$, are edge pilots in every symbol except for the P1 and P2 symbol(s). They are inserted in order to allow frequency interpolation up to the edge of the spectrum. The modulation of these cells is exactly the same as for the scattered pilots.

4.5.4 Insertion of Frame closing symbols

When any of the combinations of FFT size, guard interval and scattered pilot pattern listed in **Table 4.9** (for SISO mode) is used, the last symbol of the frame is a special frame closing symbol. Frame closing symbols are always used in MISO mode, except with pilot pattern PP8, when frame closing symbols are never used.

Table 4.9: Combinations of FFT size, guard interval and pilot pattern for which frame closing symbols are used in SISO mode

FFT size	Guard interval						
	1/128	1/32	1/16	19/256	1/8	19/128	¼
32K		PP6	PP4	PP4	PP2	PP2	NA
16K		PP7 PP6	PP4 PP5	PP4 PP5	PP2 PP3	PP2 PP3	PP1
8K		PP7	PP4 PP5	PP4 PP5	PP2 PP3	PP2 PP3	PP1
4K,2K	NA	PP7	PP4 PP5	NA	PP2 PP3	NA	PP1
1K	NA	NA	PP4 PP5	NA	PP2 PP3	NA	PP1

Finally the frame closing pilots are boosted and modulated by the same factor as the scattered pilots, $A_{SP.}$

4.5.5 Designed functions for Pilot Insertion

- **modulador_OFDM:**

The objective of this function is to return a complete OFDM symbol between 1024 and 32768 carriers longitude, including the pilot carriers, depending on the selected OFDM mode from the input symbols.

The first step is to generate polynomial PRBS sequence to modulate the pilots following the pattern described in *Section 4.5*. The next stage is to generate the carrier positions of the scattered and continual pilots in the OFDM symbol, in that case the scattered pilot positions are generated each OFDM symbol using

the algorithms described in DVB-T2 bluebook [3]. Otherwise, the continual pilot positions are static through time, and they only depends on the pilot pattern selected allowing the possibility to be loaded from a text file in order to reduce the work load.

Once the continual, scattered and edge pilots carrier positions are modulated and inserted into their corresponding carriers following the described parameters, the data symbols are mapped determining the free carriers in the OFDM symbol **(Fig. 4.9)**.

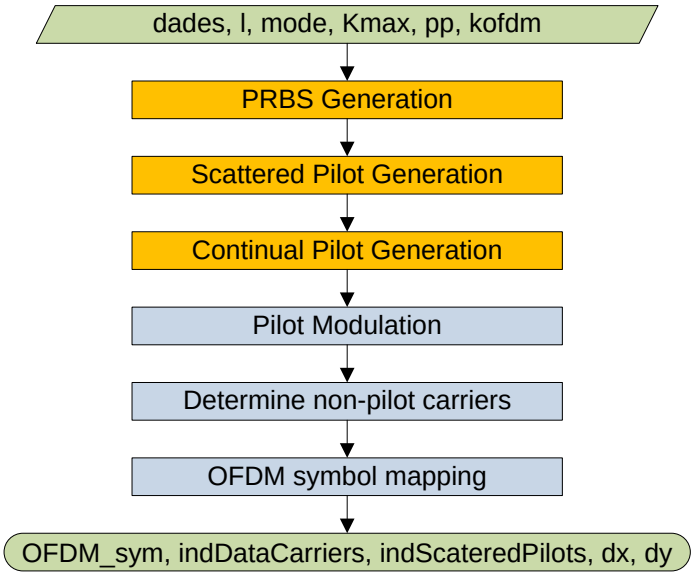

Fig. 4.9: Flux Diagram *modulador_OFDM*

- Input Parameters:
  - dades: input symbol data vector.
  - l: frame OFDM symbol number.
  - mode: OFDM selected mode.
  - Kmax: total data carrier number in one OFDM symbol.
  - pp: selected pilot pattern (PP1, PP2, etc...).
  - kofdm: total carrier number in one OFDM symbol.
- Output Parameters:
  - OFDM_sym: vector containing the OFDM to be transmitted through the channel.
  - inDataCarriers: data carriers positions (indexed).
  - inScatteredPiltos: pilot carriers positions (indexed).
  - dx and dy: scattered pilot pattern sequence generation depending on the selected parameters.

4.6 IFFT – OFDM Modulation and Guard Interval

This section specifies the OFDM structure to use for the transmission mode. Any cell $c_{m,l,k}$ in the P2 or data symbols which has not been designated as a pilot or as a reserved tone shall carry one of the data cells from the MISO processor, i.e. $c_{m,l,k} = e_{m,l,p}$. The cells $e_{m,l,p}$ for symbol l in T2-frame m shall be taken in increasing order of the index p, and assigned to $c_{m,l,k}$ of the symbol in increasing order of the carrier index k for the values of k in the range $K_{min} \leq k \leq K_{max}$ designated as data cells.

The transmitted signal is organized in frames. Each frame has duration of T_F, and consists of L_F OFDM symbols. N_{T2} frames constitute one super-frame. Each symbol is constituted by a set of K_{total} carriers transmitted with a duration T_S. It is composed of two parts: a useful part with duration T_U and a guard interval with a duration Δ. The guard interval consists of a cyclic continuation of the useful part, T_U, and is inserted before it. The allowed combinations of FFT size and guard interval are defined in **Table 4.10**.

The symbols in an OFDM frame (excluding P1) are numbered from 0 to L_F–1. All symbols contain data and reference information. Since the OFDM signal comprises many separately-modulated carriers, each symbol can in turn be considered to be divided into cells, each corresponding to the modulation carried on one carrier during one symbol. The carriers are indexed by $k \in [K_{min}; K_{max}]$ and determined by K_{min} and K_{max}. The spacing between adjacent carriers is $1/T_U$ while the spacing between carriers K_{min} and K_{max} are determined by $(K_{total}–1)/T_U$.

The detailed definition of the OFDM parameters can be found in *Section 9.5 of the DVB-T2 BlueBook* [3].

Seven different guard interval fractions (Δ/T_u) are defined. **Table 4.10** gives the absolute guard interval duration Δ, expressed in multiples of the elementary period T for each combination of FFT size and guard interval fraction. Some combinations of guard interval fraction and FFT size shall not be used and are marked 'NA' in the table.

Table 4.10: Duration of the guard intervals in terms of the elementary period T

FFT size	Guard interval fraction (Δ/T_U)						
	1/28	**1/32**	**1/16**	**19/256**	**1/8**	**19/128**	**1/4**
32K	256T	1024T	2048T	2432T	4096T	4864T	NA
16K	128T	512T	1024T	1216T	2048T	2432T	4096T
8K	64T	256T	512T	608T	1024T	1216T	2048T
4K	NA	128T	256T	NA	512T	NA	1024T
2K	NA	64T	128T	NA	256T	NA	512T
1K	NA	NA	64T	NA	128T	NA	256T

The emitted signal includes the insertion of guard intervals when PAPR reduction is not used. If PAPR reduction is used, the guard intervals shall be inserted following PAPR reduction.

4.6.1 Designed functions for IFFT Modulation and Guard Interval

- **TX_canal_RX:**

The objective of the main function from the channel and modulation block is to transmit and receive a complete OFDM symbol, including the channel distortion, estimation and reception stage. That function is the largest stage of the simulator platform, it includes a lot of sub-functions and calculations processes, and it is composed by 10 main subblocks **(Fig. 4.11)**.

First of all, the *TX_canal_RX* function starts with the *OFDM_modulation* function described in *Section 4.5.5*, which allows the creation of a complete OFDM symbol ready to be transmitted. The *OFDM_modulation* function performs the pilot modulation and carrier insertion, returning a complete mapped OFDM symbol ready to be passed through the channel transmission block.

In the transmission block, zero padding is used to reach the correct symbol length depending on the selected mode. IFFT (Inverse Fast Fourier Transform) is applied to the signal, using the Matlab library defined function *ifft(x)* in order to convert the signal into time domain. The last step into the transmission process is the addition of the guard interval at the beginning of the OFDM symbol.

At that point, the OFDM symbol is ready to be passed through the channel. Four possible channels are allowed to be selected: Gaussian, Ricean (P11), Rayleigh (F11) and TU6 mobile channel, all of them detailed specifically at *Chapter 2.* Immediately, an AWGN (Additive White Gaussian Noise) is added to simulate channel noise.

After the channel distortion block, the tail of the previous symbol is added into the guard interval of the actual OFDM symbol to simulate the possible delay interferences. In a parallel way, the tail of the current symbol is extracted in order to be added to the next symbol for the future iteration.

At the receiver, the first step is to erase the tails and the guard interval of the transmitted OFDM symbol, maintaining the carriers destined to data and pilots. The FFT (Fast Fourier Transform), *fft(x)* in *Matlab* library, is applied in order to recover the original sent signal in the frequency domain. It is important to mention that an erasure of the previous zero padding carriers is needed to receive the transmitted symbol samples, for example to pass from 2048 symbol carriers to 1705 data carriers in the 2K mode.

The next step is the channel estimation. The simulator platform is capable to calculate the channel estimation process in three different ways. The first one is the ideal estimator, where the symbol is ideally estimated knowing the PDP (Power Delay Profile) of the channel. At the second estimator option, a

frequency average estimator is implemented, performing linear average regression estimation between consecutive pilots. To conclude, a 2-D Estimator is implemented, realizing an average estimation simultaneously in frequency (between carriers) and in time domain (between OFDM symbols), as it can be seen in **Fig. 4.10**.

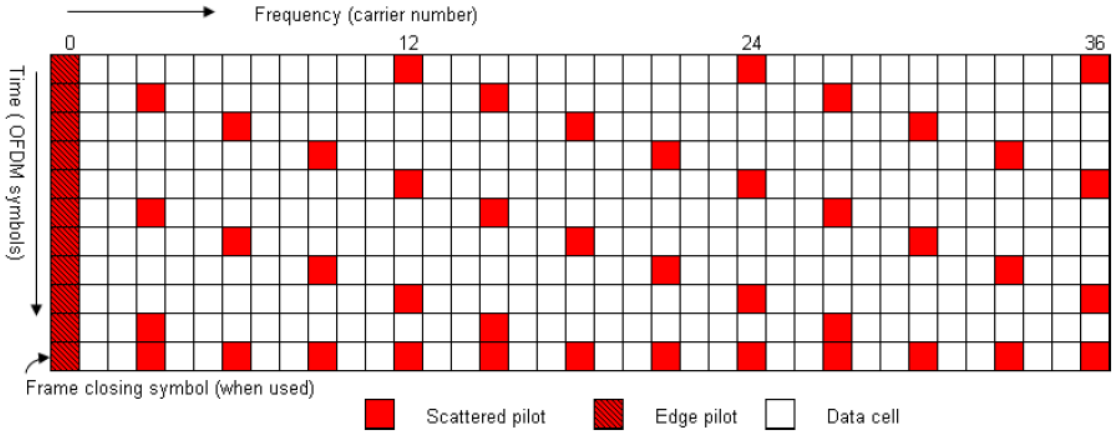

Fig. 4.10: Scattered Pilot Pattern PP1

Finally, the channel estimation vector is applied to the data symbol to counteract the channels effects, demodulating the OFDM symbol and extracting the non-information carriers in order to achieve the transmitted data symbol vector **(Fig. 4.11)**.

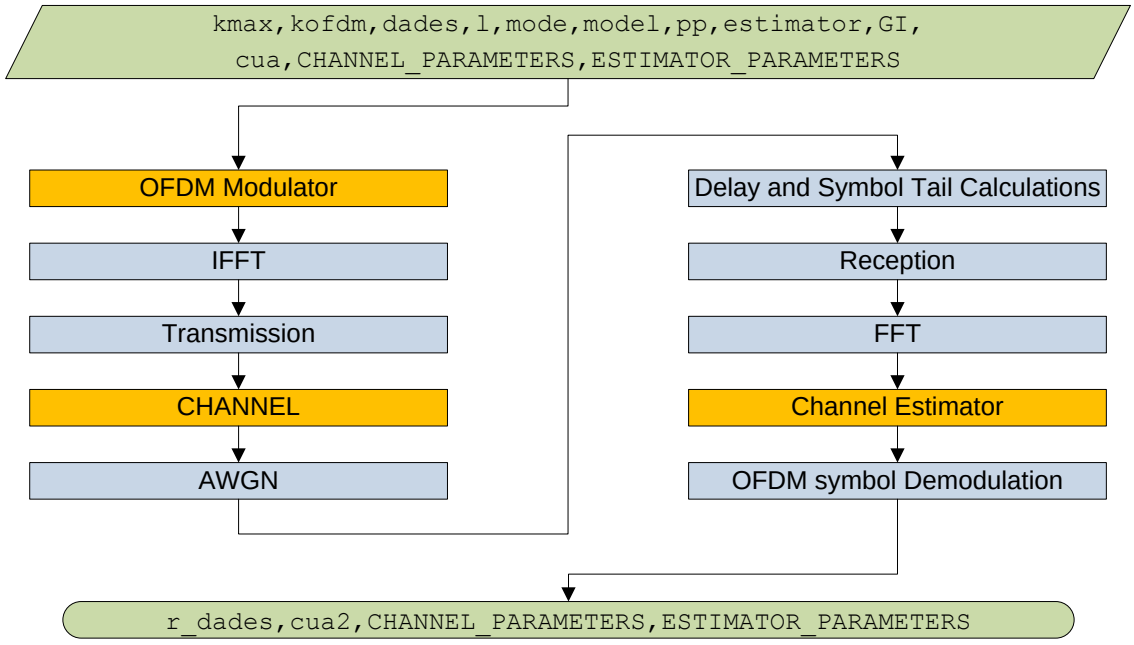

Fig. 4.11: Flux Diagram *TX_canal_RX*

- Input Parameters:
  - kmax: total data carrier number in one OFDM symbol.
  - kofdm: total carrier number in one OFDM symbol.
  - dades: input symbol data vector.
  - l: frame OFDM symbol number.
  - mode: selected OFDM mode (2K, 8K, 32K, etc...).
  - model: selected channel model (Gaussian, Ricean, etc...).
  - pp: selected pilot pattern (PP1, PP2, etc...).
  - estimator: selected estimator (ideal, 2-D estimator, etc...).
  - GI: selected guard interval for the transmission.
  - cua: OFDM symbol prefix (from the previous OFDM symbol).
  - CHANNEL_PARAMETERS: range of parameters needed to the correct channel definition.
  - ESTIMATOR_PARAMETERS: range of parameters needed to the correct channel definition.

- Output Parameters:
  - r_dades: received data vector (in symbols).
  - cua2: OFDM symbol tail (to be added in the next channel iteration).
  - CHANNEL_PARAMETERS: range of parameters needed to the correct channel definition.
  - ESTIMATOR_PARAMETERS: range of parameters needed to the correct channel definition.

CHAPTER 5: SIMULATION RESULTS

Along this chapter the different results obtained with the simulator platform are exposed and commented. The figures include channel comparative graphical results of the different modulation rates and some comparison among codification rates and modes.

The *Chapter* also includes an analysis between different operational modes and a study of the improvements introduced with the constellation rotation in hostile channels. Finally, at the end of the chapter, the performance of both standards, DVB-T and DVB-T2 is given.

5.1 Channel Comparative

The Channel models included in the simulation platform are deeply explained in *Chapter 2*. All of them have been programmed and tested in the simulation platform. The next figure **(Fig. 5.1)** shows the behaviour of the different implemented channels, including: Gaussian, Rice, Rayleigh, Memoryless Rayleigh and TU6 model.

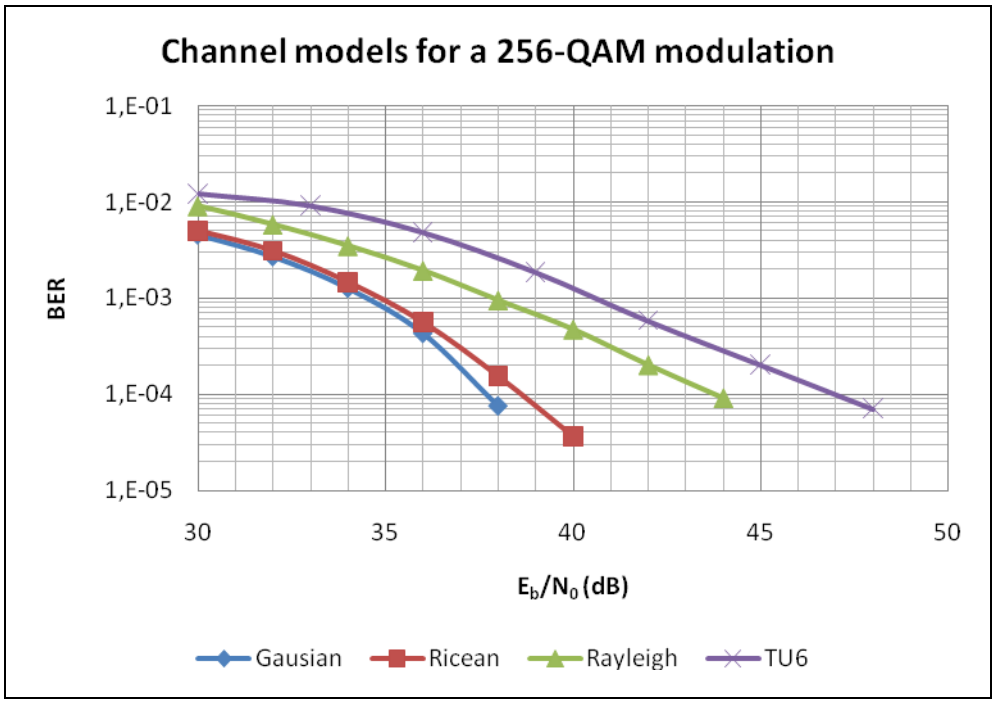

Fig. 5.1: Implemented channel models comparison for a 256-QAM modulation

As it can be seen, at low E_b/N_0 values, all channel models have similar bit error rates. Despite of that fact, when the E_b/N_0 values are higher, the channels have different slopes according to the hostility of the channel. Following this line, it is appreciated that the Gaussian channel requires the lowest E_b/N_0 to achieve the

Quasi Error Free (QEF) probability while, on the other hand, TU6 is clearly the worst channel.

It also has to be mentioned that the Memoryless Rayleigh Channel was defined to test the maximum improvement offered by the constellation rotation process. That channel is completely fictitious in the terrestrial broadcasting environments, where the reiterated randomized carrier erasures for a determined error probability value never occur.

However, taking into account the processing requirements of all the simulations, three channel models have been deeply studied: Gaussian, Rayleigh and TU6.

Those channels are selected in order to cover the most frequently environmental conditions in real scenarios. The Gaussian represents the standard theoretical channel (accounting only for thermal noise degradation), being useful for a first approximation in the early test stage of the simulation platform. The Rayleigh channel provides a real hostile scenario for the typical broadcasting environments with selective fading **(Fig. 5.2)**. On the other hand, one of the main goals of the DVB Organization was to introduce mobility capabilities to the DVB-T2 terminals. For that reason TU6 channel has been implemented in order to test the mobility conditions of the simulation platform.

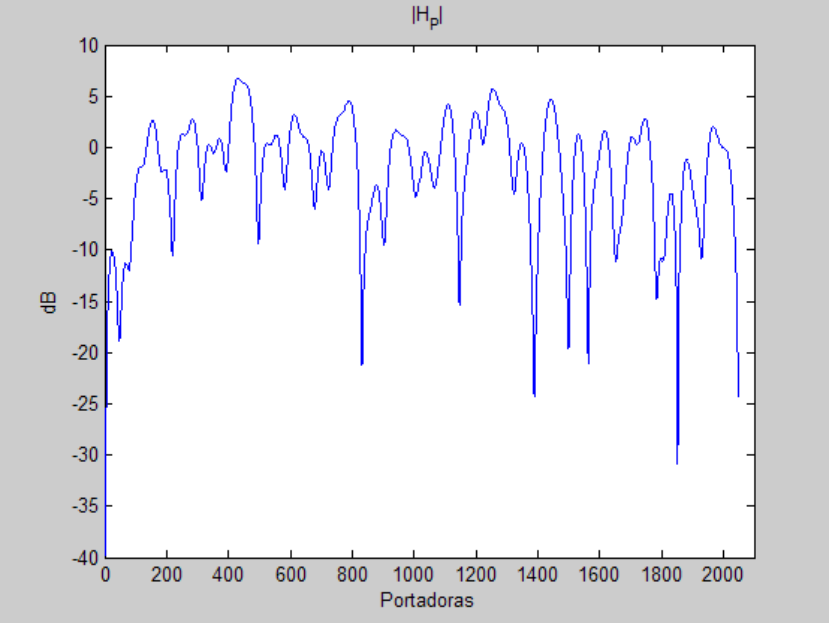

Fig. 5.2: Transfer Function of the DVB-T2 Rayleigh Channel

5.2 2K Mode simulation results

The obtained results of the simulation platform for the 2K operational mode of the DVB-T2 standard are shown at the table below **(Table 5.1)**.

Although the expected operating mode will be the 32K, the error probability values are equal in all the different modes as it will be described in next section (*Section 5.3*). The 2K mode simulations are selected to reduce computing consumption, therefore increasing the results rate.

Table 5.1: Required E_b/N_0 (dB) to achieve a BER=1×10^{-12} after the BCH decoder for all combinations of coding rates and modulation types at 2K Mode

			Required E_b/N_0 (dB) BER= 10^{-12} After BCH decoding		
Constellation	Code Rate	Effective Code Rate	Gaussian Channel	Rayleigh Channel	TU6 Channel
QPSK	1/2	4/9	-1.8	-1.2	4.3
	3/5	3/5	-0.5	1.2	5.8
	2/3	2/3	0.1	1.8	6.4
	3/4	11/15	1.1	2.8	7.2
	4/5	7/9	1.6	3.6	9
	5/6	37/45	2.2	5	9.6
16-QAM	1/2	4/9	-0.6	2.7	6.3
	3/5	3/5	0.8	4.8	8.1
	2/3	2/3	1.5	6.8	11.9
	3/4	11/15	2.2	8.9	12.8
	4/5	7/9	2.8	10.6	13.4
	5/6	37/45	3.6	11.2	14.4
64-QAM	1/2	4/9	0.6	5.3	9.3
	3/5	3/5	2.6	8.15	10
	2/3	2/3	4.2	11.4	13.4
	3/4	11/15	5.8	13.7	18
	4/5	7/9	6.5	15.5	19.2
	5/6	37/45	7.1	16.7	20.3
256-QAM	1/2	4/9	3.7	6.7	9.8
	3/5	3/5	6.3	9.9	12
	2/3	2/3	7.8	12.2	16.5
	3/4	11/15	9.8	15.3	19
	4/5	7/9	10.6	18	20.5
	5/6	37/45	14.2	19.2	22

These results were simulated with the following DVB-T2 system parameters:

- Operational Mode: 2K
- Channel Bandwidth: 8 MHz
- Channel Estimator: Ideal
- Pilot Pattern: PP1
- Constellation Rotation: Active
- Guard Interval: 1/4
- Doppler Frequency (in TU6 Channel): 10 Hz

The previous table **(Table 5.1)** has been expressed in E_b/N_0 terms in order to provide a standard value due to the different manners in the C/N calculation process. As it has been defined in *Chapter 2*, the carrier to noise ratio should be calculated as following **(5.1)**:

$$C/N = \frac{E_b}{N_0} + 10\log(code\ rate) + 10\log(log_2 M) + 10\log\left(\frac{\overline{Pot}}{N_{ofdm}}\right) \quad \textbf{(5.1)}$$

For example, in a QPSK modulation in a Rayleigh Channel with 5/6 Code Rate and 2K mode with PP1 (pilot pattern 1), the conversion will result in the following C/N relationship **(5.2)**:

$$C/N = 5\ dB - 0.8\ dB + 3\ dB\ \log - 0.45\ dB = 6.75\ dB \quad \textbf{(5.2)}$$

5.2.1 QPSK Modulation

Along this section, the results obtained in the simulator platform with the QPSK modulation are shown. Comparatives show the different behaviours of the different code rates for a given modulation.

5.2.1.1 Code rate: 1/2

The most robust performance for the DVB-T2 standard is the QPSK modulation with code rate 1/2 (without puncturing). That code rate allows the lowest values of required E_b/N_0 to achieve a QEF reception. That fact can be observed at **Fig. 5.3** and **Fig. 5.4**, where the QPSK simulations are shown for the Gaussian and Rayleigh channels, respectively.

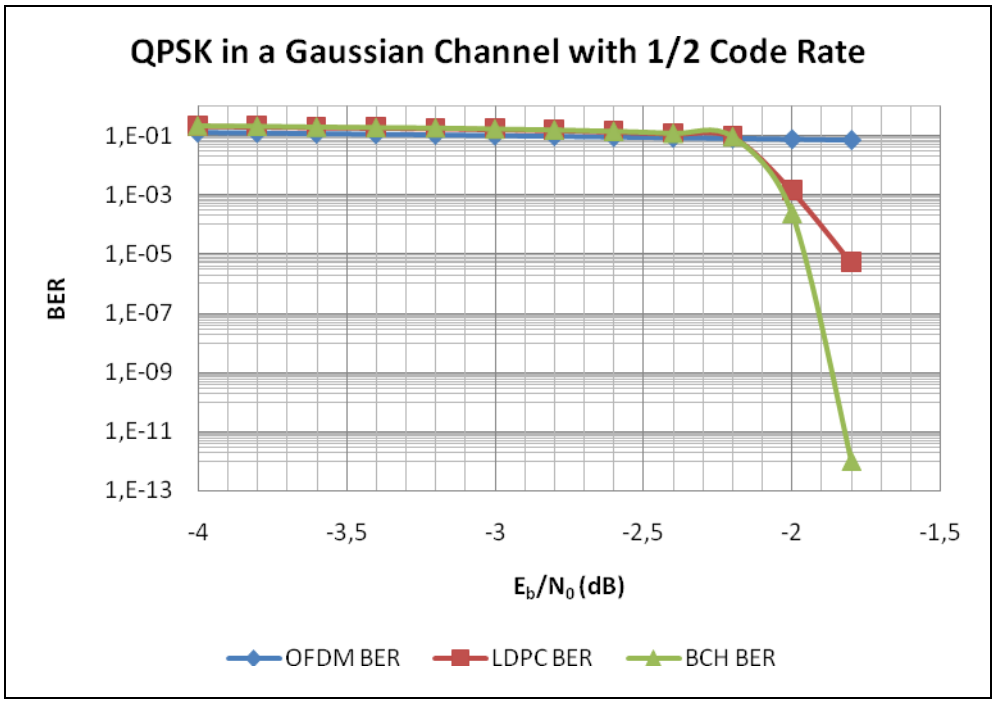

Fig. 5.3: QPSK in a Gaussian Channel with a code rate of 1/2

Notice that different channels require different E_b/N_0 values to achieve the same BER. Obviously, in that case, the Rayleigh channel requires a stronger signal to be received in equal conditions than the Gaussian channel.

It is important to mention that all the simulated figures contain three main parameters:

- **OFDM BER:** BER calculated without considering the code correction effects. Taking into account only the channel effects comparing the transmitted bits sequence before the OFDM mapping with the received bits at the output of the channel estimator.
- **LDPC BER:** BER considering the correction capabilities of the LDPC codes, including the gains introduced by the constellation rotation and the interleaving stages.
- **BCH BER:** The final BER of the system taking into account the effects introduced by the whole system, after the BCH correction block.

This representation is useful for the interpretation of the results, showing the three different behaviours of the different interfering blocks, including the degradation stage (channel errors) and the correction stage (code and interleavers). At last, it also has to be mentioned that the simulations have been realized with a BER probability of 10^{-7} after the LDPC decoder, in order to achieve the corresponding required limit of QEF of 10^{-12} after the BCH decoding block.

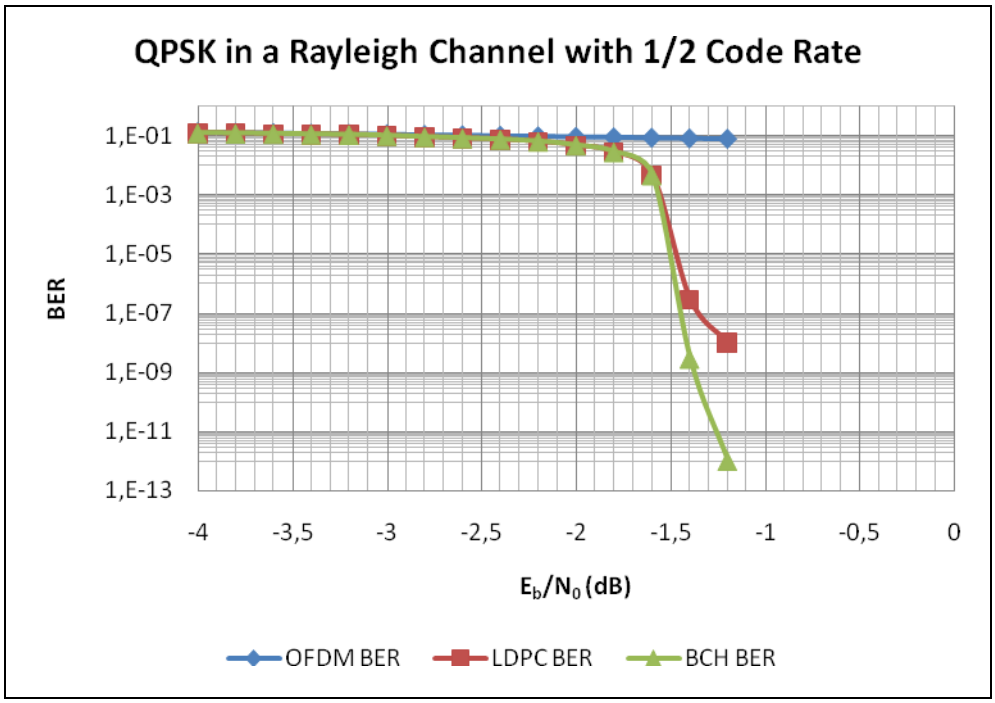

Fig. 5.4: QPSK in a Rayleigh Channel with a code rate of 1/2

5.2.1.2 Code rate: 3/5, 2/3, 3/4, 4/5 and 5/6

Increasing the puncturing pattern, the capabilities of the systems get worse. That fact is due to the less redundant information by coded blocks, making the system more sensitive to the errors and channel fading. In this way, increasing the E_b/N_0 relationship the previous described behaviour is compensated, allowing the correct demodulation **(Fig. 5.5** and **Fig. 5.6)**.

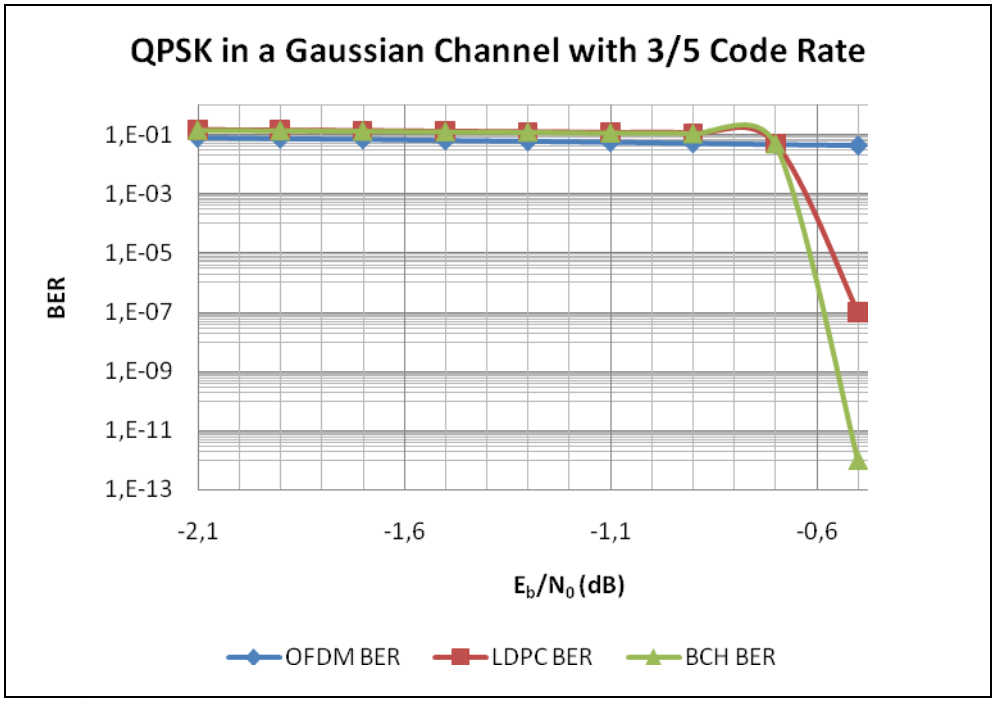

Fig. 5.5: QPSK in a Gaussian Channel with a code rate of 3/5

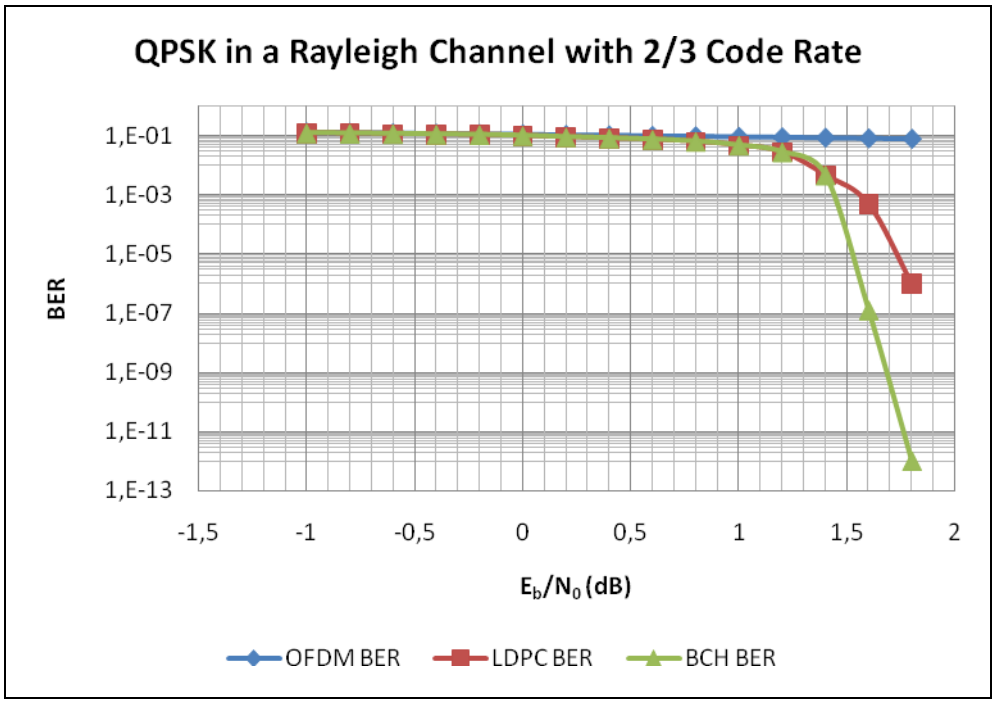

Fig. 5.6: QPSK in a Rayleigh Channel with a code rate of 2/3

Despite of performance of the LDPC-BCH coding block, which is near to the Shannon Limit, it can be observed at **Fig. 5.7** that a plane zone between the theoretical Shannon Limit and the QEF still remains present.

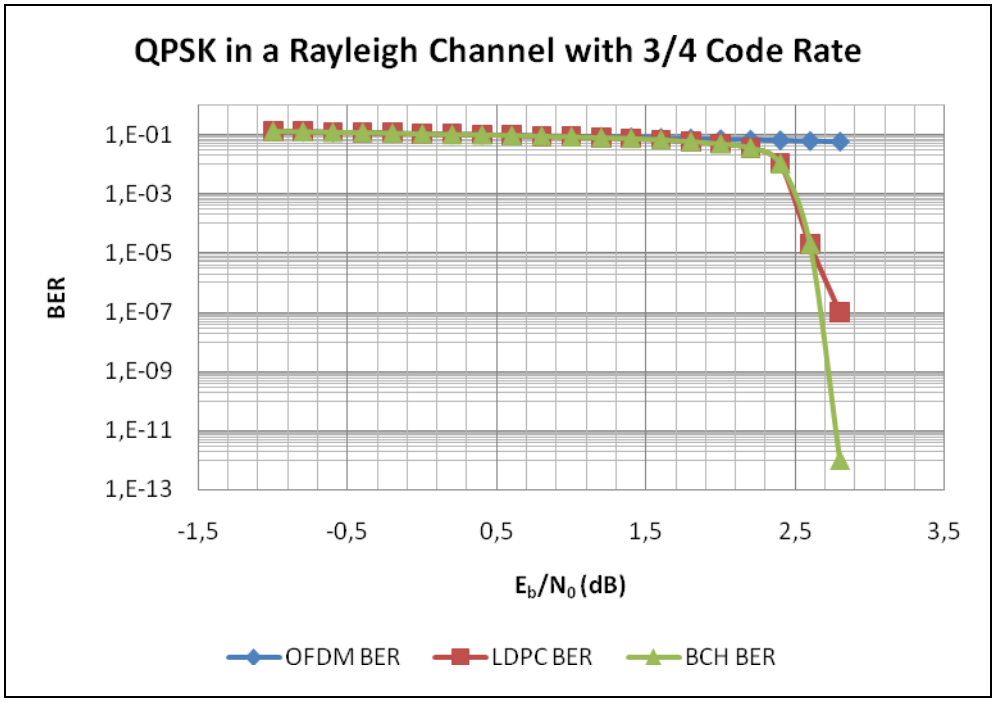

Fig. 5.7: QPSK in a Rayleigh Channel with a code rate of 3/4

That effect is clearly at higher code rates, where the LDPC-BCH behaviours decrease **(Fig. 5.8)**, these effects are more evident in hostile channels. On the other hand, the use of a higher code rate implies the improvement of the information bit rate, allowing better services and features.

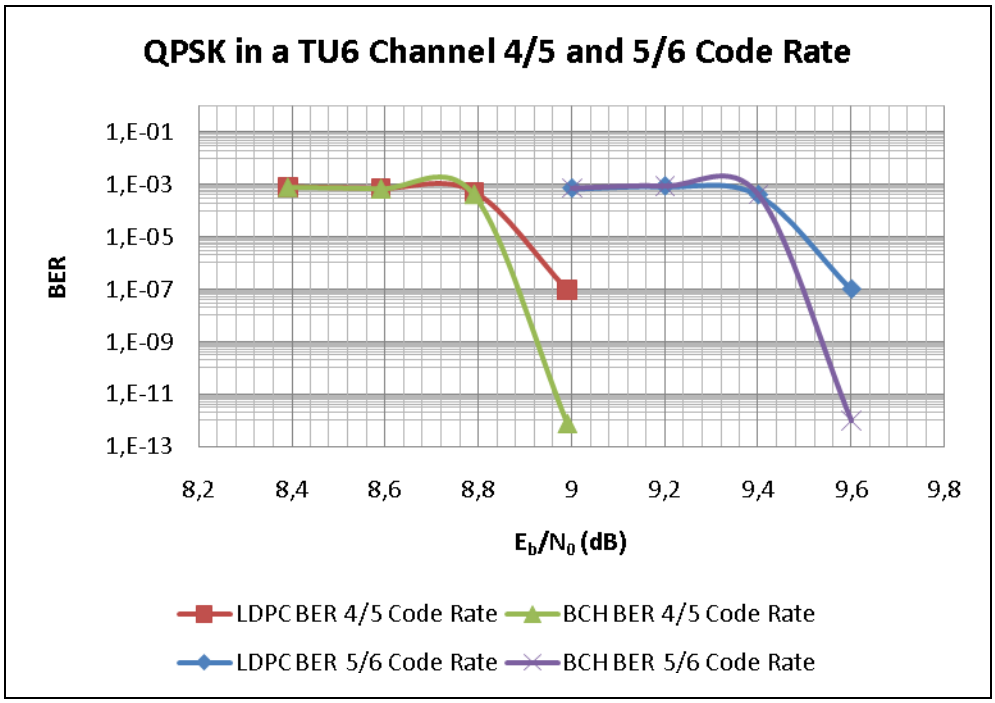

Fig. 5.8: QPSK in a TU6 Channel with a code rate of 4/5 and 5/6

5.2.2 16QAM and 64QAM Modulations

At higher modulation rate, the behaviour described in the previous section can be obtained but with higher E_b/N_0 requirements **(Fig. 5.9)**. The reduction of the decision areas corresponding to each symbol when modulation order is increased causes that at the same noise levels, the symbol error rate is worse. To compensate this effect, the required bit energy needs to be increased for the correct demodulation.

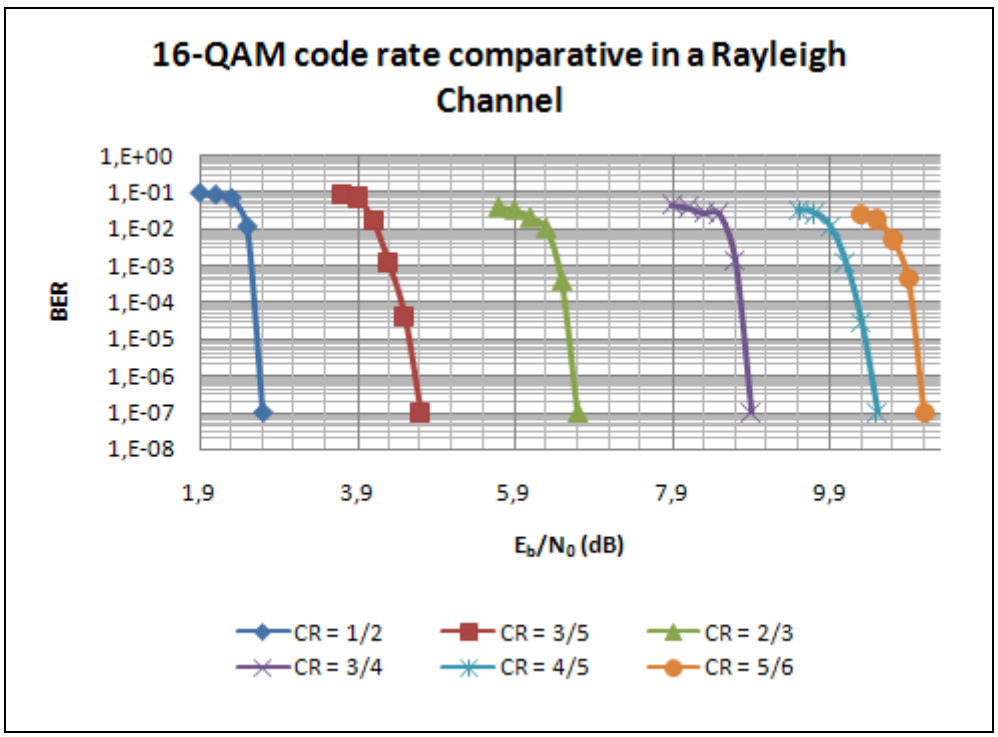

Fig. 5.9: 16-QAM code rate comparative in a Rayleigh Channel

In the 64QAM modulation **(Fig.5.10)** the required E_b/N_0 takes the highest values to reach the QEF received signal. These values are around 15 dB for the higher punctured pattern (close to one), so it is expected that this modulation will work only in low noise environments with the actual standard system definitions.

The simulation results can be used to measure differences between the different code rates and other parameters between channels, obtaining:

- Differences between Channels (Gaussian, Rayleigh and TU6).
- Differences between code rate for a same channel model.
- Differences between different modulation schemes (see *Section 5.2.3*).

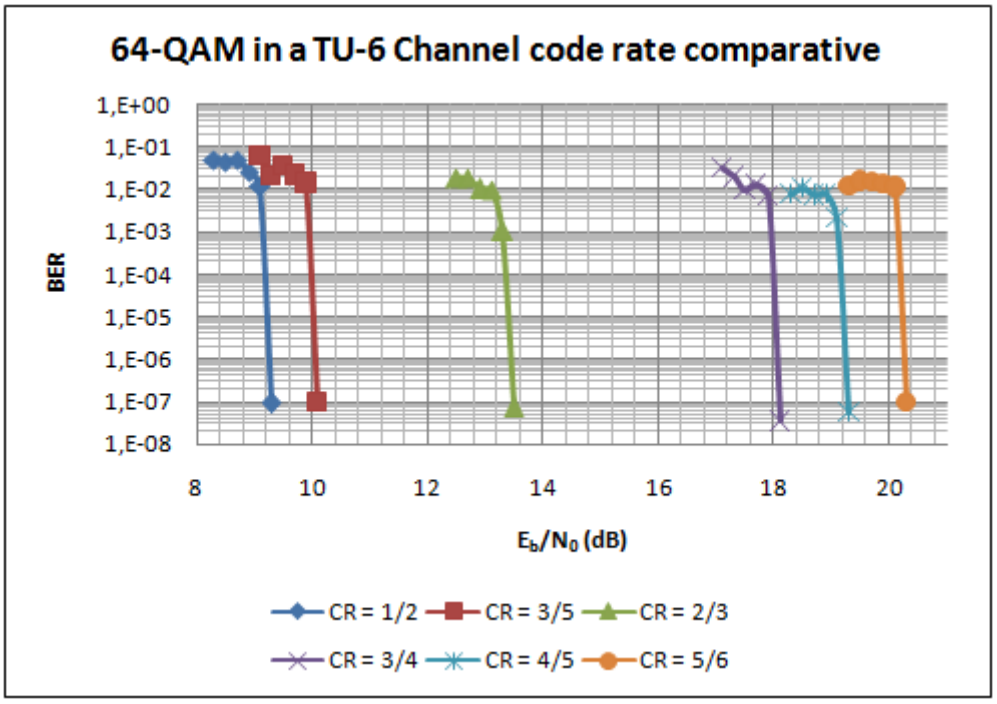

Fig. 5.10: 64-QAM code rate comparative in a TU6 Channel

5.2.3 256QAM Modulation

Finally, the comparison between the different modulations shows all the effects that have been described during this section **(Fig. 5.11)**. The 256-QAM modulation is the one that requires higher E_b/N_0 due to the small decision distance between symbols, to achieve the QEF probabilities.

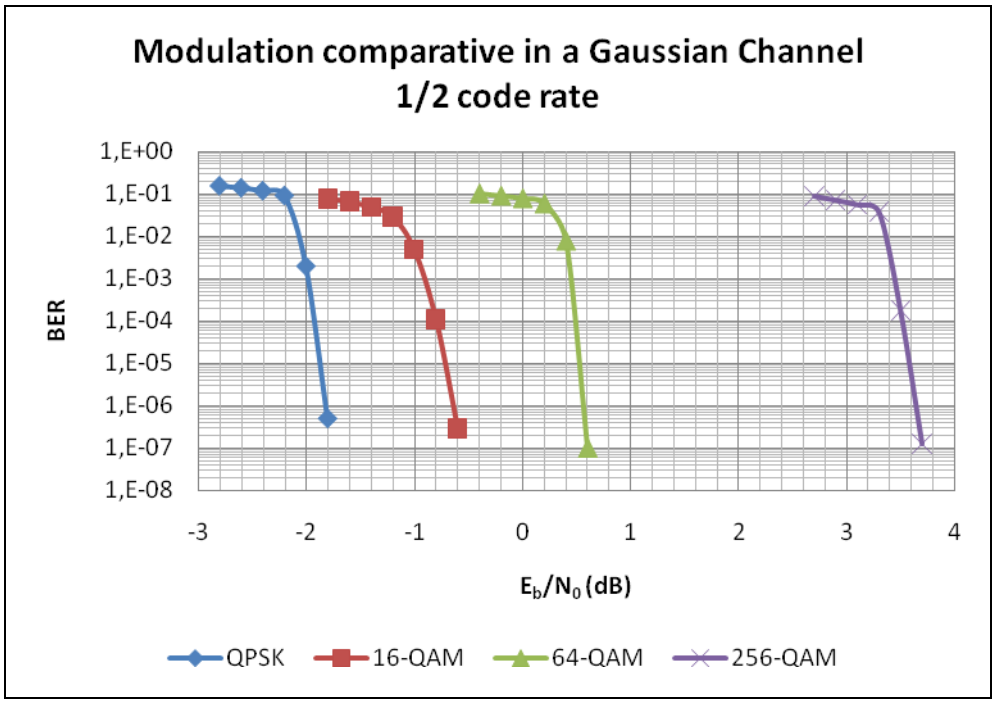

Fig. 5.11: Modulation comparative in a Gaussian Channel for 1/2 code rate

For the same channel model, it can be seen that depending of the employed modulation and code rate, the difference between different required E_b/N_0 can be as high as 20 dB. In that case, the operator service providers have a huge margin of possibilities to offer different services and data rates depending on the environmental conditions, allowing a better matching to the requirements of the users with different power transmission quality levels **(Fig. 5.12** and **Fig. 5.13)**.

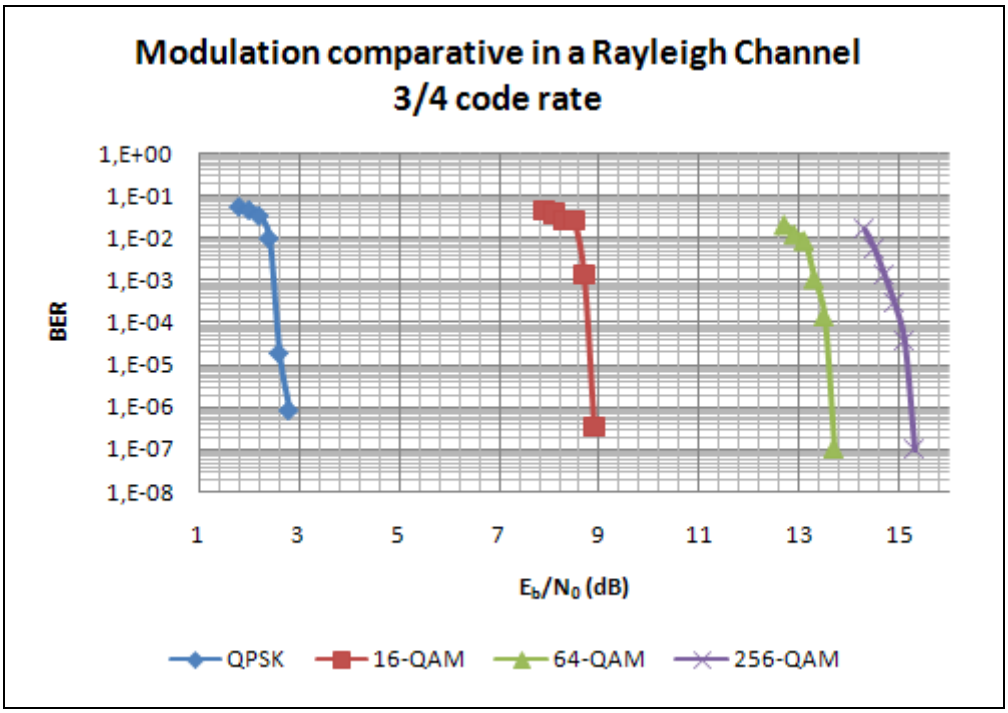

Fig. 5.12: Modulation comparative in a Rayleigh Channel for a 3/4 code rate

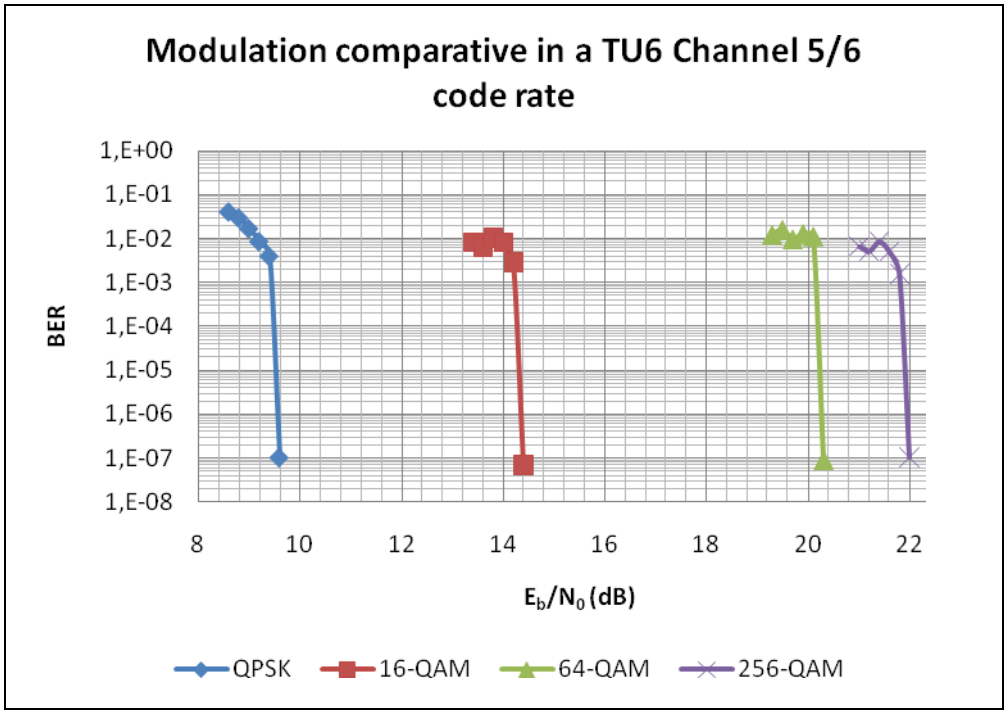

Fig. 5.13: Modulation comparative in a TU6 Channel for a 5/6 code rate

5.3 Comparative between 2K and 32K modes

One of the most important design parameters of the DVB-T2 system is the subcarrier spacing. Since the total bandwidth is fixed, a higher number of subcarriers mean smaller subcarrier spacing.

Greater the number of subcarrier implies a better protection against multipath delay spread, but on the other hand, the effects of phase noise must also be considered. Generally as the subcarrier spacing becomes narrower, the overall system becomes more susceptible to phase noise. Phase noise effects have been studied by several authors [13][14][15][16].

Despite of that fact, the 32K OFDM mode available in the DVB-T2 specifications [3] allows a maximum guard interval of over 500 µs, making it ideal for large, nationwide single frequency networks (SFN) without increasing the guard interval overhead. That guard interval is flexible, allowing more payload bandwidth when long guard intervals are not needed.

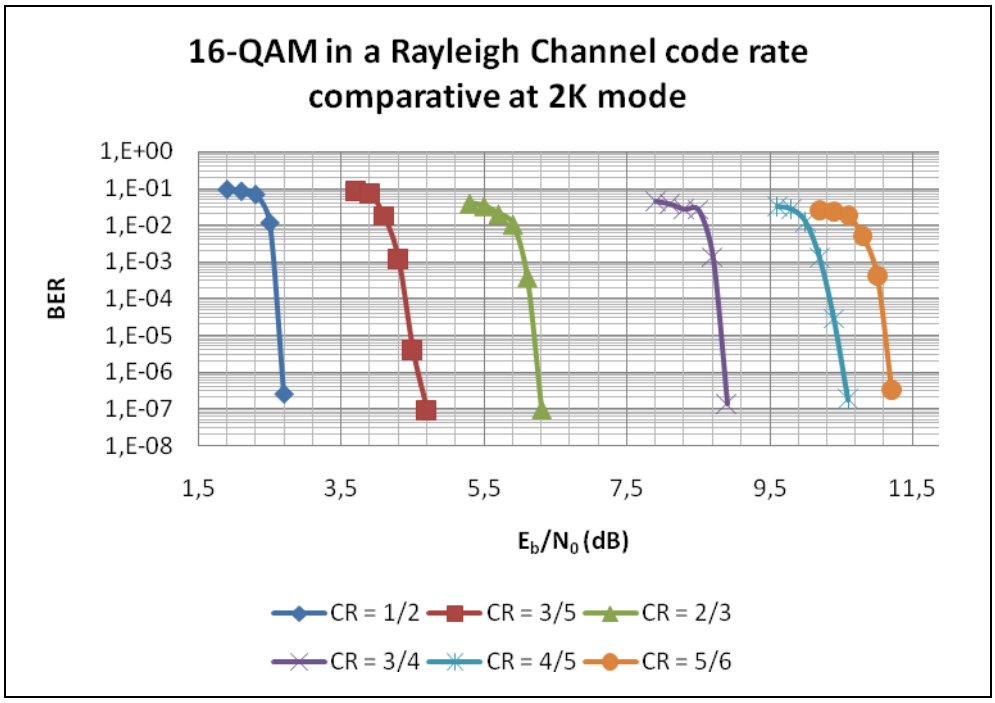

Fig. 5.14: 16-QAM in a Rayleigh Channel code rate comparative at 2K mode

At the DVB-T2 standard and at the implementation guidelines of the DVB-T2 standard the E_b/N_0 values required for the different operation modes are not specified since the carrier spacing doesn't affects to the BER probabilities **(Fig. 5.14** and **Fig. 5.15)**. That fact is due to the bit energy per symbol requirements, which remains constant independently of the number of subcarriers introduced in the OFDM symbol.

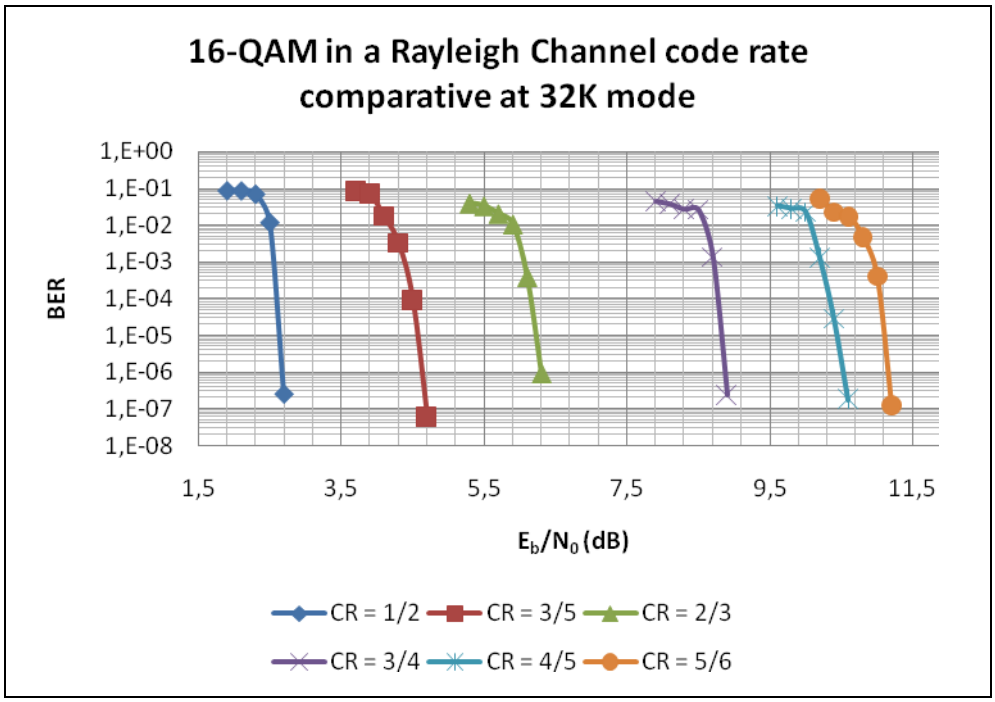

Fig. 5.15: 16-QAM in a Rayleigh Channel code rate comparative at 32K mode

5.4 Constellation Rotation Improvement

As it can be noticed along this *Chapter*, the use of the constellation rotation only allows improvements in the power transmission requirements, achieving the required BER values with slow values of SNR.

The comparison of the system between the use of the constellation rotation and the use of traditional modulation schemes are shown in **Fig. 5.16**. As it can be seen, the use of that technique can achieve an improvement in the system behaviour up to 9.8 dB. On the other hand, the inclusion of that technique did not introduce higher levels of hardware complexity, however, the calculation cost increases in a 2^M factor (where M is the modulation number).

Furthermore, its use is unadvisable in situations where the ACE PAPR techniques introduce higher gains, because they are incompatible. It is also important to be mentioned that the gain introduced by the constellation rotation improves at worse correction conditions (higher code rates and hostile channels). On the other hand, that technique works worse at higher order modulations **(Fig. 5.17)**, where the constellation symbols are closer and the constellation rotation lose their efficiency. That fact is due to the reduction in the symbol projection over the axis, decreasing the decision zone and increasing the error probabilities.

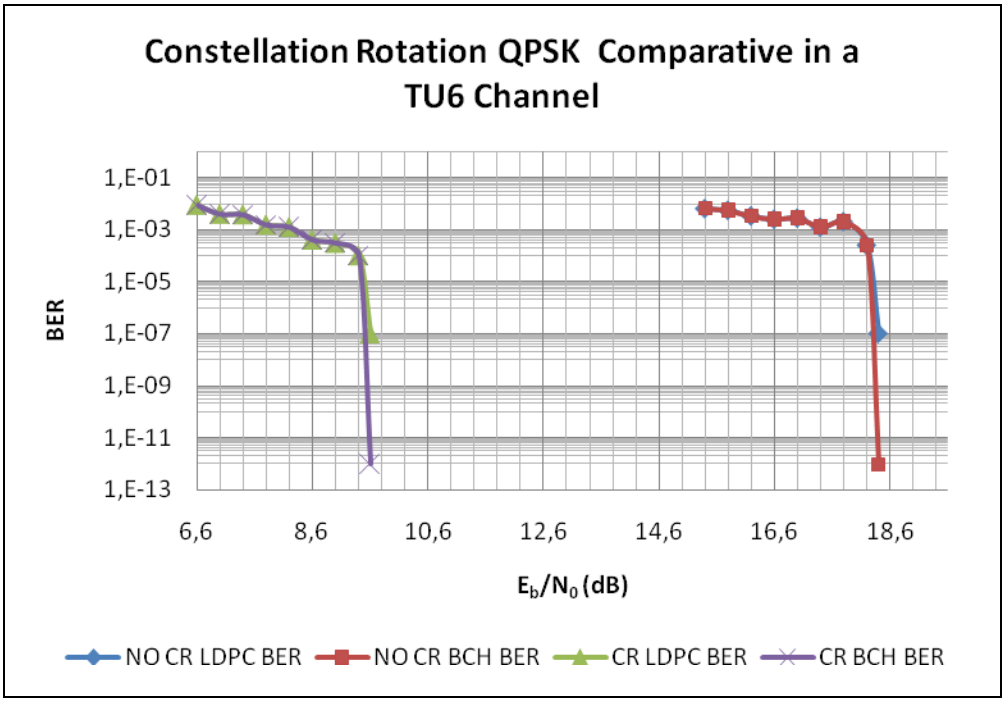

Fig. 5.16: Comparative between constellation rotation and conventional modulation for a QPSK modulation at 5/6 Code Rate in a TU6 channel model

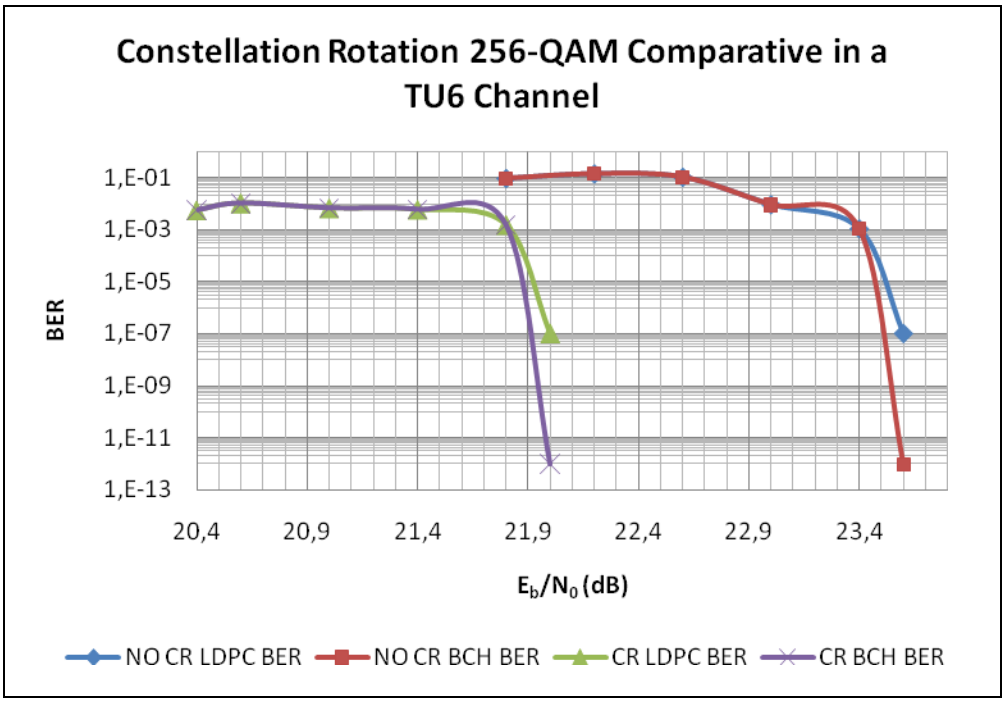

Fig. 5.17: Comparative between constellation rotation and conventional modulation for a 256-QAM modulation at 5/6 Code Rate in a TU6 channel model

5.5 DVB-T2 vs. DVB-T

To conclude the simulation platform results chapter, a study between the two Terrestrial Digital Video Broadcasting standard versions is done. As it is mentioned at *Chapter 1*, one of the main requirements of the new standard version was to increase in a 30% the overall system capacity.

Table 5.2 shows the comparison between the two absolute maximum data throughput of both standards. As it can be seen, the difference between modulations is about 31%, accomplishing one of the main objectives.

Table 5.2: Absolute maximum Bit Rate for the DVB-T2 standard

Modulation	Absolute maximum Bit Rate for DVB-T2 Standard	Absolute maximum Bit Rate DVB-T Standard
QPSK	12.53 Mbps	8.71 Mbps
16-QAM	25.16 Mbps	17.42 Mbps
64-QAM	37.68 Mbps	26.13 Mbps
256-QAM	50.34 Mbps	-

However, it is important to be mentioned that in terms of E_b/N_0 requirements the total gain introduced by the new standard can be higher than that 30%.

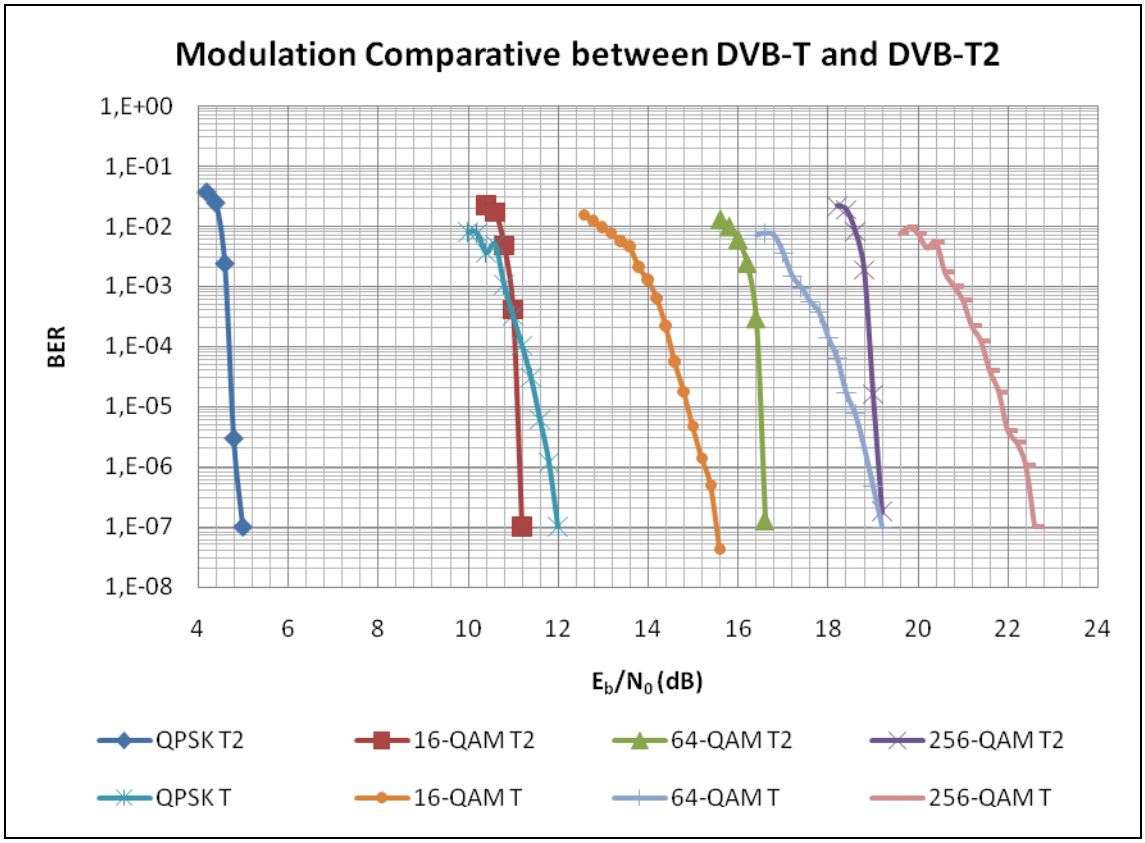

Fig. 5.18: Modulation Comparative between DVB-T and DVB-T2 standards at 5/6 code rate in a Rayleigh Channel

As it can be seen in the figure above **(Fig. 5.18)**, the 64-QAM modulation with a code rate of 5/6 in the DVB-T standard requires 18.4 dB to achieve QEF. On the other hand, the 256-QAM at the same conditions for the DVB-T2 standard requires 19.4 dB, providing a higher maximum bit rate with a marginal difference between both in the E_b/N_0 requirements.

One of the main factors to achieve that gain between both standards is the BICM module. It is seen that the LDPC code outperforms the concatenated code in AWGN, Rayleigh and TU6 f_D=10Hz channels with all studied code rates. It was also observed, that by adding a time interleaver, the performance of the LDPC coded system in mobile channels, such as TU6, can be enhanced. As for the error distributions after the decoding, it was observed that LDPC decoding provides more dense error bursts than the concatenated decoding scheme.

CHAPTER 6: NETWORK OPTIMIZATION WITH SIMULATED ANNEALING

In the context of the FURIA project, new objectives at network level have been defined to lead the joint optimization of the future DVB-T2 standard deployment. After the test and validation of the simulation platform, I2CAT-UPC consortium has been elected as coordinators for the network optimization stage. Next subsection will depict the problems of this network optimization process, as well as the solutions proposed oriented to the network enhancement and closely related with the first trials and driving tests of this new technology.

Within this framework I2CAT-UPC consortium has started a collaborative project with a national telecommunications provider to evaluate and optimize the current DVB-T network deployment in Catalonia. Using real system parameters allows validating the optimization software for a real network, assuring that when used to test DVB-T2 network topology performance, will help to find the optimal solution. For the accomplishment of this purpose the work methodology has been structured in four different steps:

- 1st Step: Definition and study of the problematic in the DVB-T network topology.
- 2nd Step: Development and implementation of new solutions to optimize the quality of the network.
- 3rd Step: Use of a commercial network planning software to perform a realistic coverage study.
- 4th Step: Design and implementation of an optimization software using Simulated Annealing for the improvement of the current network.

The first, second and third step have already been done and tested as is described in next subsections. However the third one has not been implemented yet, because we still don't have permission to use the date coming from the real network deployment.

6.1 Problematic in DVB-T network planning

Different optimization problems in DVB-T network planning have been investigated by choosing different sets of transmitter parameters as decision variables (see [17] for a general framing). Namely, in emission powers and antenna heights are optimized by simulated annealing [18]; in a local search algorithm and a mixed integer programming model are presented for power and frequency assignment [19]; in [20], emission powers are optimized by a LP-based heuristic. The common feature among these problems is that the statistical receiver coverage assessment model recommended for implementation purposes [17, 20] makes difficult to identify a mathematical structure exploitable in algorithms design.

Along this chapter, a study of the optimization of the transmitters time offset (already introduced in [19]) is performed. The time offset problem (TOP) does not arise in analog systems, since it originates from specific features of the orthogonal frequency division multiplexing (OFDM) scheme, adopted by DVB-T and DVB-T2. The practical relevance of TOP has three major motivations:

- Any private broadcaster may implement its own time offset configuration for a network without affecting the service of other operating networks;
- Unlike the case of frequencies, changing time offsets does not require a remarkable economical effort;
- Optimized time offset configurations improve significantly the coverage (especially) of single frequency networks (SFNs), in which all transmitters are assigned with the same frequency.

6.2 Proposed solutions for DVB-T/T2 network planning

General descriptions of the DVB-T system are extensively presented in technical reports from major bodies involved in the DVB-T project, such as [16, 21]. For that reason the proposed solution for the network optimization is based in an analysis of some features of the signal reception and the system exploiting.

A broadcasting network is designed to distribute video programs within a given territory portion called *target area*. This is decomposed into a set Z of “small”, approximately squared, areas (e.g., 2×2 km) called testpoints (TPs). For instance, the Catalonia territory is decomposed into 8,000 TPs. A TP is described by latitude, longitude, altitude and number of inhabitants, represents the behaviour of any receiver (i.e., a user receiving antenna) within it, which is supposed to have fixed directivity (which although it is a limitation of the model it seems quite reasonable).

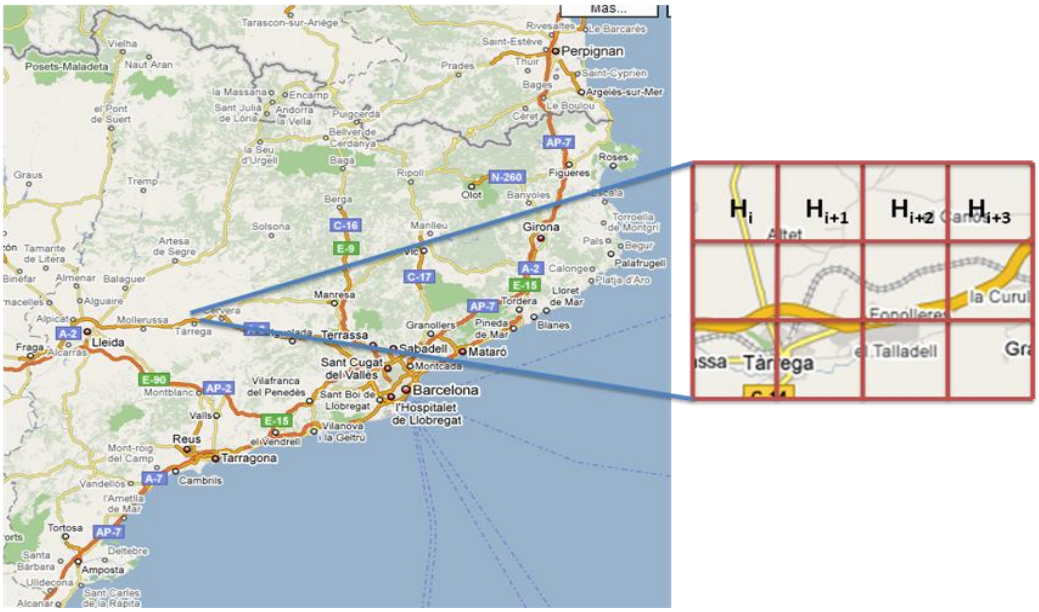

Fig. 6.1: Decomposition in square areas of the Catalonian area

The signal emitted by a transmitter propagates according to transmitter directivity and orography. Taking into account that a transmission consists of a stream of symbols and the propagation delay, the arriving time of a symbol emitted by transmitter *i* in TP_j has the expression:

$$t_{ij} = t_i + \Delta_{ij} \quad \textbf{(6.1)}$$

The power density P_{ij} ($\mu W/m^2$) received in TP_j from a transmitter *i* is proportional to the emitted power P_i, for example, $P_{ij} = P_i \cdot A_{ij}$. Thus a matrix [i,j] with the received power densities can be defined as seen in figure **(Fig. 6.2)**.

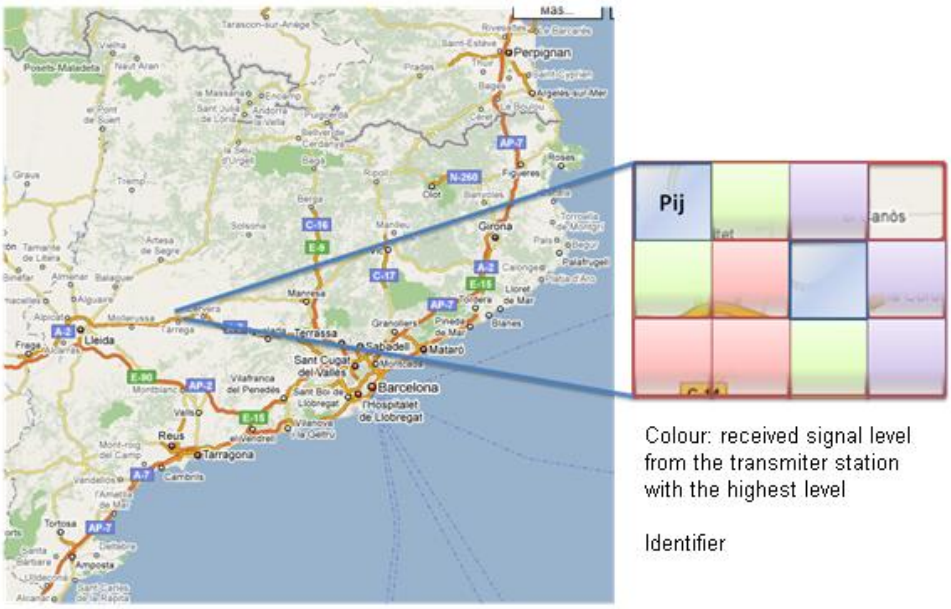

Fig. 6.2: Received density power matrix example

In fact associated with the received signal from each transmitting station a single contribution is not received. The reception stage receives different copies of the signal due to multipath (reflections, diffraction and combinations of both) effects. However, these delays are in general quite close to $\Delta\tau_{ij}$, and are considered negligible in this study. Just in some special environments (as for example coverage in rural and mountain areas) different delays from a transmitter station are possible due to the travelled distance differences between the signals. A delay matrix (similar to the previous figures) can be defined.

At the TP_j the signal of a certain number of stations is received: T(j) indicates the T subgroup detected at *j*. In this way a graphical representation for each TP can be performed with the following parameters:

- Number of transmission stations detected T(j).
- Power level (or power density level) received at each station.
- Total associated delay.

In the definition of the TOP problem the key notion in the coverage assessment is the notion of interference. In analog systems, different signals arriving on a receiver with the same frequency always interfere (co-channel interference). Due to the OFDM scheme, this is not always the case in digital systems. In fact, the receiver (in TP) *j* locates at time τ_j a detection window: all signals falling into the window are wanted, whilst the others are interfering. Figure **(Fig. 6.3)** shows an example of the different received signals at a given point.

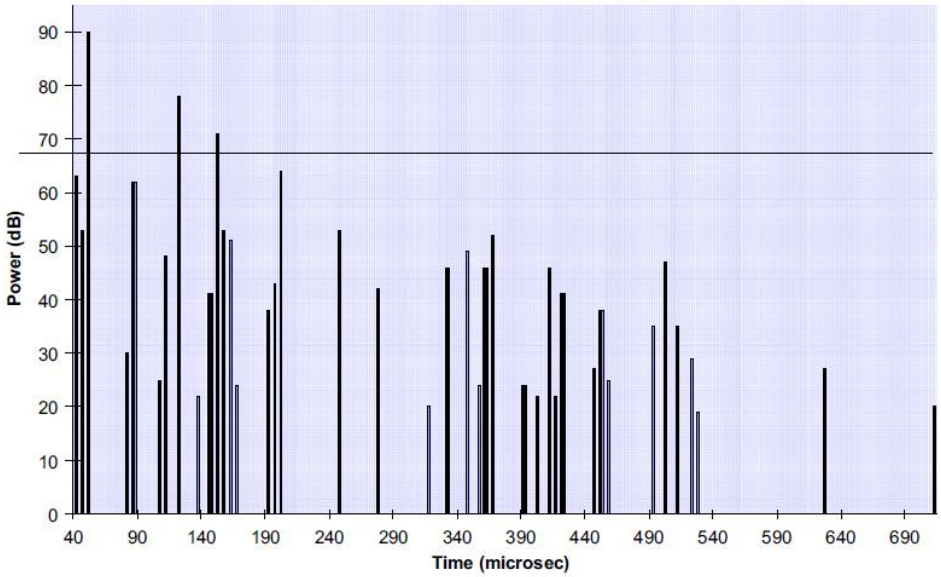

Fig. 6.3: Received signals at the receiver

If the shape of the detection windows is considered as it can be seen in figure below **(Fig. 6.4)** a signal (symbol) from transmitter *h* arriving in TP_j at time τ_{hj} contributes to the wanted signal if $\tau_{hj} \leq \tau_j$ +Tg (Guard intervals are defined in *Chapter 4* at **Table 4.10**) while it is interfering if $\tau_{hj} > \tau_j$ + Tg.

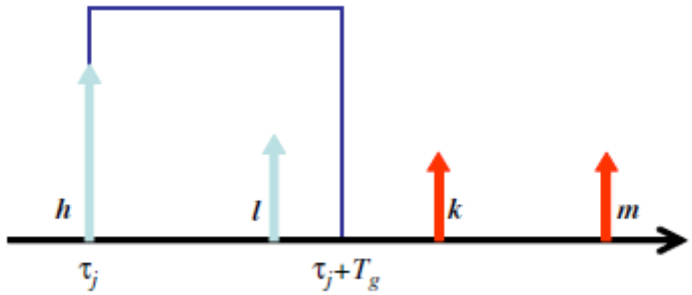

Fig. 6.4: Detection window in TP j and synchronized with signal h: signals h and l are fully wanted; k and m are fully interfering

Another point that has to be taken into consideration is that the different transmitter stations are configured with certain guard intervals periods, and these guard intervals can be different from one station to another. An optimal

definition of the guard interval periods could also reduce the interference at a given reception point.

Once the problematic has been defined the proposed solution for the TOP problem is based in the Simulated Annealing algorithm. Simulated Annealing allows obtaining the optimal temporal offset of each transmitter station, minimising the absolute cost in the entire region. It is based in the measure of the interference level, specially penalising the produced interferences in highly populated TPs. It also provides:

- If a new transmitter or repeater station is added, the network calculations can be easily remade, obtaining the new optimal network configuration.
- If a problematic zone is detected, the algorithm allows a relatively fast calculation if the problem can be solved modifying the configuration of certain transmitter stations, and detecting the influence of these modifications over other TPs.
- Finally if the problem does not have a solution with the present stations, it allows to quickly detecting if the addition of a new transmitter or repeater station could reduce the problematic.

6.3 Description of the Simulated Annealing optimization

Simulated Annealing has proven to be one of the most efficient tools for the frequency deployment optimization in GSM-GPRS and TETRA networks, obtaining a great cost reduction (interferences) in front of other heuristic techniques (iterative and non iterative). It also has been employed in the 3G networks for the optimization of the pilot levels, base station antennas downtilt, terminal Active Set parameters, etc.

The Simulated Annealing is a metaheuristic algorithm that optimizes the cost function of the defined TOP problem. However for the solution implementation the different scenario parameters have to be well defined. In the next points a description of the scenario parameters and the estimated optimal values are shown.

6.3.1 Propagation model

One of the main parameters that have to be defined for the network modelling is the signal level (dBm) or the received power density in each TP, originating from the different transmitter station. At this point two options can be used:

- Measures results.
- Propagation model (for the DVB-T standard the ITU organization has defined the ITU-R 526_100 [22] as the recommended channel for the DVB-T network planning).

6.3.2 Receiver considerations

In the SFN networks, different stations simultaneously transmit the same program. The signal originating from different sources at a given point can be considered as a constructive or destructive interference, depending on the delay of the signals from the dominant.

As it has been described in the previous section, the received signals at the receiver have time differences depending on the transmitter distance to the TP. If these time phase shifts allow the arriving of the desired signal out of the guard interval the auto-interference problem will take place on the SFN network.

Following this line, the receiver also has an important role since depending on the receiver type the synchronization with the desired signal is different. Currently two different synchronization methods have been deployed on the commercial systems:

- First echo receivers: These receivers evaluate the delay of the different signals from the dominant signal (see **Fig. 6.5**). This delay is a function of the distance difference between the transmitters and the TP and also the relative delays from the transmitters.

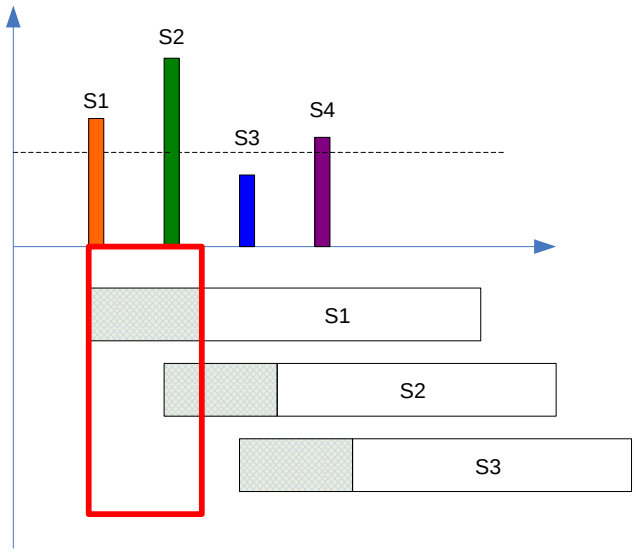

Fig. 6.5: Synchronization in first echo receivers

- Best echo receivers: These receivers establish the transmitter whose signal imposes the reference symbol (see **Fig. 6.6**). This transmitter can be whatever the desired one, or the transmitter that has whose signal has arrived first with a signal level above a certain threshold.

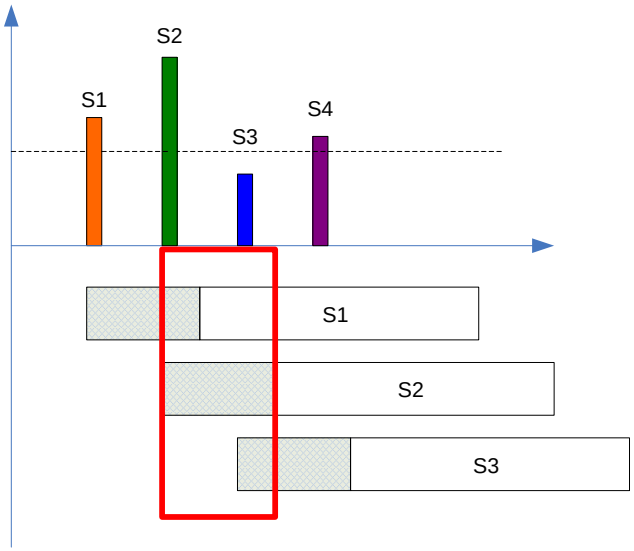

Fig. 6.6: Synchronization in best echo receivers

6.3.3 Radio planning scenario

The first parameter that has to be considered for the design of the proposed solution is the differences from the transmitter stations parameters. The most important parameter is the guard interval which may be different for many different groups of transmitter stations.

In other hand it also has to be considered that the group T(j), listened transmitter stations at the TP_j can be classified in two categories:

- $W(j,\tau_j)$ as desired contributions
- $I(j,\tau_j)$ as interference contributions

Different studies point out that a TP_j is covered if the following condition is satisfied:

$$\sum_{i \in W(j,\tau_j)} P_{ij} \geq K \sum_{i \in I(j,\tau_j)} P_{ij} \qquad \textbf{(6.2)}$$

Once all the parameters are lineally defined a K constant is defined. This parameter depends on the required CIR (*carrier to interference ratio*) which can vary between 20 to 40 dB depending on the environment and the kind of the scenarios. Therefore the solution has to:

- Fixed Offset: test if with the different τ_j possible values (this values match up with the arrival times from the signals received at the TP_j) there is anyone that satisfies the previous defined equation **(6.2)**.
- Unsettled Offset: assign to every transmitter a T_i optimal offset value that satisfies the previous defined equation **(6.2)**.

In this case it could be said that the TP_j is well covered. The subset of covered TPs is noted as C. The function to be optimized, also denominated “global coverage area” is **(6.3)**:

$$\sum_{j \in C} w_j \qquad \textbf{(6.3)}$$

Where w_j, usually in practice represents the weight function, which is equal to H_j (the number of inhabitants at the TP_j). The reason of taking the number of inhabitants as the optimization parameter is defined in order to prioritize the maximization of the reception over populated areas instead of inhabited areas where the maximization of the coverage area would not suppose an added value for the service providers. The higher value of the function represents a better solution obtained, furthermore in the Simulated Annealing tool, the cost function (that has to be minimized) will be inverse proportional to the global coverage area.

6.2.4 TOP definition

For the formulation of the algorithm, the first that has to be taken in to account are the following two considerations:

1. Given a TP_j, it can be defined from the received stations T(j), that a subgroup S constitutes a coverage group if the differences between the different delays τ_{ij} , two-by-two from all of them, is lower than the guard interval time Tg. It is possible that a TP could have different coverage groups; the subset of coverage groups is noted as ψ_j. The TP_j will be covered (in the case of a fixed time offset) if it exists a coverage group whose all the received signals are inside the detection window (Tg). This coverage group would be the active coverage group. For the optimal reception it must exist at least one in each TP.

2. General case (for unsettled time offsets): the temporal offset values have to be found in order to guarantee the condition that at least an active coverage group is found at each TP. This is a complex problem where it may not exist a solution depending on the scenario.

The mathematical description of the algorithm is as follows:

As it has been defined every TP can accept more than one coverage group. For example a TP_j can accept $S_1(j)$, $S_2(j)$ …$S_{rj}(j)$ coverage groups.

At this point two binary variables are defined:

- x_j (1 if there is not a coverage group at TP_j, otherwise it will be 0).
- y_{hj} (1 if the h coverage group is active, and 0 otherwise).

With both variables and the optimization parameter the algorithm tries to satisfy the following conditions:

$$\min \sum_j w_j x_j \quad for\ all\ j$$
$$x_j + \sum_{h=1,\dots r_j} y_{hj} \geq 1 \quad for\ all\ j$$
$$\left|\tau_{ij} - \tau_{kj}\right| + M \cdot y_{hj} \leq T_g + M \quad for\ h = 1, \dots r_j\ , \quad i,k \in S_h(j) \qquad \textbf{(6.4)}$$

This method requires knowing the ψ_j set, this is all the coverage groups, for every single TP_j which in fact can result in a computationally expensive method. However this calculation can be simplified with the following consideration:

$$\sum_{i \in S} P_{ij} \geq K \sum_{i \in TPj \setminus S} P_{ij}$$
$$P_{kj} > \frac{1}{K} \sum_{i \in TPj \setminus \{k\}} P_{ij} \quad for\ k \in TPj \qquad \textbf{(6.5)}$$

If this condition is satisfied, k belongs to all the TP_j coverage groups. Defining S as the transmitter stations contained in all the TP_j coverage groups, and being S a coverage group, it can also be demonstrated that the group S is the only coverage group of TP_j. This assumption allows simplifying the computational complexity with an error value that can be considered negligible.

6.3.4 Simulated Annealing algorithm

Along the previous section it was explained that radio planning optimization can be posed as a combinatorial optimization problem. Indeed combinatorial optimization aims at finding the set of parameters that maximizes (or minimizes) an arbitrary cost function, in this case defined by the radio planning engineer. In this sense, the most popular resolution approach was the Local Search (LS), which can be roughly summarized as an iterative search procedure that, starting from an initial feasible solution S, progressively improves it with a series of modifications. In particular, the set of new solutions that can be generated from the current one is the solution neighborhood N(S) and all the possible solutions conforms the solutions space. The search terminates when it encounters a solution that cannot be improved with any modification. Thus, with almost all likelihood the algorithm will not reach the best possible solution and will get trapped in a local minimum.

SA (Simulated Annealing) is one of the algorithms that enjoy more popularity in the resolution of combinatorial optimization problems. SA attempts to mathematically capture this process of controlled cooling and apply it to combinatorial optimization problems. The cooling process is formulated as the search of the solution implying a lower cost (energy). Every new solution is generated by applying a slight perturbation over the current one. In this case one of the paramount components of SA is the transition between solutions and the process that describes them. In particular, the transition depends on the T parameter, which is the probability that a system has a particular energy state is given by the Boltzmann- Gibbs probability distribution of statistical mechanics:

$$P\,(energy\ state = x) = c_t\, exp\left(\frac{-x}{k_B T}\right) \quad \textbf{(6.6)}$$

Where:

- c_T : Normalizing constant ($c_T > 0$).
- k_B: The Boltzmann constant ($1{,}38 \cdot 10^{-23}$J/K).

Likewise, from a physical viewpoint, there is some non-zero probability of reaching a higher energy state. As a consequence uphill movements are allowed with a certain probability too, which decreases as the temperature is lowered. Thanks to this strategy, the algorithm is able to escape from local minima, especially at the beginning of the optimization and facilitating a more efficient exploration of the solutions space.

In order to make of SA a robust procedure, it is desirable that the quality of the final solution is independent of the initial one. Thus, the value of T0 must be high enough so that most of transitions are accepted; otherwise the algorithm could be conditioned to be trapped in local minima.

The initial value can be easily found starting with a small value of T_0 and multiplying it by a value greater than 1 until the ratio of accepted solutions is close to 100%. In the simulations of this work the search is stopped when this ratio is higher than 85%.

On the other hand another important parameter is the cooling strategy. In this case, for a slow enough cooling strategy, if stationary is achieved at level n, in the next one (n+1) the number of required iterations will be lower because results are going to be very similar and stationary will appear sooner. Hence, and outlining the importance of having a long enough iteration at T_0 several authors have proposed as the most appropriate cooling update the following equation:

$$T_{n+1} = \frac{T_n}{1 + \frac{T_n \cdot (1+\partial)}{3\,\sigma_n}} \quad \textbf{(6.6)}$$

The aggressiveness in the reduction of T_n can be controlled with δ so that simulation time can be adjusted to the available one. On the other hand, σ_n represents the standard deviation of the cost evolution with temperature T_n. The optimization of both parameters is the key point in order to obtain the optimal solution of the Simulated Annealing algorithm. In this report different values of δ and σ_n have been tested in order to obtain the optimal preliminary result. However in a real data network optimization stage these parameters should be found in order to exploit the Simulated Annealing algorithm benefits.

6.4 Preliminary Results

The goal of this first approach to the DVB-T and DVB-T2 planning optimization solution is to test the enhancement of this solution with the Simulated Annealing algorithm, since as it has been defined at the beginning of this chapter, the idea is to optimize the whole Catalonian area network. This first approach will be very useful in order to ask for the real data of the current implemented network and it also will show the improvement of the network with this almost implementation cero cost solution.

Thus the resources available for the network planning optimization are the following:

- Forsk Atoll
- Matlab
- Catalonia digital elevation model (20x20 m.)
- Catalonia ortophoto image (20x20 m.)

The Forsk Atoll tool is a very powerful network planning tool that allows to generate the coverage maps of different mobile communications systems (as for example GSM, WiMax, LTE, etc) and manage its parameters. However for the development of the project this tool has not been used in this stage since no network parameters (antenna allocation, transmitted power, offset parameters and population data) have been available. For that reason a previous Matlab scenario has been considered to test the functionalities of the Simulated Annealing algorithm.

The implementation has been done with the Catalonia digital elevation model available, in order to take into account the coverage area of the different transmitters with the selected channel model. In this first evaluation of the proposed Simulated Annealing based solution stage, it has been defined a possible scenario over the Lleida province **(Fig. 6.7)**.

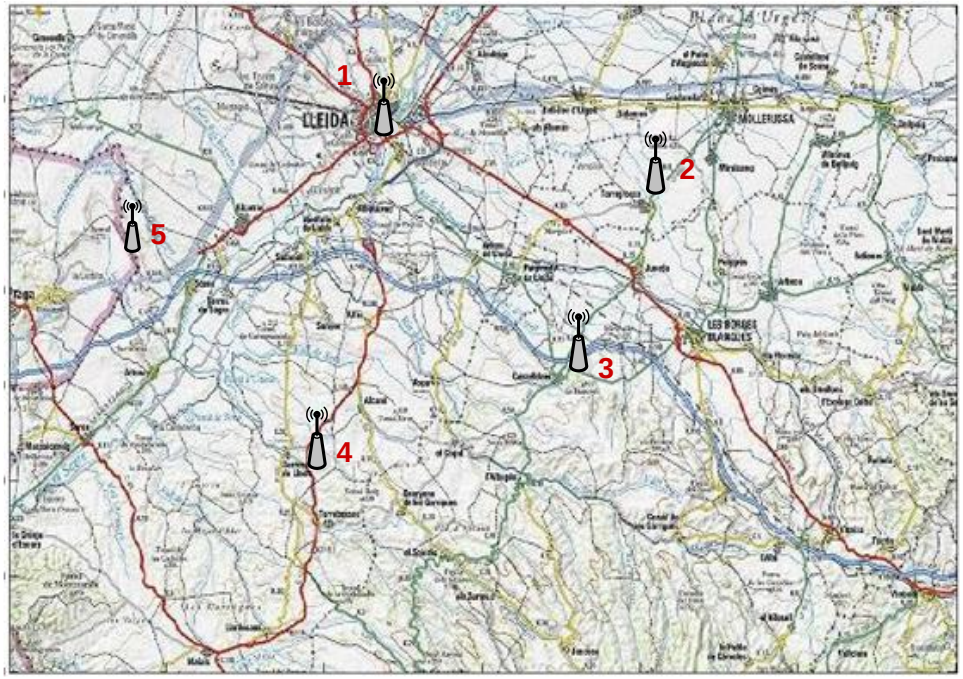

Fig. 6.7: Studied area for the network optimization

The parameters of this possible DVB-T network configuration are the following:

- Number of transmitting antennas: 5.
- Sites allocation: Lleida (1), Torregrossa (2), Puigverd de Lleida (3), Sarroca de Lleida (4), Lo Puntal (5).
- Initial transmission delay: 0 μs for all the transmitter stations
- Antennas: Omnidirectional.
- Transmitted power: 1 W for all the transmitter stations.
- Channel model: Okumura-Hata.
- Transmission mode: 32 K.
- Guard Interval: 1/128 (28 μs).
- Receiver Sensitivity: -78 dBm

For the definition of the simulation environment with Simulated Annealing the tests have been performed fixing all the transmitters with a specific guard interval value. However the simulation platform has been designed for supporting guard interval variability and it is prepared for a possible future development stage with real network parameters.

6.3.1 Coverage analysis

The first step to validate the proposed optimization solution is to generate the initial scenario coverage map **(Fig. 6.8)**. In this context with the previous defined parameters a study of the coverage area is performed.

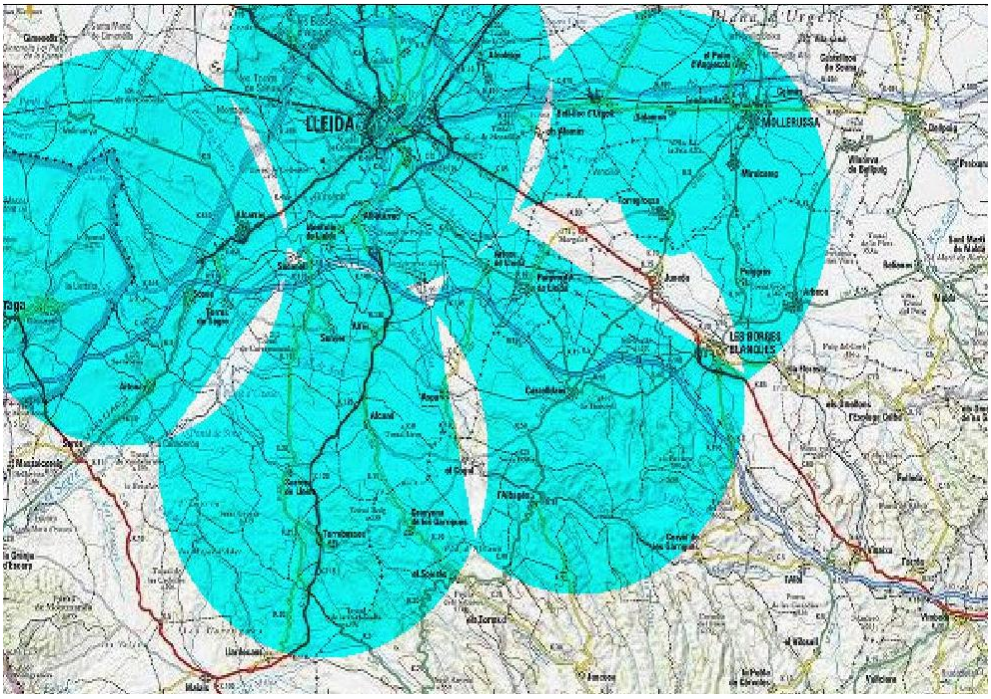

Fig. 6.8: Initial coverage map

The coverage represented in figure **(Fig. 6.8)** is defined as the received power above the receiver's minimal sensitivity (-78 dBm) and taking into consideration the interferences produced by the different antennas at a given point. These interference signals generate a lack of coverage if the difference between the contributing signals (inside the guard interval) and the interfering signals (outside the guard interval) is bellow than a defined margin. The defined margin for this scenario is 20 dB, as it is defined in the DVB-T standard [7].

As it can be seen on the figure the omnidirectional antennas placed on the defined sites cover large areas of the Lleida province. With the channel model defined (Okumura-Hata) and taken into account that the scenario orography is almost flat; the coverage area of each site is almost a circular form. However in the neighbouring between sites there are small zones without signal coverage. The reason of this lack of coverage in these small zones is the time offset problem defined in the previous sections.

With these initial scenario definitions several tests have been performed in order to obtain the optimal cooling strategy for the Simulated Annealing algorithm and thus to optimize the overall network coverage. These parameters are the following **(Table 6.1)**:

Table 6.1: Final cooling parameters

Cooling parameters	
δ	0.1
σ_n	0.5

With both parameters defined the final coverage map of the scenario is shown at the figure bellow **(Fig. 6.9)**

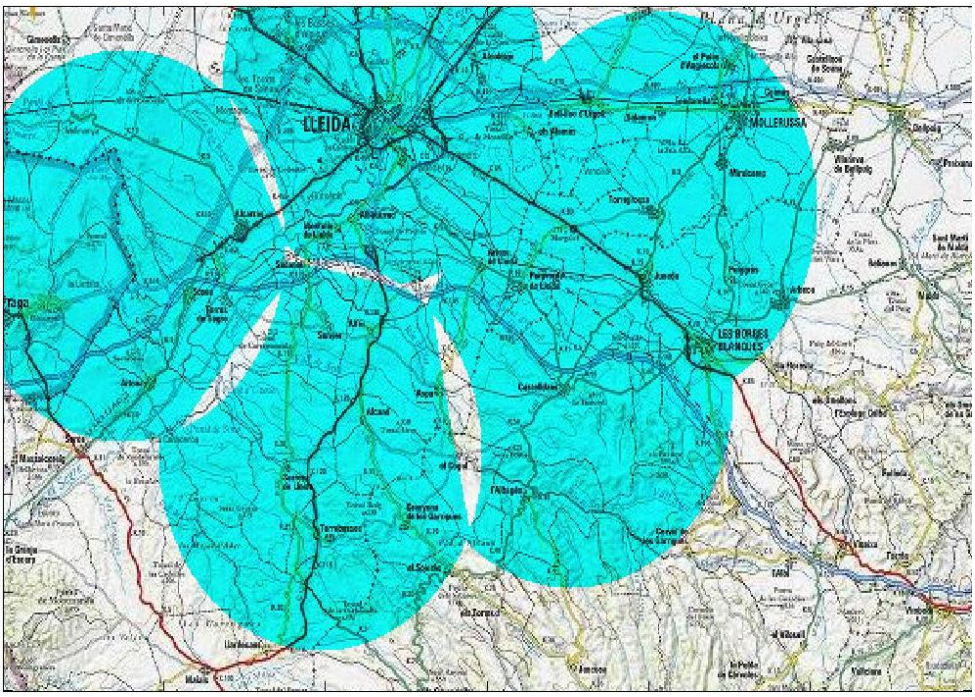

Fig. 6.9: Final coverage map

The final result after applying the simulated annealing algorithm is a coverage improvement of all the neighbouring zones. As it can be seen in the final map the worst affected zone (the east part of the map) is the one that has experienced a higher improvement and no uncovered pixels are found. Also the other neighbouring zones have reduced its lack of coverage.

Furthermore making a calculation of the pixels covered in both situations it can be seen that an increase of around a 5% in the number of coverage pixels is obtained.

On the other hand, the definition of the initial scenario was defined with a zero delay time synchronisation scheme. In figure **(Table 6.2)** the time offset for each site is also represented.

Table 6.2: Offset parameters introduced by Simulated Annealing Algorithm

Offset Parameters		
Site Number	Allocation	Time Offset (μs)
1	Lleida	0
2	Torregrossa	32
3	Puigverd de Lleida	87
4	Sarroca de Lleida	78
5	Lo Puntal	38

Finally in order to validate the obtained results a figure representing the evolution of the cost function is shown at figure **(Fig. 6.10)**.

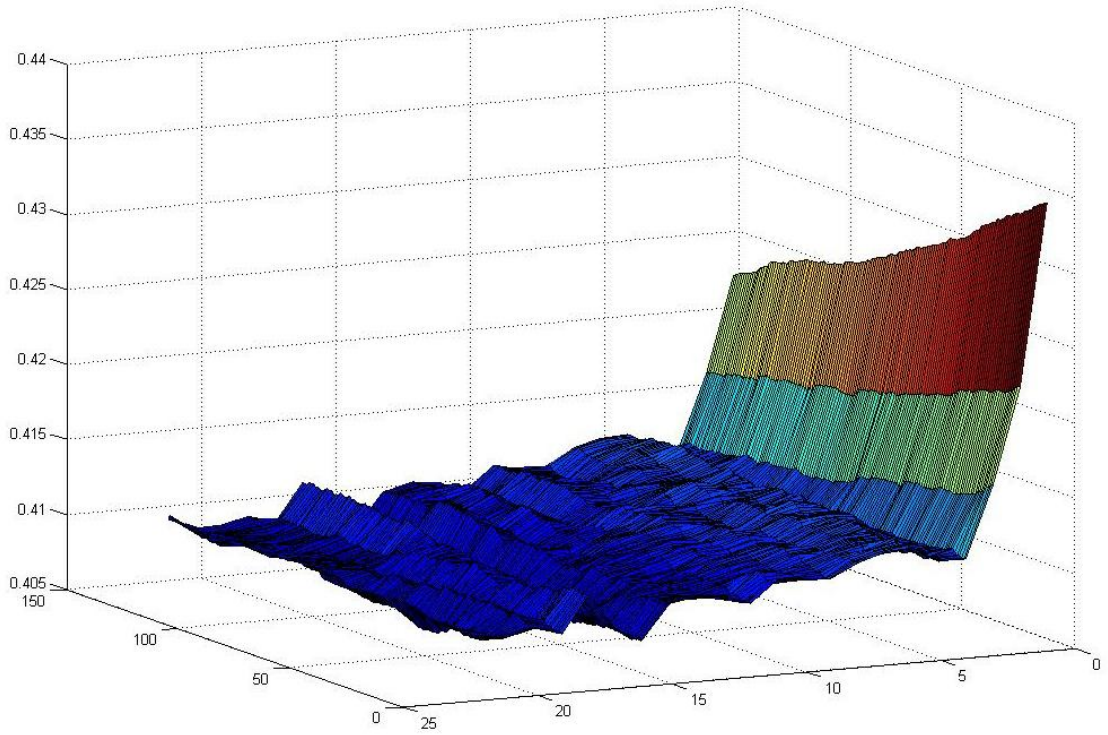

Fig. 6.10: Cost function evolution

Thus as it was expected the cost function experiments increasing and decreasing processes during a given temperature value, and it also experiences the same effect with the temperature cooling. However after a temperature change the increase/decrease value is more abrupt than in a same temperature value.

Another important point that can be observed in the previous figure is the presence of local minima over the whole simulation process. The most important task in this stage is to evaluate which is the global minimum of the function in order to obtain the best possible solution. This result can only be achieved after a long iterative simulation stage.

As previously mentioned along the *Chapter*, it is expected to improve all this parameters and simulations in order to achieve the absolute minima in a real scenario in the near future.

CONCLUSIONS

During the realisation of this project, the study, design and implementation of a simulator platform capable to test the next generation of the digital terrestrial video broadcasting has been realized. The main goals of the project have been accomplished, including additional research and studies of improving methods for the DVB-T and DVB-T2 network planning. It is important to mention that the whole project has been done inside the FURIA project (a national AVANZA project with the participation of the most representative companies and research teams of the audiovisual technologies at national level).

The experience has been long and hard, but on the other hand it has been edifying and beneficial for our future career. Specially thanks to our teachers and tutors along that project: Silvia Ruiz, Luis Alonso and Mario García. Also thanks to the people that have contributed in the development of the simulator platform along that years.

As it can be seen along this report, the simulator platform is capable to test all the possible parameters and enhancements introduced in the new DVB-T2 standard, including: operational modes, modulations, code rates, pilot patterns and channel parameters. Referred to that part, five channel models are programmed and three are fully tested to ensure that the software simulator works properly.

Following that argumentation, the main goal of the project has been successfully achieved, the test of the new enhancements introduced by the DVB-T2 in front of the DVB-T standard. The main conclusion extracted from the graphical results confirms that the goal defined for this new standard, a 30% improvement in terms of data rate capacity, is accomplished. That enhancement allows better services and new user experiences, such as the HDTV. Furthermore, the simulator platform allows quantifying those improvements in all the operational modes and configurations, making it suitable for the future network implementation process.

On the other hand, as has been said during the report, the project is based into the DVB Bluebook A122-TM3980 Rev.5, expecting the official ETSI standard for the new DVB-T generation. At that point the simulator is deeply prepared to face future modifications and extensions, adapting it to numerous simulation situations or possible changes introduced by the new ETSI standard structure.

In a future perspective study, it has also been defined a network optimization tool to improve the capabilities of DVB-T and DVB-T2 network implementation. That tool is based into a meta-heuristic iterative algorithm (Simulated Annealing) that performs an exhaustive search of the optimal time offset parameters for its transmitting antenna of the network.

That tool can significantly simplify the operator planning decisions, providing a support for the network parameters choice in conjunction with an assessment and an identification of the geographical areas that are best / worst treated.

This work has been chosen to optimize the time offsets between transmitters (that should be synchronized by using GPS); however, this is just an example. The tool can be used to adjust any parameter of the network or even a combination of parameters. The operator can decide to maintain the offset parameters and calculate the best power levels for each zone (to not exceed the interference level with large delays that can degrade the performance in certain areas) or the best length of the guard intervals in each transmitter station.

The Simulated Annealing tool also allows the optimization of several parameters simultaneously. Once adjusting the requirement of the simulations, it is considered suitable to expand the optimization into other parameters to maximize the improvement of the network. In that case, it is important to define the next optimized parameter, the cost function calculation and the new equation in order to consider the improvements of both parameters. However, this action is more costly in meaning of runtime and programming stage.

BIBLIOGRAPHY

[1] C. Enrique, C. López, S. Ruiz, L. Alonso; “Design of a simulation platform to test next generation of terrestrial DVB”, Bachelor thesis, July 2007, Escola Politècnica Superior de Castelldefels (EPSC).

[2] FURIA Project: Official webpage of FURIA council. www.furiapse.com

[3] DVB-T2 Document A122: Frame structure channel coding and modulation for a second generation digital terrestrial television broadcasting system”, TM 3980 Rev. 5, June 2008.

[4] IEEE 802.11y-2008: “IEEE Standard for Information Technology-Telecommunications and Information Exchange between systems”. 2008 Edition.

[5] DVB Organization: Official webpage of DVB European Organization. www.dvb.org

[6] ETSI EN 300 421: “Digital Video Broadcasting (DVB); Framing structure, channel coding and modulation for 11/12 GHz satellite services”.

[7] ETSI EN 302 307: “Digital Video Broadcasting (DVB); Second generation framing structure, channel coding and modulation systems for Broadcasting, Interactive Services, News Gathering and other broadband satellite applications”.

[8] IBC: International Broadcasting Center. www.ibc.org

[9] ETSI EN 300 744: “Digital Video Broadcasting (DVB); Framing structure, channel coding and modulation for digital terrestrial television (DVB-T)”. November 2004.

[10] DVB-T2 Document A133: Implementation guidelines for a second generation digital terrestrial television broadcasting system (DVB-T2) (draft TR 102 831 V1.1.1).

[11] ISO/IEC 13818 (Parts 1 to 3): “Information technology – Generic coding of moving pictures and associated audio information”.

[12] DVB-C2 Document A138: Frame structure channel coding and modulation for a second generation digital transmission system for cable systems (DVB-C2).

[13] T. Pollet, M. Van Bladel and M. Moeneclaey. BER sensitivity of OFDM systems to carrier frequency offset and wiener phase noise. *IEEE Transactions on Communications* 43(2/3/4) (February/ March/April 1995).

[14] L. Tomba. On the effect of Wiener phase noise in OFDM systems, *IEEE communications*, Vol. 46 Issue: 5, May 98.

[15] M.S. El-Tanany, Wu Yiyan, L. Hazy. .Analytical modeling and simulation of phase noise interference in OFDM-based digital television terrestrial broadcasting systems. Broadcasting, IEEE Transactions, Vol. 47 Issue: 1, Mar 01.

[16] A.G. Armada, M. Calvo, .Phase noise and sub-carrier spacing effects on the performance of an OFDM communication system., *IEEE communication letters,* VOL. 2, No.1, JAN. 98.

[17] R. Beutler, Frequency Assignment and Network Planning for Digital Terrestrial Broadcasting Systems, Kluwer Academic Publishers, Dordrecht, 2004.

[18] A. Ligeti, J. Zander, Minimal cost coverage planning for single frequency networks, IEEE Trans. Broadcasting 45, 1999.

[19] C. Mannino, F. Rossi, S. Smriglio. The network packing problem in terrestrial broadcasting, Oper. Res. 54, 2006.

[20] The Chester 1997 Multilateral Coordination Agreement: Technical Criteria, Coordination Principles and Procedures for the Introduction of Terrestrial Digital Video Broadcasting, 25 July 1997.

[21] CEPT/EBU, Planning and Introduction of Terrestrial Digital Television (DVB-T) in Europe, Doc. FM (97) 1997.